



Spintronics in Semiconductors

C.S. Chu

**Department of Electrophysics
National Chiao Tung University**

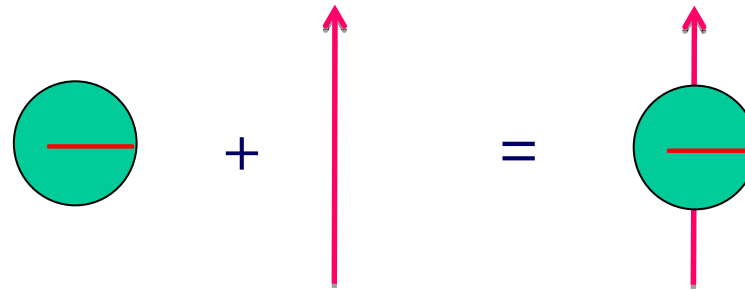


NCTU

Outline

- Introduction
- Spin-orbit interaction in semiconductors
- Spin-Hall Effect (SHE)
- Spin Dipole
- Detection of spin current:
 - a nano-mechanical proposal
- Detection of spin current: by inverse SHE
- Spin injection
- Spin-orbit interaction at metal alloy surfaces
- Summary

An electron has a **charge $-e$** and a **spin $1/2$**



Electronic industries have made good use of the **charge**.

But the **electron spin** has essentially been neglected.

**Quoted from the abstract of
“Spintronics: Fundamentals and applications”**

Spintronics, or spin electronics, involves the study of active control and manipulation of spin degrees of freedom in solid-state systems.

**in Reviews of Modern Physics,
vol. 76, p.323-410, 2004,
by I. Žutić, J. Fabian, and S. Das Sarma.**

Spintronics

Where magnetic material and magnetic field is involved:

- **GMR: giant magneto-resistive effect**
- **Memory / storage**
- **TMR, CMR**

Spin-based Quantum Computing:
uses spin of nuclei as qubits

All electrical means of generation and manipulation of spins:

- **spin-polarized transport in semiconductors**
- **spin FET, spin filter**
- **logic / storage**

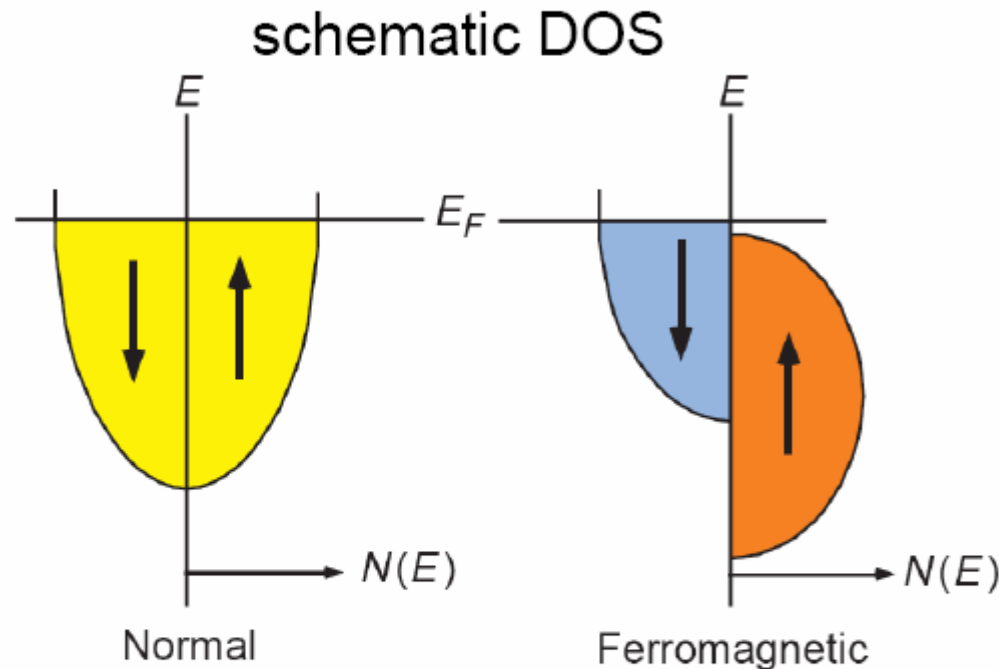
Why spintronics ?

- new physical principles
 - new challenges
 - new working principles for applications
 - new devices for technologies
-
- potentially decreases electric power consumption



Spin-polarized transport

Magnetic materials
are involved.



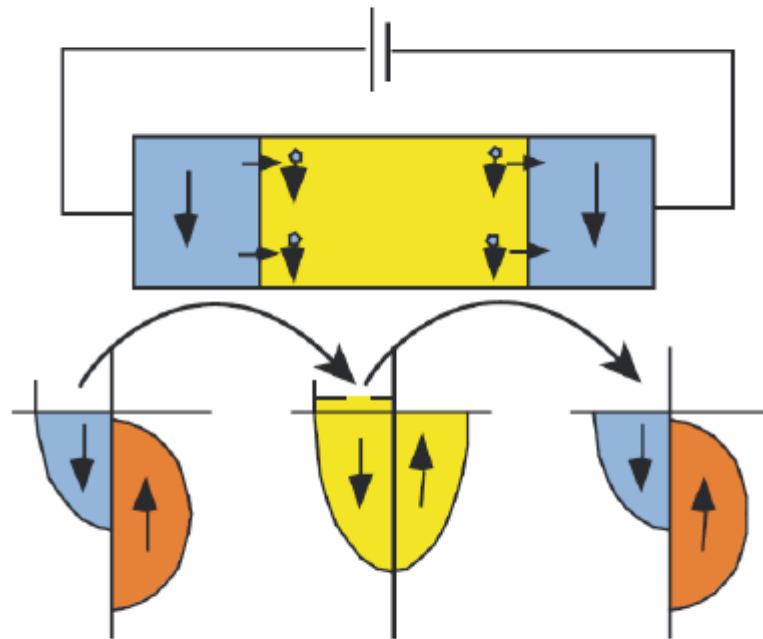
polarization:

$$P = \frac{n_{\uparrow} - n_{\downarrow}}{n_{\uparrow} + n_{\downarrow}}$$

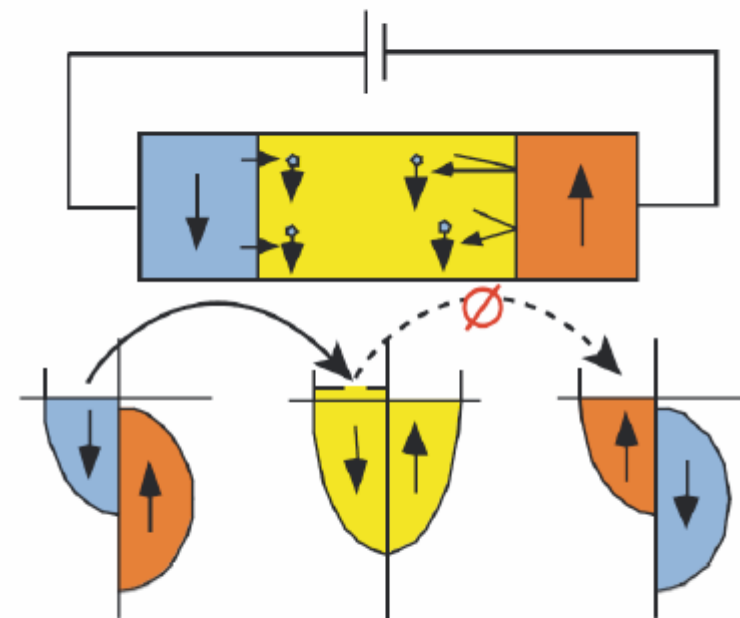
- imbalance of spin population at Fermi level leads naturally to spin-polarized transport
- commonly occurs in ferromagnetic metals (or alloys) with P up to 50 %

Magnetic materials
are involved.

Spin valve

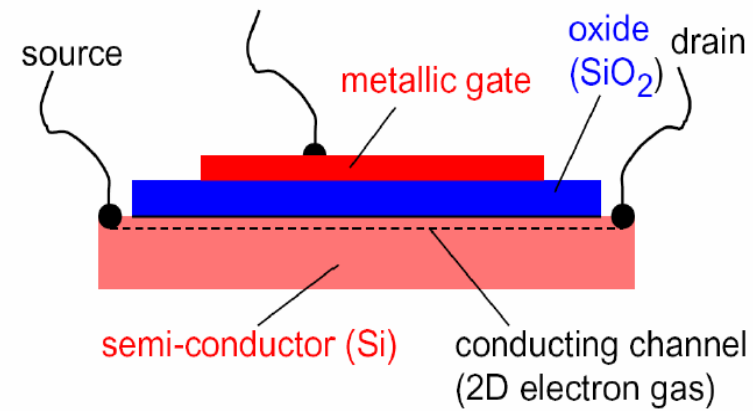


low resistance

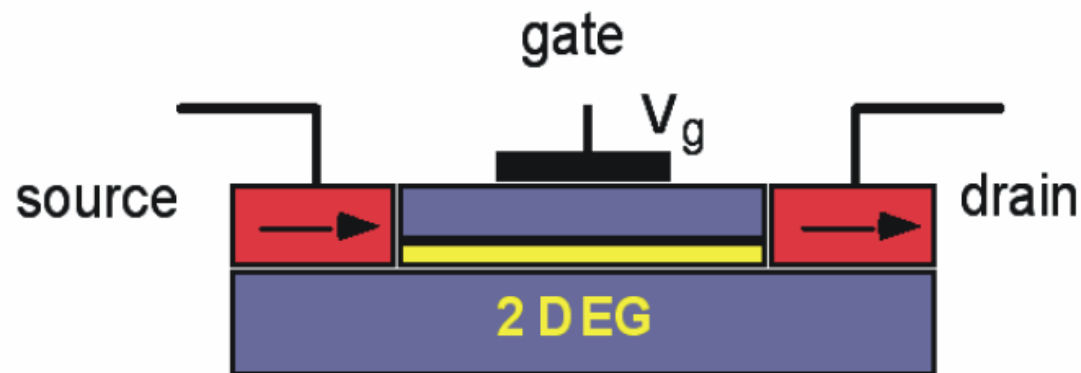


high resistance

“Normal” transistor (MOSFET)



Spin transistor



Datta and Das

Why spintronics in semiconductors ?

- **compatible with the semiconductor industries**
- **highly tunable**
- **spin-orbit interaction (SOI) is much larger than in vacuum**
- **zero magnetic field spin splitting in samples that has bulk inversion asymmetry (BIA) or structure inversion asymmetry (SIA).**

Amazing Spin-Orbit interaction in semiconductor:

In vacuum:

$$\begin{aligned} & \frac{\eta}{4m_0^2 c^2} \boldsymbol{\sigma} \cdot [\boldsymbol{\nabla} V \times \boldsymbol{p}] \\ & - \frac{\eta^2}{4m_0^2 c^2} \boldsymbol{\sigma} \cdot [\boldsymbol{k} \times \boldsymbol{\nabla} V] \\ & \lambda \boldsymbol{\sigma} \cdot (\boldsymbol{k} \times \boldsymbol{\nabla} V) \end{aligned}$$

In vacuum: $\lambda = -3.7 \times 10^{-6} \text{ \AA}^2$

In semiconductor such as GaAs: $\lambda = 5.3 \text{ \AA}^2$

In semiconductor such as InAs: $\lambda = 120 \text{ \AA}^2$

| Compound | Δ_0^{exp} (eV) | Δ_0^{theo} (eV) | f_i |
|--------------|------------------------------|-------------------------------|-------|
| C | 0.006 | 0.006 | 0 |
| Si | 0.044 | 0.044 | 0 |
| Ge | 0.29 | 0.29 | 0 |
| α -Sn | | 0.80 | 0 |
| AlN | | 0.012 | 0.449 |
| AlP | | 0.060 | 0.307 |
| AlAs | | 0.29 | 0.274 |
| AlSb | 0.75 | 0.80 | 0.250 |
| GaN | 0.011 | 0.095 | 0.500 |
| GaP | 0.127 | 0.11 | 0.327 |
| GaAs | 0.34 | 0.34 | 0.310 |
| GaSb | 0.80 | 0.98 | 0.261 |
| InN | | 0.08 | 0.578 |
| InP | 0.11 | 0.16 | 0.421 |
| InAs | 0.38 | 0.40 | 0.357 |
| InSb | 0.82 | 0.80 | 0.321 |
| ZnO | -0.005 | 0.03 | 0.616 |
| ZnS | 0.07 | 0.09 | 0.623 |
| ZnSe | 0.43 | 0.42 | 0.630 |
| ZnTe | 0.93 | 0.86 | 0.609 |
| CdS | 0.066 | 0.09 | 0.685 |
| CdSe | | 0.42 | 0.699 |
| CdTe | 0.92 | 0.94 | 0.717 |
| HgS | | 0.13 | 0.79 |
| HgSe | | 0.48 | 0.68 |
| HgTe | | 0.99 | 0.65 |

Strength of
spin-orbit
goes as Z^4 .

It is larger
for heavier
atoms.

Physical origin of this large enhancement in the SOI coupling constant:

- **a brief review of how SOI comes about,
starting from the Dirac equation.**
- **how does the SOI coupling constant gets
enhanced in semiconductors:
a $\mathbf{k}\cdot\mathbf{p}$ approach.**



How does spin-orbit interaction arises from Dirac equation, when relativity is fully taken into account ?

$$(c \boldsymbol{\alpha} \cdot \mathbf{p} + \beta m_0 c^2 + V) \psi = E \psi$$

$$\boldsymbol{\alpha} = \begin{pmatrix} 0 & \boldsymbol{\sigma} \\ \boldsymbol{\sigma} & 0 \end{pmatrix} \quad \beta = \begin{pmatrix} \mathbf{1}_{2 \times 2} & 0 \\ 0 & -\mathbf{1}_{2 \times 2} \end{pmatrix}$$

$$\psi = \begin{bmatrix} \psi_A \\ \psi_B \end{bmatrix}$$

$$\boldsymbol{\sigma} \cdot \mathbf{p} \psi_B = \frac{1}{c} (\tilde{E} - V) \psi_A ,$$

$$\boldsymbol{\sigma} \cdot \mathbf{p} \psi_A = \frac{1}{c} (\tilde{E} - V + 2m_0c^2) \psi_B$$

$$\tilde{E} = E - m_0c^2 \quad \text{and}$$

normalization of ψ gives

$$\int d\mathbf{r} \psi^\dagger \psi = \int d\mathbf{r} [\psi_A^\dagger \psi_A + \psi_B^\dagger \psi_B] = 1$$

$$\boldsymbol{\sigma} \cdot \mathbf{p} \left[\frac{c^2}{\tilde{E} - V + 2m_0c^2} \right] \boldsymbol{\sigma} \cdot \mathbf{p} \psi_A = (\tilde{E} - V) \psi_A$$

We focus upon the large component, when $E > m_0c^2$.

$$\boldsymbol{\sigma} \cdot \mathbf{p} \left[\frac{c^2}{\tilde{E} - V + 2m_0c^2} \right] \boldsymbol{\sigma} \cdot \mathbf{p} \psi_A = (\tilde{E} - V) \psi_A$$

Note that this equation cannot replace the original Dirac equation, when large and small components are coupled. This is because ψ_A alone is not normalized. From

$$\psi_B = \left[2m_0c^2 + \tilde{E} - V \right]^{-1} c \boldsymbol{\sigma} \cdot \boldsymbol{\pi} \psi_A \quad \text{we have}$$

$$\begin{aligned} \psi_B^\dagger \psi_B &= \psi_A^\dagger (c \boldsymbol{\sigma} \cdot \boldsymbol{\pi}) \left[2m_0c^2 + \tilde{E} - V \right]^{-2} (c \boldsymbol{\sigma} \cdot \boldsymbol{\pi}) \psi_A \\ &\approx \frac{1}{4m_0^2c^2} \psi_A^\dagger \left(\boldsymbol{\pi}^2 + eh \boldsymbol{\sigma} \cdot \mathbf{B} \right) \psi_A \end{aligned}$$

$$\boldsymbol{\pi} = \mathbf{p} + e\mathbf{A} \quad \text{where } e > 0$$

$$\tilde{\psi} = \left(1 + \frac{\pi^2 + e\eta \sigma \cdot B}{8m_0^2 c^2} \right) \psi_A$$

$$\psi_A = \left(1 - \frac{\pi^2 + e\eta \sigma \cdot B}{8m_0^2 c^2} \right) \tilde{\psi}$$

$$\begin{aligned} (\sigma \cdot \pi) \left[\frac{c^2}{2m_0 c^2 + \tilde{E} - V} \right] (\sigma \cdot \pi) \left(1 - \frac{\pi^2 + e\eta \sigma \cdot B}{8m_0^2 c^2} \right) \tilde{\psi} \\ = (\tilde{E} - V) \left(1 - \frac{\pi^2 + e\eta \sigma \cdot B}{8m_0^2 c^2} \right) \tilde{\psi} \end{aligned}$$

$$\frac{c^2}{2m_0 c^2 + \tilde{E} - V} \approx \frac{1}{2m_0} \left(1 - \frac{\tilde{E} - V}{2m_0 c^2} \right) \quad \text{up to order } (v/c)^2$$

$$\begin{aligned} \frac{1}{2m_0} (\boldsymbol{\sigma} \cdot \boldsymbol{\pi}) \left[1 - \frac{\tilde{E} - V}{2m_0 c^2} \right] (\boldsymbol{\sigma} \cdot \boldsymbol{\pi}) \left(1 - \frac{\pi^2 + e\eta \boldsymbol{\sigma} \cdot \boldsymbol{B}}{8m_0^2 c^2} \right) \tilde{\psi} \\ = (\tilde{E} - V) \left(1 - \frac{\pi^2 + e\eta \boldsymbol{\sigma} \cdot \boldsymbol{B}}{8m_0^2 c^2} \right) \tilde{\psi} \end{aligned}$$

$$\begin{aligned} \left(\frac{\pi^2 + e\eta \boldsymbol{\sigma} \cdot \boldsymbol{B}}{2m_0} \right) \left(1 - \frac{\pi^2 + e\eta \boldsymbol{\sigma} \cdot \boldsymbol{B}}{8m_0^2 c^2} \right) \tilde{\psi} + \frac{1}{4m_0^2 c^2} (\boldsymbol{\sigma} \cdot \boldsymbol{\pi}) V (\boldsymbol{\sigma} \cdot \boldsymbol{\pi}) \tilde{\psi} \\ - \frac{\tilde{E}}{4m_0^2 c^2} (\pi^2 + e\eta \boldsymbol{\sigma} \cdot \boldsymbol{B}) \tilde{\psi} \\ = (\tilde{E} - V) \left(1 - \frac{\pi^2 + e\eta \boldsymbol{\sigma} \cdot \boldsymbol{B}}{8m_0^2 c^2} \right) \tilde{\psi} \end{aligned}$$

$$\begin{aligned}
 & \left(\frac{\vec{p}^2 + e\hbar \vec{\sigma} \cdot \vec{B}}{2m_0} \right) \left(1 - \frac{\vec{p}^2 + e\hbar \vec{\sigma} \cdot \vec{B}}{8m_0^2 c^2} \right) \tilde{\psi} + \frac{1}{4m_0^2 c^2} (\vec{\sigma} \cdot \vec{p}) V (\vec{\sigma} \cdot \vec{p}) \tilde{\psi} \\
 & + V \left(1 - \frac{\vec{p}^2 + e\hbar \vec{\sigma} \cdot \vec{B}}{8m_0^2 c^2} \right) \tilde{\psi} \\
 & = \tilde{E} \left(1 + \frac{\vec{p}^2 + e\hbar \vec{\sigma} \cdot \vec{B}}{8m_0^2 c^2} \right) \tilde{\psi}
 \end{aligned}$$

$$\begin{aligned}
 & \left(1 - \frac{\vec{p}^2 + e\hbar \vec{\sigma} \cdot \vec{B}}{8m_0^2 c^2} \right) \left(\frac{\vec{p}^2 + e\hbar \vec{\sigma} \cdot \vec{B}}{2m_0} \right) \left(1 - \frac{\vec{p}^2 + e\hbar \vec{\sigma} \cdot \vec{B}}{8m_0^2 c^2} \right) \tilde{\psi} \\
 & + \left(1 - \frac{\vec{p}^2 + e\hbar \vec{\sigma} \cdot \vec{B}}{8m_0^2 c^2} \right) \frac{1}{4m_0^2 c^2} (\vec{\sigma} \cdot \vec{p}) V (\vec{\sigma} \cdot \vec{p}) \tilde{\psi} \\
 & + \left(1 - \frac{\vec{p}^2 + e\hbar \vec{\sigma} \cdot \vec{B}}{8m_0^2 c^2} \right) V \left(1 - \frac{\vec{p}^2 + e\hbar \vec{\sigma} \cdot \vec{B}}{8m_0^2 c^2} \right) \tilde{\psi} \\
 & = \tilde{E} \tilde{\psi}
 \end{aligned}$$

$$\begin{aligned}
 & (\hat{\sigma} \cdot \hat{\pi}) V (\hat{\sigma} \cdot \hat{\pi}) \\
 &= -i\eta \nabla V \cdot \hat{\pi} + \eta (\nabla V \times \hat{\pi}) \cdot \hat{\sigma} + V(\hat{\pi}^2 + e\eta \hat{\sigma} \cdot \hat{B})
 \end{aligned}$$

$$\left[\begin{aligned}
 & \frac{\pi^2}{2m_0} + V + \frac{eh}{2m_0} \hat{\sigma} \cdot \hat{B} - \frac{eh}{4m_0^2 c^2} \hat{\sigma} \cdot (\hat{\pi} \times \hat{\varepsilon}) + \frac{eh^2}{8m_0^2 c^2} \nabla \cdot \hat{\varepsilon} \\
 & - \frac{(\hat{\pi}^2)^2}{8m_0^3 c^2} - \frac{eh \hat{\pi}^2}{4m_0^3 c^2} \hat{\sigma} \cdot \hat{B} - \frac{(ehB)^2}{8m_0^3 c^2}
 \end{aligned} \right] \psi_0$$

$$= E_0 \psi_0$$

The spin orbit interaction term comes from the action of gradient V onto the small component wavefunction.

$$\hat{\varepsilon} = \frac{1}{e} \nabla V$$

We know now how the spin-orbit interaction comes from the relativistic effect. The Thomas precession has also been taken into account in our taking of the nonrelativistic limit.

Can we then understand the amazing enlargement of the spin-orbit coupling parameter λ in semiconductor ?

Amazing Spin-Orbit interaction in semiconductor: To refresh our memory

In vacuum:

$$\begin{aligned} & \frac{\eta}{4m_0^2 c^2} \boldsymbol{\sigma} \cdot [\nabla V \times \boldsymbol{p}] \\ & - \frac{\eta^2}{4m_0^2 c^2} \boldsymbol{\sigma} \cdot [\boldsymbol{k} \times \nabla V] \\ & \lambda \boldsymbol{\sigma} \cdot (\boldsymbol{k} \times \nabla V) \end{aligned}$$

In vacuum: $\lambda = -3.7 \times 10^{-6} \text{ \AA}^2$

In semiconductor such as GaAs: $\lambda = 5.3 \text{ \AA}^2$

In semiconductor such as InAs: $\lambda = 120 \text{ \AA}^2$

$\mathbf{k} \cdot \mathbf{p}$ Method for an electron in a periodic potential $V_0(\mathbf{r})$

The derivation of the $\mathbf{k} \cdot \mathbf{p}$ method is based on the Schrödinger equation for the Bloch functions $e^{i\mathbf{k} \cdot \mathbf{r}} u_{\nu\mathbf{k}}(\mathbf{r}) \equiv e^{i\mathbf{k} \cdot \mathbf{r}} \langle \mathbf{r} | \nu \mathbf{k} \rangle$ in the microscopic lattice-periodic crystal potential $V_0(\mathbf{r})$

$$\left[\frac{p^2}{2m_0} + V_0(\mathbf{r}) \right] e^{i\mathbf{k} \cdot \mathbf{r}} u_{\nu\mathbf{k}}(\mathbf{r}) = E_{\nu}(\mathbf{k}) e^{i\mathbf{k} \cdot \mathbf{r}} u_{\nu\mathbf{k}}(\mathbf{r}) .$$

$$\left[\frac{p^2}{2m_0} + V_0 + \frac{\hbar^2 k^2}{2m_0} + \frac{\hbar}{m_0} \mathbf{k} \cdot \mathbf{p} \right] |\nu \mathbf{k}\rangle = E_{\nu}(\mathbf{k}) |\nu \mathbf{k}\rangle .$$

If we include the spin-orbit interaction, given by

$$\frac{\eta}{4m_0^2c^2} \boldsymbol{\sigma} \cdot [\nabla V \times \mathbf{p}]$$

we get

$$\left[\frac{p^2}{2m_0} + V_0 + \frac{\hbar^2 k^2}{2m_0} + \frac{\hbar}{m_0} \mathbf{k} \cdot \boldsymbol{\pi} + \frac{\hbar}{4m_0^2c^2} \mathbf{p} \cdot \boldsymbol{\sigma} \times (\nabla V_0) \right] |n\mathbf{k}\rangle = E_n(\mathbf{k}) |n\mathbf{k}\rangle$$

where

$$\boldsymbol{\pi} := \mathbf{p} + \frac{\hbar}{4m_0c^2} \boldsymbol{\sigma} \times \nabla V_0$$



Two component
spinors

For a fixed wave vector \mathbf{k}_0 the sets of lattice periodic functions $\{|\mathbf{n}\mathbf{k}_0\rangle\}$ provide a complete and orthonormal basis. Therefore, we can expand the kets $\{|\mathbf{n}\mathbf{k}\rangle\}$ in terms of band edge Bloch functions $\{|\nu\mathbf{0}\rangle\}$ times spin eigenstates $|\sigma\rangle$

$$|\mathbf{n}\mathbf{k}\rangle = \sum_{\substack{\nu' \\ \sigma'=\uparrow,\downarrow}} c_{n\nu'\sigma'}(\mathbf{k}) |\nu'\sigma'\rangle ,$$

where

$$|\nu'\sigma'\rangle := |\nu'\mathbf{0}\rangle \otimes |\sigma'\rangle .$$

$$\sum_{\nu', \sigma'} \left\{ \left[E_{\nu'}(\mathbf{0}) + \frac{\hbar^2 k^2}{2m_0} \right] \delta_{\nu\nu'} \delta_{\sigma\sigma'} + \frac{\hbar}{m_0} \mathbf{k} \cdot \mathbf{P}_{\sigma\sigma'}^{\nu\nu'} + \Delta_{\sigma\sigma'}^{\nu\nu'} \right\} c_{n\nu'\sigma'}(\mathbf{k}) = E_n(\mathbf{k}) c_{n\nu\sigma}(\mathbf{k}) ,$$

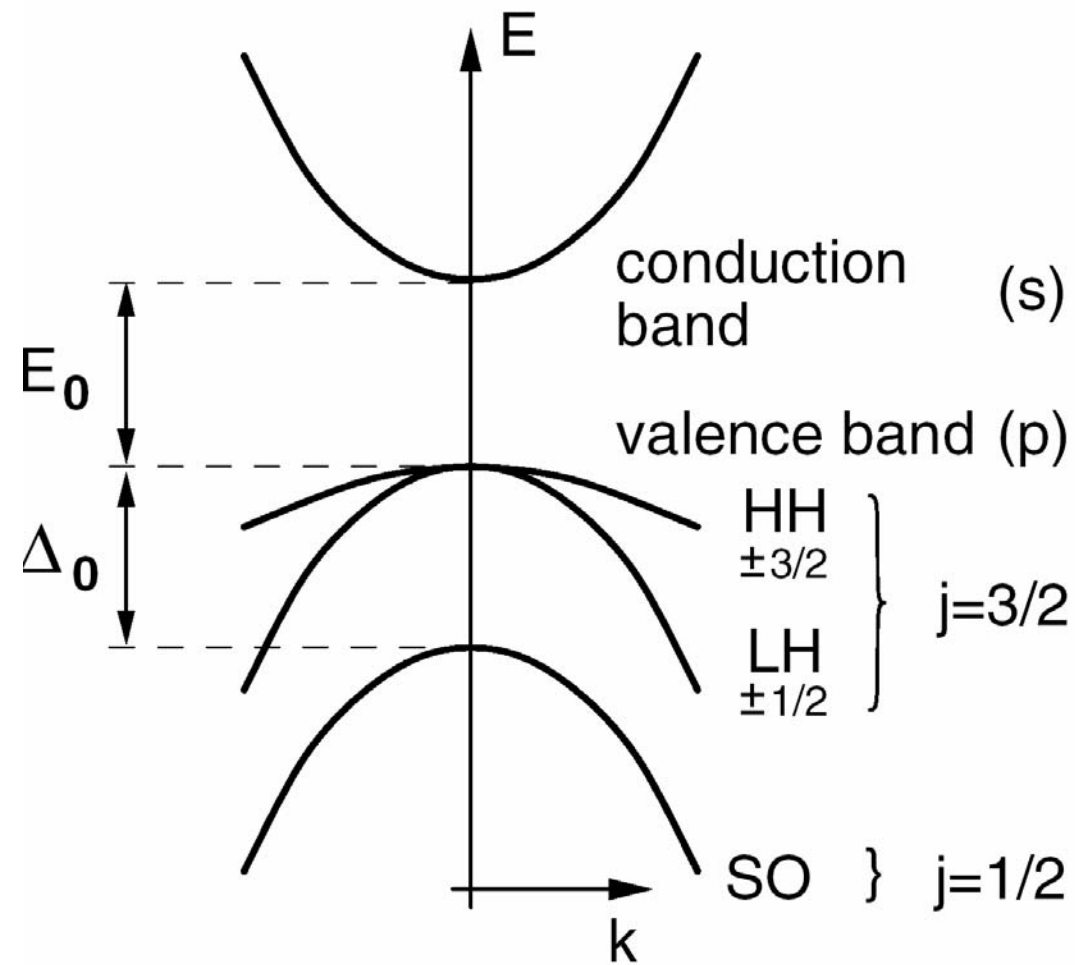
where

$$\mathbf{P}_{\sigma\sigma'}^{\nu\nu'} := \langle \nu\sigma | \boldsymbol{\pi} | \nu'\sigma' \rangle ,$$

$$\Delta_{\sigma\sigma'}^{\nu\nu'} := \frac{\hbar}{4m_0^2 c^2} \langle \nu\sigma | [\mathbf{p} \cdot \boldsymbol{\sigma} \times (\nabla V_0)] | \nu'\sigma' \rangle .$$

We choose the S and P orbitals for states $|\nu'\sigma'\rangle$.

$$\boldsymbol{\pi} := \mathbf{p} + \frac{\hbar}{4m_0 c^2} \boldsymbol{\sigma} \times \nabla V_0$$



| | | |
|------------------|-------------|----------|
| $ J, m_j\rangle$ | ψ_{jm} | $E(k=0)$ |
|------------------|-------------|----------|

| | | |
|------------------------------------|---|-------|
| $ \frac{3}{2}, \frac{3}{2}\rangle$ | $-\frac{1}{\sqrt{2}} X+iY\rangle \uparrow\rangle$ | E_v |
|------------------------------------|---|-------|

| | | |
|------------------------------------|--|-------|
| $ \frac{3}{2}, \frac{1}{2}\rangle$ | $\sqrt{\frac{2}{3}} Z\rangle \uparrow\rangle - \frac{1}{\sqrt{6}} X+iY\rangle \downarrow\rangle$ | E_v |
|------------------------------------|--|-------|

| | | |
|-------------------------------------|--|-------|
| $ \frac{3}{2}, \frac{-1}{2}\rangle$ | $\sqrt{\frac{2}{3}} Z\rangle \downarrow\rangle + \frac{1}{\sqrt{6}} X-iY\rangle \uparrow\rangle$ | E_v |
|-------------------------------------|--|-------|

| | | |
|-------------------------------------|--|-------|
| $ \frac{3}{2}, \frac{-3}{2}\rangle$ | $\frac{1}{\sqrt{2}} X-iY\rangle \downarrow\rangle$ | E_v |
|-------------------------------------|--|-------|

 Γ_8^v

| | | |
|------------------------------------|---|------------------|
| $ \frac{1}{2}, \frac{1}{2}\rangle$ | $-\sqrt{\frac{1}{3}} Z\rangle \uparrow\rangle - \frac{1}{\sqrt{3}} X+iY\rangle \downarrow\rangle$ | $E_v - \Delta_0$ |
|------------------------------------|---|------------------|

| | | |
|-------------------------------------|--|------------------|
| $ \frac{1}{2}, \frac{-1}{2}\rangle$ | $\sqrt{\frac{1}{3}} Z\rangle \downarrow\rangle - \frac{1}{\sqrt{3}} X-iY\rangle \uparrow\rangle$ | $E_v - \Delta_0$ |
|-------------------------------------|--|------------------|

 Γ_7^v

| | | | |
|--|---|------------------|--------------|
| $\left \frac{1}{2}, \frac{1}{2}\right\rangle$ | $ S\rangle \uparrow\rangle$ | E_c | Γ_6^c |
| $\left \frac{1}{2}, \frac{-1}{2}\right\rangle$ | $ S\rangle \downarrow\rangle$ | E_c | |
| $\left \frac{3}{2}, \frac{3}{2}\right\rangle$ | $-\frac{1}{\sqrt{2}} X+iY\rangle \uparrow\rangle$ | E_v | Γ_8^v |
| $\left \frac{3}{2}, \frac{1}{2}\right\rangle$ | $\sqrt{\frac{2}{3}} Z\rangle \uparrow\rangle - \frac{1}{\sqrt{6}} X+iY\rangle \downarrow\rangle$ | E_v | |
| $\left \frac{3}{2}, \frac{-1}{2}\right\rangle$ | $\sqrt{\frac{2}{3}} Z\rangle \downarrow\rangle + \frac{1}{\sqrt{6}} X-iY\rangle \uparrow\rangle$ | E_v | |
| $\left \frac{3}{2}, \frac{-3}{2}\right\rangle$ | $\frac{1}{\sqrt{2}} X-iY\rangle \downarrow\rangle$ | E_v | Γ_7^v |
| $\left \frac{1}{2}, \frac{1}{2}\right\rangle$ | $-\sqrt{\frac{1}{3}} Z\rangle \uparrow\rangle - \frac{1}{\sqrt{3}} X+iY\rangle \downarrow\rangle$ | $E_v - \Delta_0$ | |
| $\left \frac{1}{2}, \frac{-1}{2}\right\rangle$ | $\sqrt{\frac{1}{3}} Z\rangle \downarrow\rangle - \frac{1}{\sqrt{3}} X-iY\rangle \uparrow\rangle$ | $E_v - \Delta_0$ | |

Table C.1. Basis functions $|jm\rangle$ of the extended Kane model. The quantization axis of angular momentum is the crystallographic direction [001]. In accordance with time reversal symmetry, we have chosen the phase convention that $|X\rangle$, $|Y\rangle$, and $|Z\rangle$ are real and $|S\rangle$, $|X'\rangle$, $|Y'\rangle$, and $|Z'\rangle$ are purely imaginary. Note that our definition of the basis functions $|jm\rangle$ agrees with common definitions of angular-momentum eigenfunctions (see e.g. [1])

| | | |
|--------------|---|--|
| Γ_8^c | $\left \frac{3}{2} \quad \frac{3}{2} \right\rangle_{c'} = -\frac{1}{\sqrt{2}} \begin{vmatrix} X' + iY' \\ 0 \end{vmatrix}$ | $\left \frac{3}{2} \quad \frac{1}{2} \right\rangle_{c'} = \frac{1}{\sqrt{6}} \begin{vmatrix} 2Z' \\ -X' - iY' \end{vmatrix}$ |
| | $\left \frac{3}{2} \quad -\frac{1}{2} \right\rangle_{c'} = \frac{1}{\sqrt{6}} \begin{vmatrix} X' - iY' \\ 2Z' \end{vmatrix}$ | $\left \frac{3}{2} \quad -\frac{3}{2} \right\rangle_{c'} = \frac{1}{\sqrt{2}} \begin{vmatrix} 0 \\ X' - iY' \end{vmatrix}$ |
| Γ_7^c | $\left \frac{1}{2} \quad \frac{1}{2} \right\rangle_{c'} = -\frac{1}{\sqrt{3}} \begin{vmatrix} Z' \\ X' + iY' \end{vmatrix}$ | $\left \frac{1}{2} \quad -\frac{1}{2} \right\rangle_{c'} = -\frac{1}{\sqrt{3}} \begin{vmatrix} X' - iY' \\ -Z' \end{vmatrix}$ |
| | $\left \frac{1}{2} \quad \frac{1}{2} \right\rangle_c = \begin{vmatrix} S \\ 0 \end{vmatrix}$ | $\left \frac{1}{2} \quad -\frac{1}{2} \right\rangle_c = \begin{vmatrix} 0 \\ S \end{vmatrix}$ |
| Γ_8^v | $\left \frac{3}{2} \quad \frac{3}{2} \right\rangle_v = -\frac{1}{\sqrt{2}} \begin{vmatrix} X + iY \\ 0 \end{vmatrix}$ | $\left \frac{3}{2} \quad \frac{1}{2} \right\rangle_v = \frac{1}{\sqrt{6}} \begin{vmatrix} 2Z \\ -X - iY \end{vmatrix}$ |
| | $\left \frac{3}{2} \quad -\frac{1}{2} \right\rangle_v = \frac{1}{\sqrt{6}} \begin{vmatrix} X - iY \\ 2Z \end{vmatrix}$ | $\left \frac{3}{2} \quad -\frac{3}{2} \right\rangle_v = \frac{1}{\sqrt{2}} \begin{vmatrix} 0 \\ X - iY \end{vmatrix}$ |
| Γ_7^v | $\left \frac{1}{2} \quad \frac{1}{2} \right\rangle_v = -\frac{1}{\sqrt{3}} \begin{vmatrix} Z \\ X + iY \end{vmatrix}$ | $\left \frac{1}{2} \quad -\frac{1}{2} \right\rangle_v = -\frac{1}{\sqrt{3}} \begin{vmatrix} X - iY \\ -Z \end{vmatrix}$ |

$$\mathcal{H}_{8 \times 8} = \begin{pmatrix} (E_c + V) \mathbf{1}_{2 \times 2} & \sqrt{3} P \mathbf{T} \cdot \mathbf{k} & -\frac{1}{\sqrt{3}} P \boldsymbol{\sigma} \cdot \mathbf{k} \\ \sqrt{3} P \mathbf{T}^\dagger \cdot \mathbf{k} & (E_v + V) \mathbf{1}_{4 \times 4} & 0 \\ -\frac{1}{\sqrt{3}} P \boldsymbol{\sigma} \cdot \mathbf{k} & 0 & (E_v - \Delta_0 + V) \mathbf{1}_{2 \times 2} \end{pmatrix}$$

$$= \begin{pmatrix} E_c + V & 0 & \frac{-1}{\sqrt{2}} P k_+ & \sqrt{\frac{2}{3}} P k_z & \frac{1}{\sqrt{6}} P k_- & 0 & \frac{-1}{\sqrt{3}} P k_z & \frac{-1}{\sqrt{3}} P k_- \\ 0 & E_c + V & 0 & \frac{-1}{\sqrt{6}} P k_+ & \sqrt{\frac{2}{3}} P k_z & \frac{1}{\sqrt{2}} P k_- & \frac{-1}{\sqrt{3}} P k_+ & \frac{1}{\sqrt{3}} P k_z \\ \frac{-1}{\sqrt{2}} P k_- & 0 & E_v + V & 0 & 0 & 0 & 0 & 0 \\ \sqrt{\frac{2}{3}} P k_z & \frac{-1}{\sqrt{6}} P k_- & 0 & E_v + V & 0 & 0 & 0 & 0 \\ \frac{1}{\sqrt{6}} P k_+ & \sqrt{\frac{2}{3}} P k_z & 0 & 0 & E_v + V & 0 & 0 & 0 \\ 0 & \frac{1}{\sqrt{2}} P k_+ & 0 & 0 & 0 & E_v + V & 0 & 0 \\ \frac{-1}{\sqrt{3}} P k_z & \frac{-1}{\sqrt{3}} P k_- & 0 & 0 & 0 & 0 & E_v - \Delta_0 + V & 0 \\ \frac{-1}{\sqrt{3}} P k_+ & \frac{1}{\sqrt{3}} P k_z & 0 & 0 & 0 & 0 & 0 & E_v - \Delta_0 + V \end{pmatrix}.$$

$$P = \frac{\hbar}{m_0} \langle S | p_x | X \rangle$$

$$\Delta_0 = - \frac{3i\hbar}{4m_0^2 c^2} \langle X | [(\nabla V_0) \times \mathbf{p}]_y | Z \rangle$$

$$\begin{bmatrix} (E_c + V)1_{2 \times 2} & \sqrt{3}PT \cdot \hat{k}^{\rho} & -\frac{1}{\sqrt{3}}P\hat{\sigma} \cdot \hat{k}^{\rho} \\ \sqrt{3}PT^+ \cdot \hat{k}^{\rho} & (E_v + V)1_{4 \times 4} & 0 \\ -\frac{1}{\sqrt{3}}P\hat{\sigma} \cdot \hat{k}^{\rho} & 0 & (E_c - \Delta_0 + V)1_{2 \times 2} \end{bmatrix} \begin{bmatrix} \psi_c \\ \psi_{v+} \\ \psi_{v-} \end{bmatrix} = E \begin{bmatrix} \psi_c \\ \psi_{v+} \\ \psi_{v-} \end{bmatrix}$$

$$\sqrt{3}PT^+ \cdot \hat{k}^{\rho} \psi_c = (\tilde{E} + E_0 - V) \psi_{v+}$$

or

$$\psi_{v+} = \frac{\sqrt{3}P}{\tilde{E} + E_0 - V} T^+ \cdot \hat{k}^{\rho} \psi_c$$

$$-\frac{P}{\sqrt{3}}\hat{\sigma} \cdot \hat{k}^{\rho} \psi_c = (E - E_v + \Delta_0 - V) \psi_{v-}$$

or

$$\psi_{v-} = -\frac{P}{\sqrt{3}(\tilde{E} + E_0 + \Delta_0 - V)} \hat{\sigma} \cdot \hat{k}^{\rho} \psi_c$$

$$\left[T \cdot k \frac{3P^2}{\tilde{E} - V + E_0} T^\dagger \cdot k + \sigma \cdot k \frac{P^2/3}{\tilde{E} - V + E_0 + \Delta_0} \sigma \cdot k \right] \psi_c$$

$$= (\tilde{E} - V) \psi_c,$$

From normalization consideration

$$\psi_c^+ \psi_c + \psi_{v+}^+ \psi_{v+} + \psi_{v-}^+ \psi_{v-}$$

$$= \psi_c^+ \left[1 + T \cdot k \frac{3P^2}{(E_0 + \tilde{E} - V)^2} T^\dagger \cdot k + \sigma \cdot k \frac{P^2}{3(E_0 + \tilde{E} + \Delta_0 - V)^2} \sigma \cdot k \right] \psi_c$$

$$= \psi_c^+ \left[1 + 3P^2 \frac{(T \cdot \hat{\pi})(T^\dagger \cdot \hat{\pi})}{\eta^2 E_0^2} + \frac{P^2}{3} \frac{(\sigma \cdot \hat{\pi})(\sigma \cdot \hat{\pi})}{\eta^2 (E_0 + \Delta_0)^2} \right] \psi_c$$

$$(T \cdot \hat{\pi})(T^\dagger \cdot \hat{\pi}) = \frac{(2\pi^2 - e\eta \sigma \cdot B)}{9}$$

Physical meaning of P^2 :

$$\left[\mathbf{T} \cdot \mathbf{k} \frac{3P^2}{\tilde{E} - V + E_0} \mathbf{T}^\dagger \cdot \mathbf{k} + \boldsymbol{\sigma} \cdot \mathbf{k} \frac{P^2/3}{\tilde{E} - V + E_0 + \Delta_0} \boldsymbol{\sigma} \cdot \mathbf{k} \right] \psi_c$$

$$= (\tilde{E} - V) \psi_c ,$$

Taking the $E_0 \gg \Delta_0$:

$$\frac{3P^2}{E_0} \frac{(2\pi^2 - e\eta \boldsymbol{\sigma} \cdot \mathbf{B})}{9\eta^2} \psi_c + \frac{P^2}{3E_0} \frac{(\pi^2 + e\eta \boldsymbol{\sigma} \cdot \mathbf{B})}{\eta^2} \psi_c$$

$$= (\tilde{E} - V) \psi_c$$

$$\frac{P^2}{3E_0} \frac{3\pi^2}{\eta^2} \psi_c = (\tilde{E} - V) \psi_c$$

$$\frac{1}{2m^*} = \frac{P^2}{\eta^2 E_0} \quad \mathbf{P}^2 \text{ and } \mathbf{E}_0 \text{ combined to give the effective mass of the electron}$$

Define a normalized wavefunction

$$\tilde{\psi}_c = \left[1 + \frac{P^2}{6\eta^2} \left(\frac{2\pi^2 - e\eta \boldsymbol{\sigma} \cdot \mathbf{B}}{E_0^2} + \frac{\pi^2 + e\eta \boldsymbol{\sigma} \cdot \mathbf{B}}{(E_0 + \Delta_0)^2} \right) \right] \psi_c$$

$$\left[\mathbf{T} \cdot \mathbf{k} \frac{3P^2}{\tilde{E} - V + E_0} \mathbf{T}^\dagger \cdot \mathbf{k} + \boldsymbol{\sigma} \cdot \mathbf{k} \frac{P^2/3}{\tilde{E} - V + E_0 + \Delta_0} \boldsymbol{\sigma} \cdot \mathbf{k} \right] \psi_c$$

$$= (\tilde{E} - V) \psi_c,$$

$$\begin{aligned}
 & \left[1 - \frac{P^2}{6\eta^2} \left(\frac{2\kappa^2 - e\eta \boldsymbol{\sigma} \cdot \mathbf{B}}{E_0^2} + \frac{\kappa^2 + e\eta \boldsymbol{\sigma} \cdot \mathbf{B}}{(E_0 + \Delta_0)^2} \right) \right] \frac{P^2}{3\eta^2 E_0} (2\kappa^2 - e\eta \boldsymbol{\sigma} \cdot \mathbf{B}) \left[1 - \frac{P^2}{6\eta^2} \left(\frac{2\kappa^2 - e\eta \boldsymbol{\sigma} \cdot \mathbf{B}}{E_0^2} + \frac{\kappa^2 + e\eta \boldsymbol{\sigma} \cdot \mathbf{B}}{(E_0 + \Delta_0)^2} \right) \right] \tilde{\psi}_c \\
 & + \frac{3P^2}{\eta^2 E_0^2} (T \cdot \kappa) V (T^+ \cdot \kappa) \tilde{\psi}_c \\
 & + \frac{P^2}{3\eta^2 (E_0 + \Delta_0)^2} \left[1 - \frac{P^2}{6\eta^2} \left(\frac{2\kappa^2 - e\eta \boldsymbol{\sigma} \cdot \mathbf{B}}{E_0^2} + \frac{\kappa^2 + e\eta \boldsymbol{\sigma} \cdot \mathbf{B}}{(E_0 + \Delta_0)^2} \right) \right] (\kappa^2 + e\eta \boldsymbol{\sigma} \cdot \mathbf{B}) \left[1 - \frac{P^2}{6\eta^2} \left(\frac{2\kappa^2 - e\eta \boldsymbol{\sigma} \cdot \mathbf{B}}{E_0^2} + \frac{\kappa^2 + e\eta \boldsymbol{\sigma} \cdot \mathbf{B}}{(E_0 + \Delta_0)^2} \right) \right] \tilde{\psi}_c \\
 & + \frac{P^2}{3\eta^2 (E_0 + \Delta_0)^2} (\boldsymbol{\sigma} \cdot \kappa) V (\boldsymbol{\sigma} \cdot \kappa) \tilde{\psi}_c \\
 & + \left[1 - \frac{P^2}{6\eta^2} \left(\frac{2\kappa^2 - e\eta \boldsymbol{\sigma} \cdot \mathbf{B}}{E_0^2} + \frac{\kappa^2 + e\eta \boldsymbol{\sigma} \cdot \mathbf{B}}{(E_0 + \Delta_0)^2} \right) \right] V \left[1 - \frac{P^2}{6\eta^2} \left(\frac{2\kappa^2 - e\eta \boldsymbol{\sigma} \cdot \mathbf{B}}{E_0^2} + \frac{\kappa^2 + e\eta \boldsymbol{\sigma} \cdot \mathbf{B}}{(E_0 + \Delta_0)^2} \right) \right] \tilde{\psi}_c \\
 & = \tilde{E} \tilde{\psi}_c
 \end{aligned}$$

$$\begin{aligned}
 & \left\{ \frac{P^2}{3} \left[\frac{2}{E_0} + \frac{1}{E_0 + \Delta_0} \right] \left(\frac{\rho^2}{\eta^2} \right) + V \right. \\
 & \quad - \frac{P^2}{3} \left[\frac{1}{E_0} - \frac{1}{E_0 + \Delta_0} \right] \frac{e}{\eta} \boldsymbol{\sigma} \cdot \boldsymbol{B} \\
 & \quad - \frac{eP^2}{3\eta} \left[\frac{1}{E_0^2} - \frac{1}{(E_0 + \Delta_0)^2} \right] \boldsymbol{\sigma} \cdot (\boldsymbol{\varepsilon} \times \boldsymbol{\pi}) \\
 & \quad \left. + \frac{eP^2}{6} \left(\frac{2}{E_0^2} + \frac{1}{(E_0 + \Delta_0)^2} \right) \boldsymbol{\nabla} \cdot \boldsymbol{\varepsilon} \right\} \tilde{\psi}_c \\
 & = \tilde{E} \tilde{\psi}_c
 \end{aligned}$$

$$\lambda \propto \left(\frac{P}{k} \times \nabla V \right)$$

$$\frac{1}{2m^*} = \frac{P^2}{\eta^2 E_0}$$

In semiconductor :

$$\begin{aligned} \lambda &= \frac{P^2}{3} \left[\frac{1}{E_0^2} - \frac{1}{(E_0 + \Delta_0)^2} \right] \\ &= \frac{\eta^2}{3} \frac{P^2}{\eta^2 E_0} \left[\frac{1}{E_0} - \frac{E_0}{(E_0 + \Delta_0)^2} \right] \\ &= \frac{\eta^2}{6m^* E_0} \left[1 - \frac{E_0^2}{(E_0 + \Delta_0)^2} \right] \end{aligned}$$

In vacuum :

$$\lambda_{\text{vac}} = -\frac{\eta^2}{4m_0^2 c^2} = -\frac{\eta^2}{4m_0(m_0 c^2)}$$

The enhancement factor for InAs:

$$\begin{aligned} \left| \frac{\lambda}{\lambda_{\text{vac}}} \right| &\approx \frac{m_0 c^2}{E_0} \times \frac{m_0}{m^*} \times \frac{2}{3} \\ &= \frac{0.5 \text{ MeV}}{0.418 \text{ eV}} \times \frac{1}{0.023} \times \frac{2}{3} = 34.7 \times 10^6 \end{aligned}$$

Compare with the actual values :

$$\left| \frac{\lambda}{\lambda_{\text{vac}}} \right| = \frac{120 \text{ A}^2}{3.73 \times 10^{-6} \text{ A}^2} = 32 \times 10^6$$

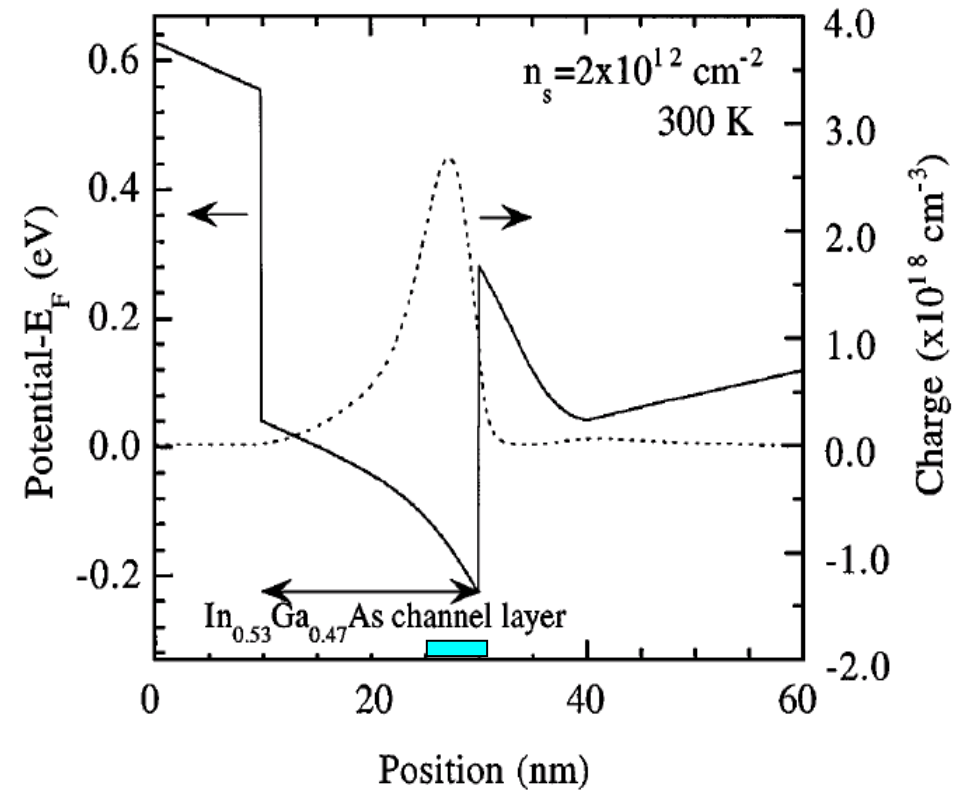


SOI due to Structure Inversion Asymmetry

Rashba SOI

| |
|---|
| ud-In _{0.52} Al _{0.48} As gate Schottky layer (20 nm) |
| ud-In _{0.53} Ga _{0.47} As channel layer (20 nm) |
| ud-In _{0.52} Al _{0.48} As spacer layer (6 nm) |
| n ⁺ -In _{0.52} Al _{0.48} As carrier-supply layer (7 nm , n=4 x 10 ¹⁸ cm ⁻³) |
| ud-In _{0.52} Al _{0.48} As buffer layer |
| S. I.-InP substrate |

Schematic layer structure of an inverted
In_{0.53}Ga_{0.47}As / In_{0.52}Al_{0.48}As
heterostructure.
(Nitta *et al.* Phys. Rev. Lett.**78**, 1355(1997))



Calculated conduction band diagram (solid line) and electron distribution (dash line).
(Nitta *et al.* Physica E, **2**, 527(1998))

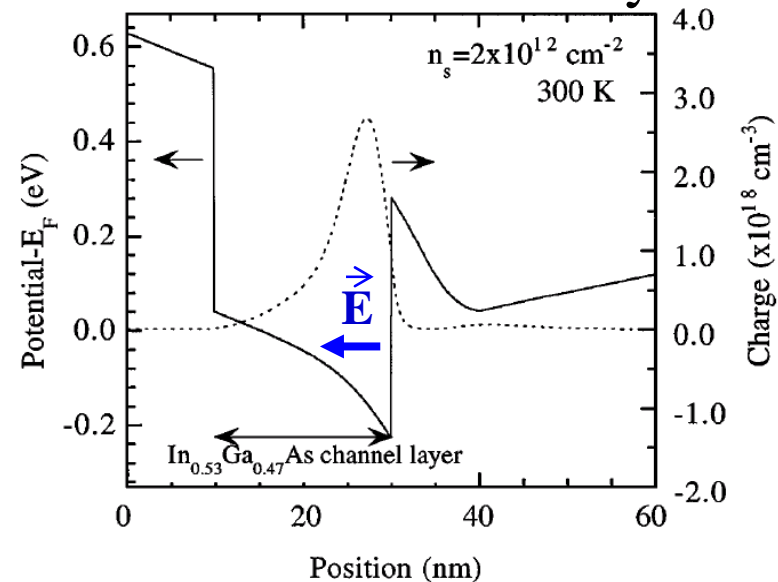


Rashba effect (spin-orbit interaction)

Asymmetric Heterostructure:

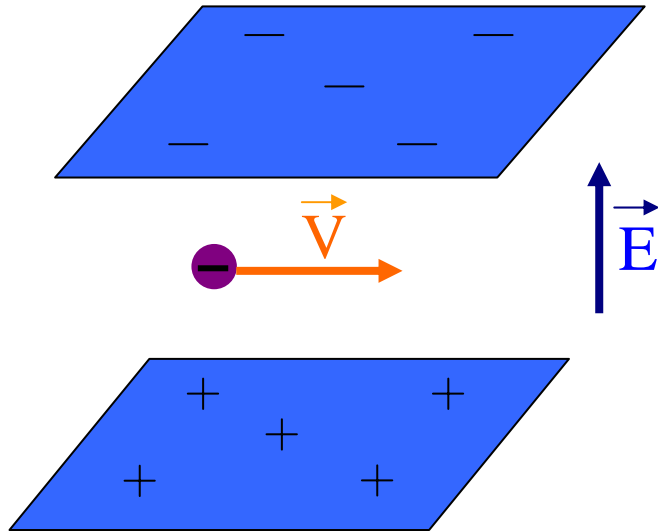


Structure inversion asymmetry:





An electron moves between two charged plane



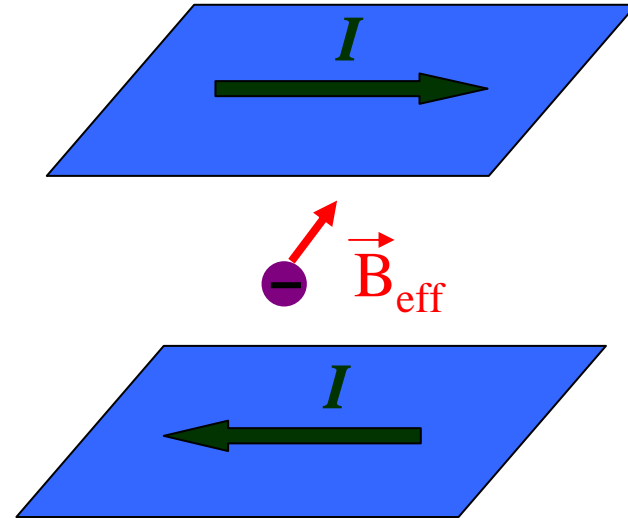
In Lab. frame

The SOI hamiltonian is given by

$$H = -\vec{\mu} \cdot \vec{B}_{eff} \propto \vec{\sigma} \cdot (-\vec{v} \times \vec{E})$$

$$H_{Rashba} \equiv \alpha_0 (\vec{p} \times \hat{z}) \cdot \vec{\sigma}$$

Effective magnetic field induced by the effective current I .



In the rest frame of an electron

where α_0 is called the Rashba constant.



Rashba spin-orbit interaction (SOI)

- SOI is significant in **narrow gap semiconductor heterostructures**.
- Large variation (up to 50%) of the SOI coupling constant α , tuned by metal gates, has been observed experimentally.

[Nitta *et. al.* PRL **78** (1997)

Engels *et. al.* PRB **55** (1997)

Grundler, PRL **84** (2000)]

- Static gate control of α has been the focus of previous proposals on spin polarized transistors.

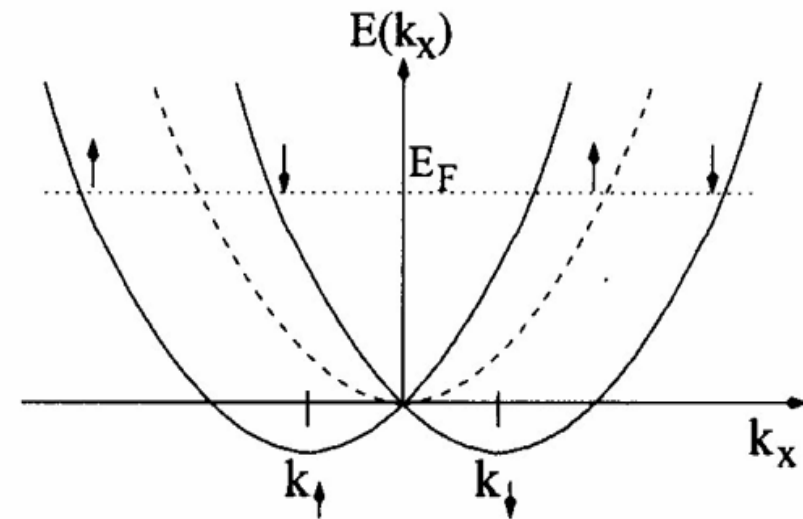
[Datta *et. al.* APL **56** (1990),]

Rashba term:

$$H_{\text{so}} = \alpha \left(\frac{\mathbf{r}}{p} \times \hat{\mathbf{v}} \right) \cdot \hat{\boldsymbol{\sigma}}$$

$\hat{\mathbf{v}}$: normal to interface

$\hat{\boldsymbol{\sigma}}$: the Pauli spin operator



$$E_{2D} = k_x^2 + k_y^2 \pm \alpha_0 \sqrt{k_x^2 + k_y^2}$$

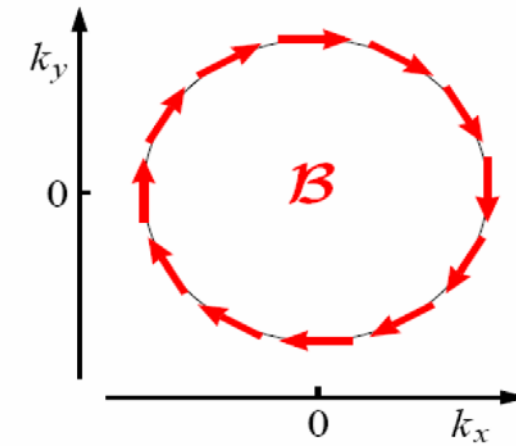
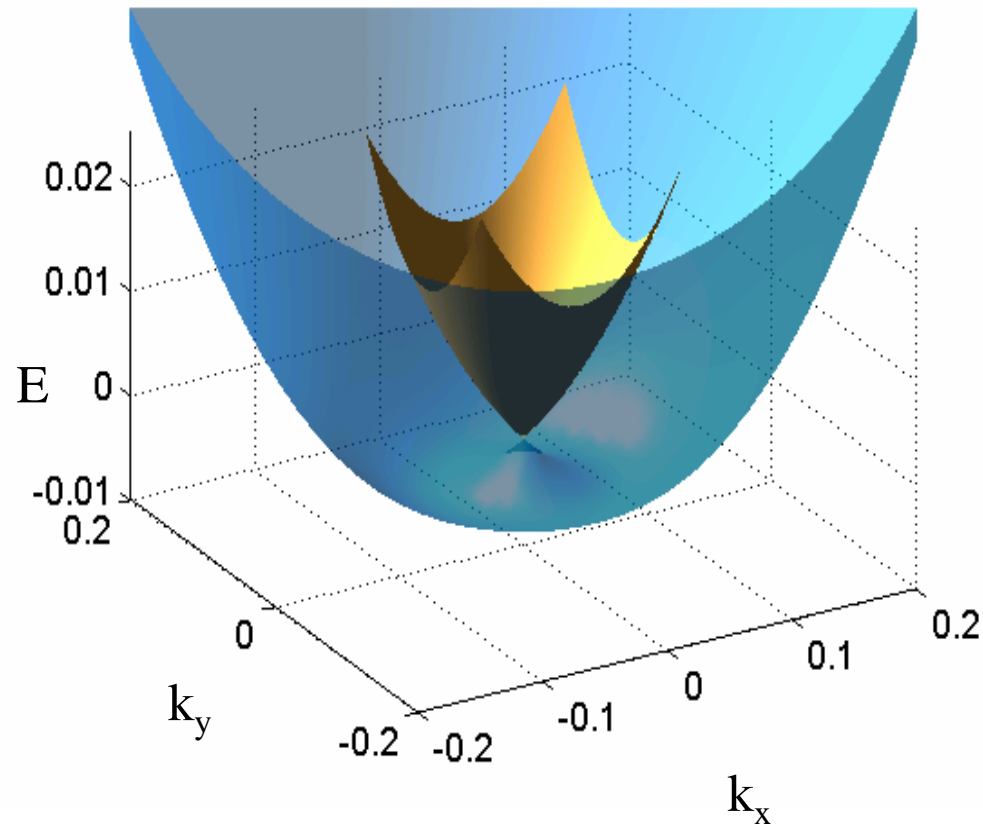
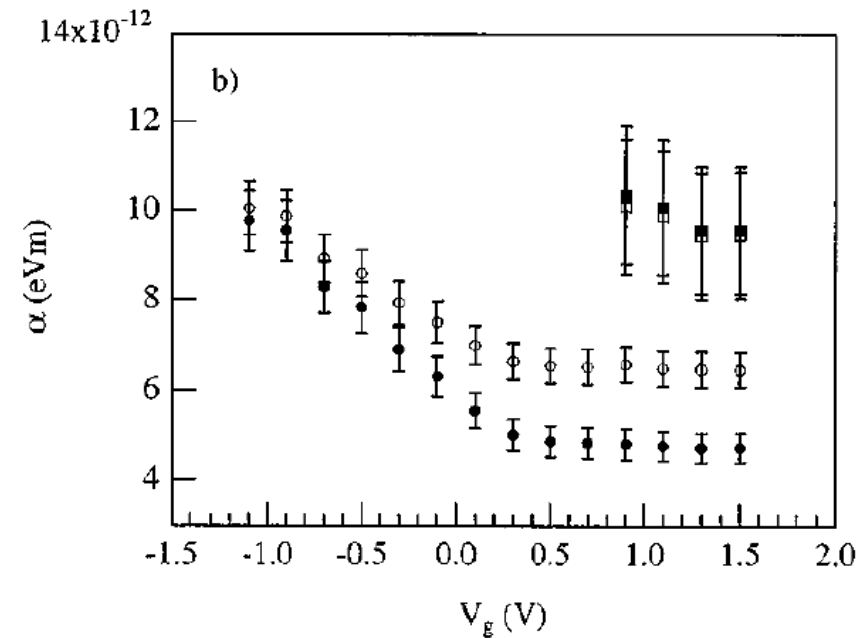
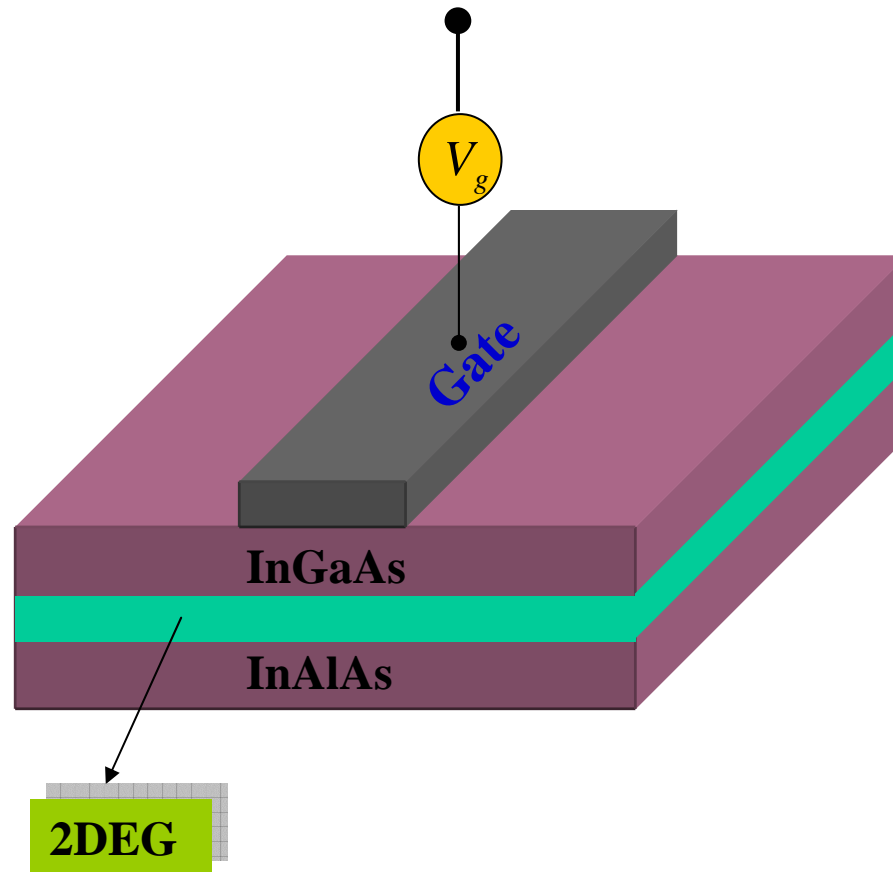


Figure 13: SIA (001) effective field.

Fig.3. Dispersion relation for a 2D Rashba-type system and the Rashba constant $\alpha_0 = 0.13$.



Tuning of the coupling constant α_0 by a metal gate



Spin-orbit coupling parameter α of the first (circle) and second (square) subband as a function of the gate voltage: including (solid) and not including (open) band nonparabolicity correlation.

(Nitta. *et al.* Phys.Rev.B **60**,7736(1999))



SOI due to Bulk Inversion Asymmetry Dresselhaus SOI

Examples: Zincblende structures GaAs, InAs

$$H_{\text{SOI}} = \hbar \mathbf{r}_p \cdot \boldsymbol{\sigma}$$

$$h_k^x = \beta k_x (k_y^2 - \kappa^2);$$

$$h_k^y = -\beta k_y (k_x^2 - \kappa^2)$$

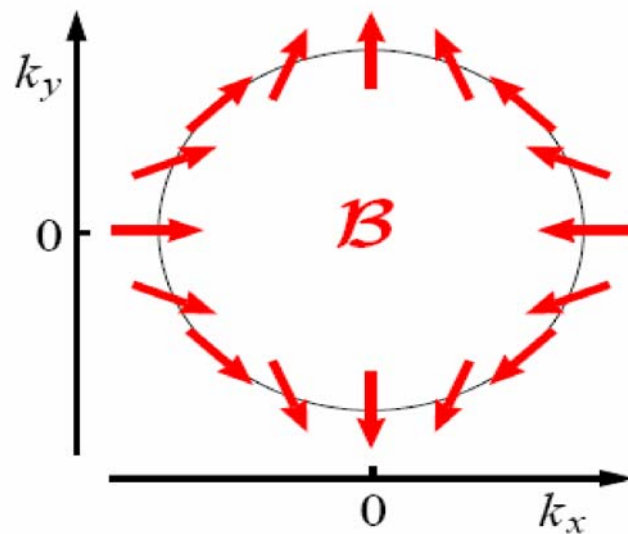


Figure 11: BIA (001) effective field.

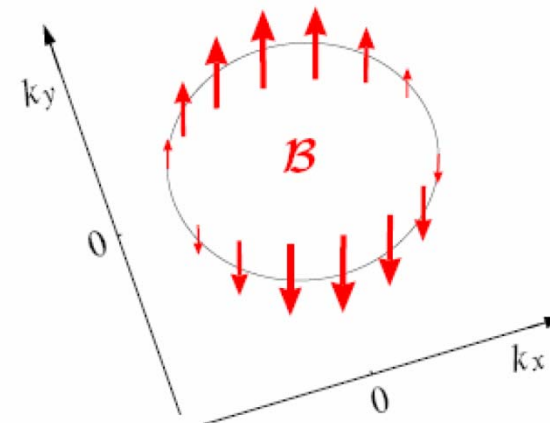


Figure 12: BIA (110) effective field.



Summary: Physical origin of SOI

Extrinsic origin:
SOI impurity

$$\lambda \boldsymbol{\sigma} \cdot (\mathbf{k} \times \nabla V)$$

Intrinsic origin:
Structural effect

$$H_{\text{SOI}} = \hbar \mathbf{r}_p \cdot \boldsymbol{\sigma}$$

Dresselhaus SOI:
Bulk Inversion asymmetry

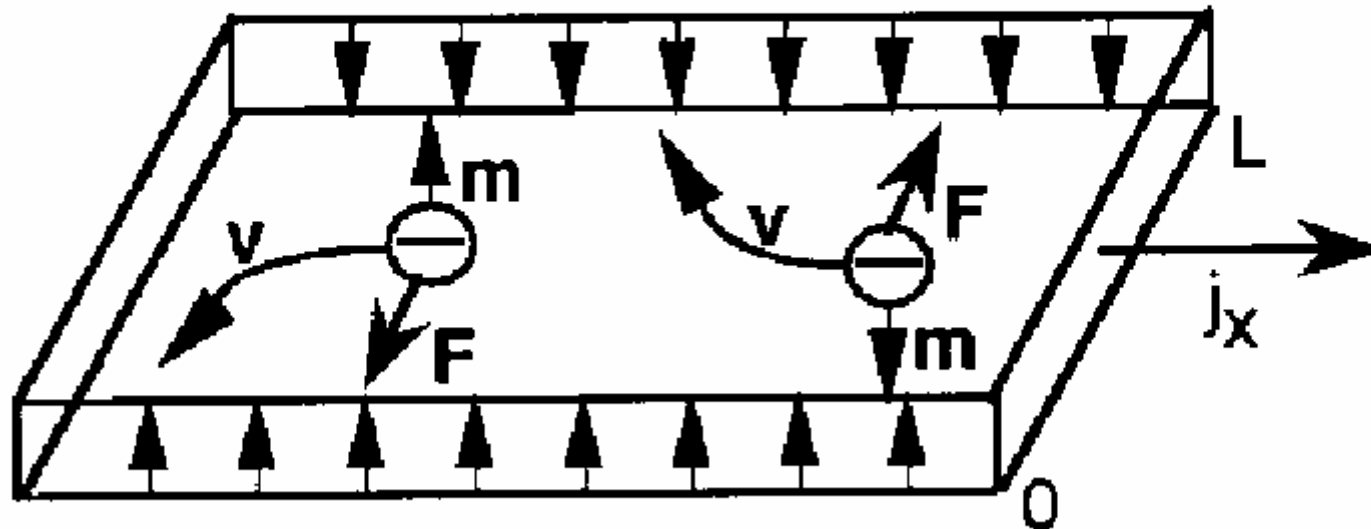
$$\begin{aligned} h_k^x &= \beta k_x (k_y^2 - \kappa^2); \\ h_k^y &= -\beta k_y (k_x^2 - \kappa^2) \end{aligned}$$

Rashba SOI:
Structure inversion asymmetry

$$\hbar \mathbf{r}_k = \alpha (\mathbf{k} \times \hat{z})$$

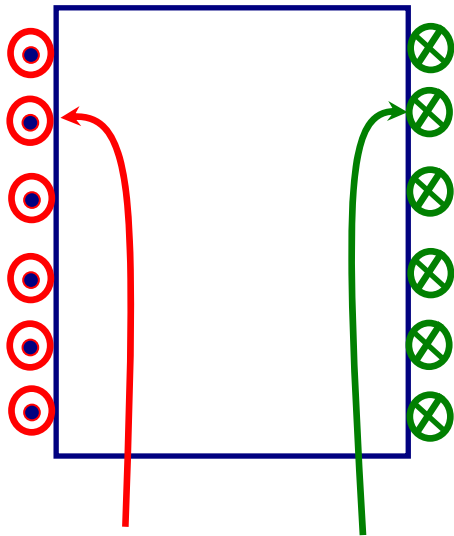
A simple picture for the extrinsic spin Hall effect

Spin Hall effect



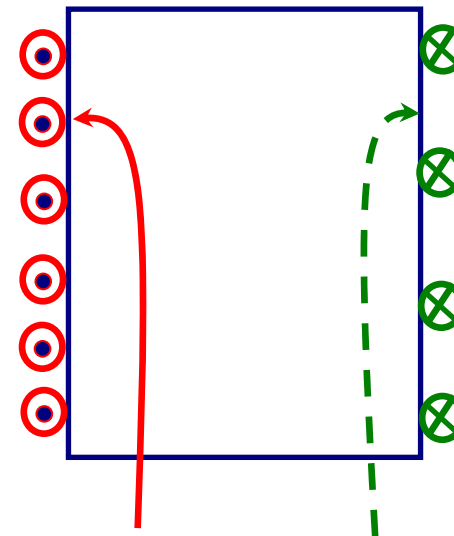
J.E. Hirsch, PRL 83, 1834 (1999)

Spin accumulation & Spin Hall Effect: Spin-dependent deflection of injected carriers produces spin accumulation at lateral edges



**Injection of
unpolarized current:**

**Spin accumulation
without charge
accumulation**



**Injection of partially
polarized current:**

**Spin accumulation is
accompanied by charge
accumulation**

Earliest proposal:

An electrical current passes through a sample with spin-orbit interaction induces a *spin polarization near the lateral edges*, with opposite polarization at opposing edges (M.I. D'yakonov and V.I. Perel', *JEPT Lett.*, 13, 467 (1971)).

This effect does not require an external magnetic field or magnetic order in the equilibrium state before the current is applied.

The M.I. D'yakonov and V.I. Perel' (1971) paper was titled: “*Possibility of orienting electron spins with current*” in which an *extrinsic mechanism* was proposed for the spin Hall effect.

V.M. Edelstein, *Solid State Commun.* 73, 233 (1990)
“Spin polarization of conduction electrons induced
by electric current in two-dimensional asymmetric
electron systems”

S. Murakami, N. Nagaosa, S.C. Zhang,
Science 301, 1348 (2003)

$$\dot{j}_j^i = \sigma_s \epsilon^{ijk} E_k$$

“Dissipationless quantum spin current at room
temperature”

J. Sinova, D. Culcer, Q. Niu, N.A. Sinitsyn, T.
Jungwirth, and A.H. MacDonald,
Physical Review Letters 92, 126603 (2004)

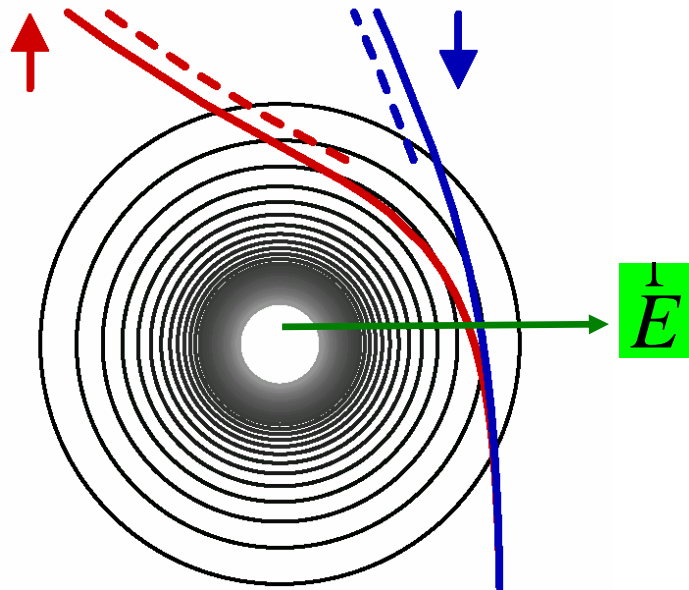
“Universal Intrinsic Spin Hall Effect”

A simple picture for the extrinsic SOI effect

$$H = \frac{p^2}{2m} + V(\vec{r}) + \lambda e \vec{\sigma} \cdot (\vec{p} \times \vec{E})$$

$$m\vec{v} = -\vec{\nabla} V + \lambda m e \frac{d}{dt} (\vec{E} \times \vec{\sigma}) - \lambda e \vec{\nabla} [\vec{\sigma} \cdot (\vec{p} \times \vec{E})]$$

$$m\vec{v} = -\vec{\nabla} V + \lambda m e \vec{\sigma} (\vec{v} \times \hat{z}) [dE/dr + E/r]$$



$e > 0$; $\vec{\sigma}$ along \hat{z} , and linear in λ .

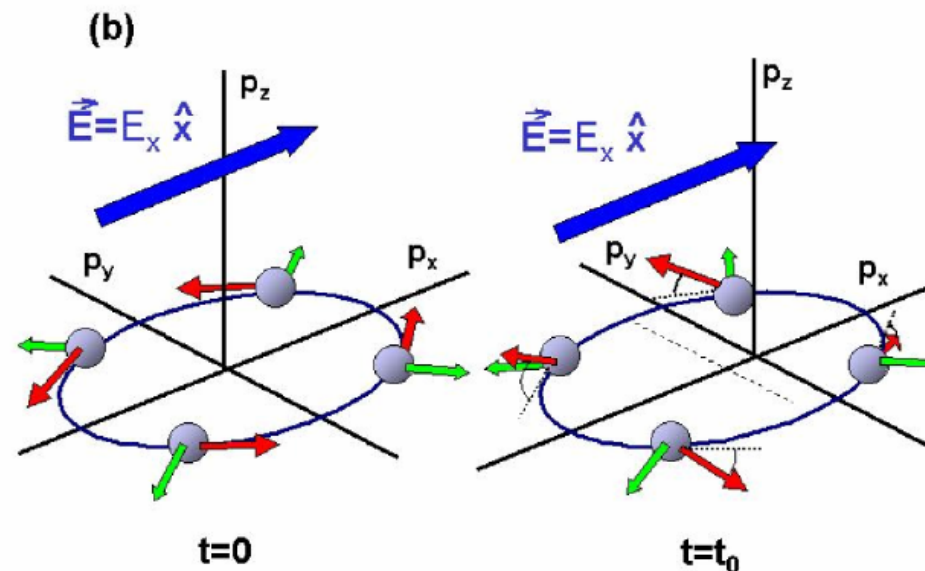
For an attractive scatterer with $E \sim r^{-n}$ ($n > 1$), **spin up electron** is deflected more to the **left** and **spin down electron** is deflected more to the **right**.

In the presence of an electric field the Fermi surface (circle) is displaced an amount $|eE_x t_0 / \hbar|$ at time t_0 (shorter than typical scattering times). While moving in momentum space, electrons experience an effective torque which tilts the spins up for $p_y > 0$ and down for $p_y < 0$, creating a spin current in the y direction.

J. Sinova, *et al* PRL 92, 126603 (2004)

Green arrows:
wavevector

Green arrows:
Effective
magnetic field
direction



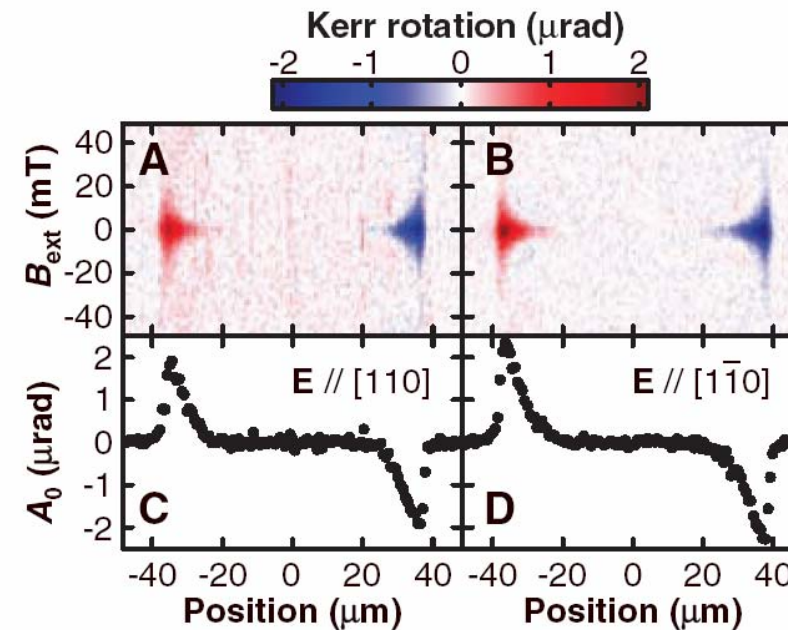
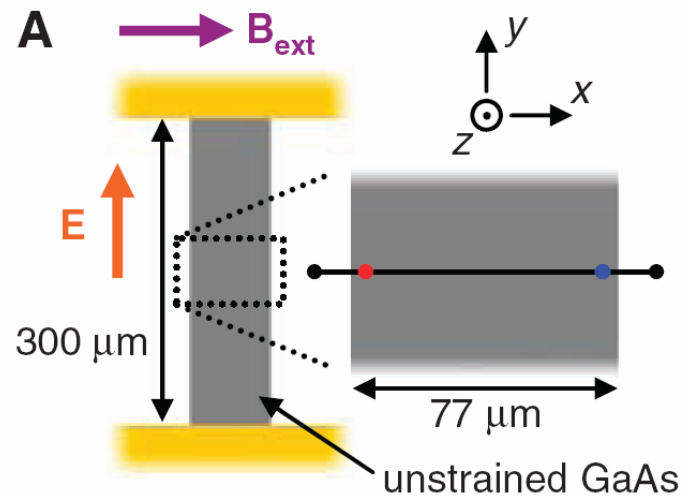
J. Sinova, *et al* PRL 92, 126603 (2004)

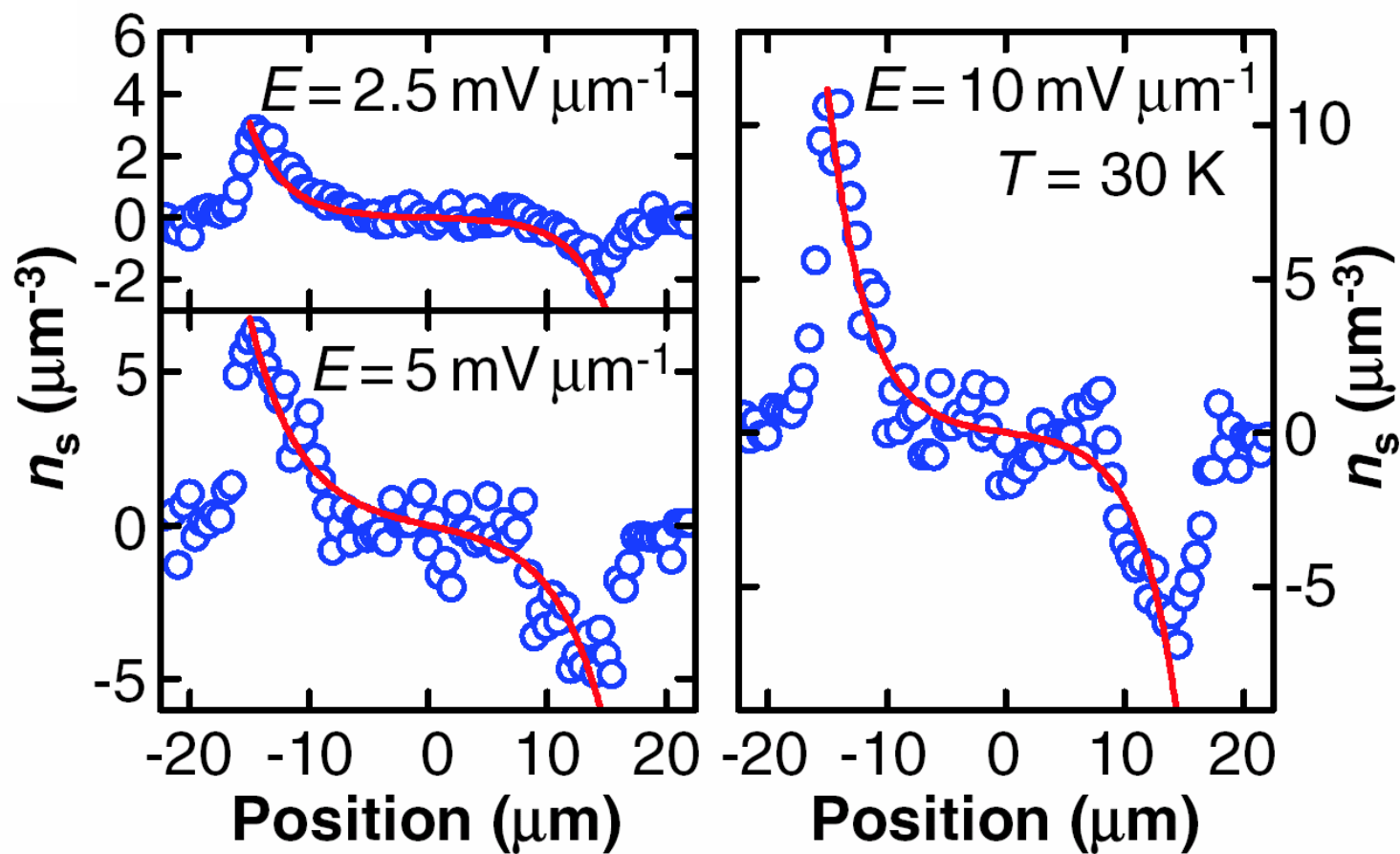
This picture is not correct because it has not taken into account 2 features:

- 1. the effect of background impurities;**
- 2. the form of SOI: linear or non-linear in k ?**

Experimental observation of **extrinsic** spin Hall Effect in thin 3D layers (weak dependence on crystal orientation)

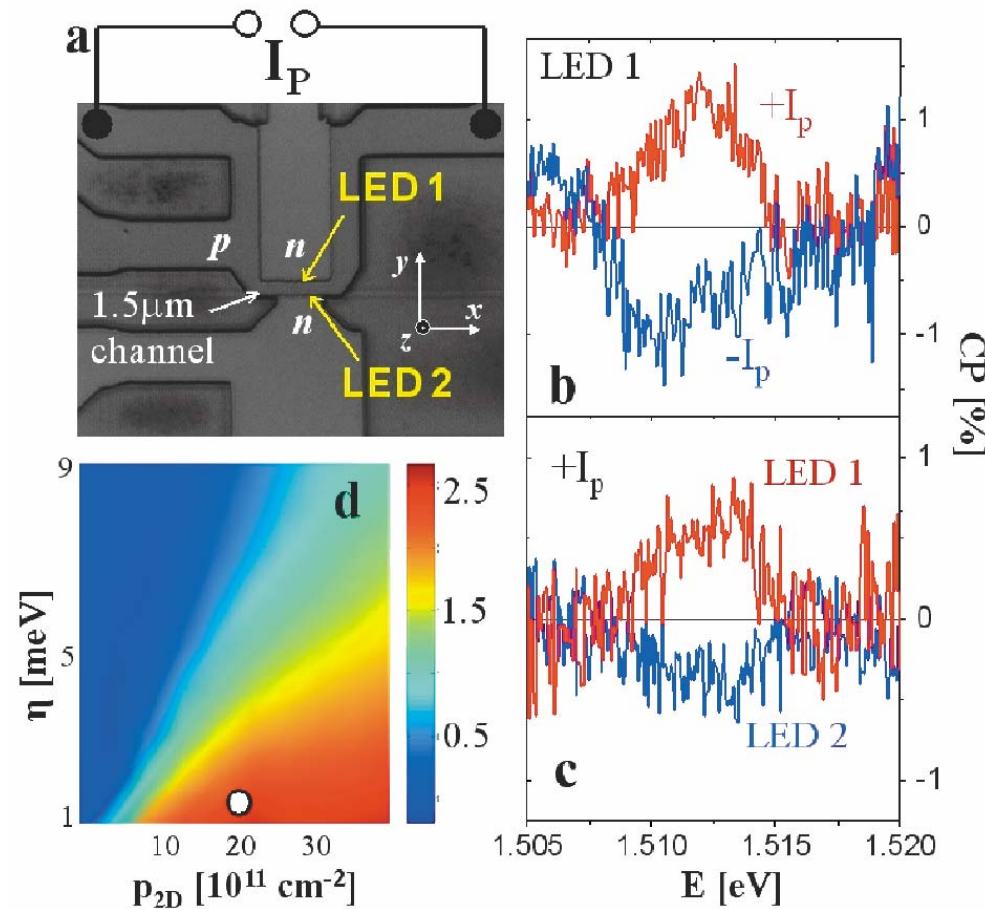
Y.K. Kato, R.C. Myers, A.C. Gossard, D.D. Awschalom, Science 306, 1910 (2004)



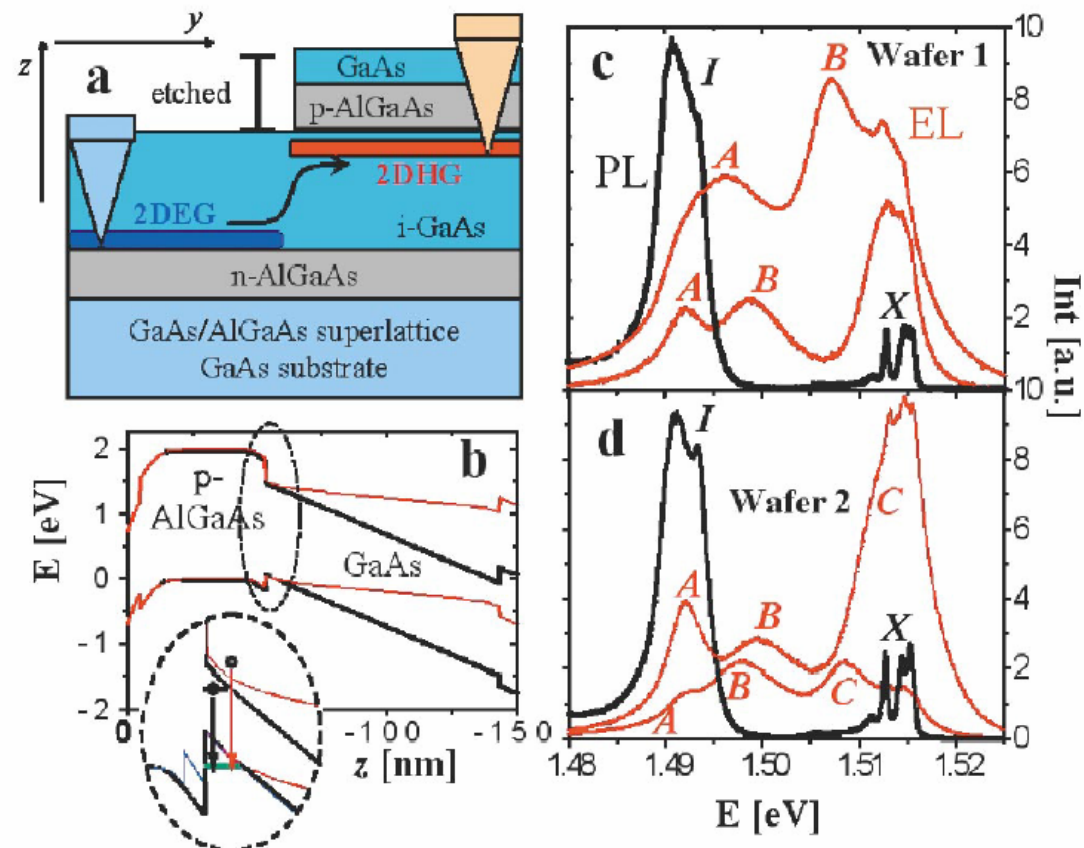


Experimental confirmation of spin Hall Effect in a 2D hole gas (intrinsic SHE)

J. Wunderlich, B. Kaestner, J. Sinova, and T. Jungwirth, Phys. Rev. Lett. 94, 047204 (2005)



J. Wunderlich, B. Kaestner, J. Sinova, and T. Jungwirth, Phys. Rev. Lett. 94, 047204 (2005)



Spin is not conserved:

$$\frac{\partial S_z}{\partial t} + \nabla \cdot \mathbf{J}_s = \mathcal{T}_z.$$

Torque density

**and definition of spin current remains an issue
(Shi J, Zhang P, Xiao D, and Nui Q, Phys. Rev.
Lett. 96 76604(2006)).**

$$\mathcal{T} \equiv \frac{d\hat{s}_z}{dt} \equiv (1/i\hbar) [\hat{s}_z, \hat{H}]$$

**Experiments measure spin accumulation, not
spin current.**

**Spin accumulation, not spin current, is the key
physical quantity of our interest.**

Derivation of a spin diffusion equation

$$H_{\text{SOI}} = \vec{h}_p^r \cdot \vec{\sigma}$$

Dresselhaus SOI:

$$h_k^x = \beta k_x (k_y^2 - \kappa^2);$$
$$h_k^y = -\beta k_y (k_x^2 - \kappa^2)$$

Dresselhaus SOI contains
cubic term in k

Rashba SOI:

$$\vec{h}_k^r = \alpha (\vec{k} \times \hat{z})$$

H' :
Perturbing
Hamiltonian

$$H' = V(\mathbf{r}, t) + \mathbf{B}(\mathbf{r}, t) \cdot \boldsymbol{\sigma} = \sum_i \Phi_i(\mathbf{r}, t) \tau^i$$

where $\tau^0 = 1$, and $\tau^i = \sigma^i$ for $i = x, y, z$.

Four vector density $D_i(\mathbf{r}, t)$:

$$D_0(\mathbf{r}, t) = n(\mathbf{r}, t)$$

$$D_i(\mathbf{r}, t) = 2 S_i(\mathbf{r}, t)$$

$$D_i(\mathbf{r}, t) = -i \text{Tr} \left[\tau^i \mathcal{G}^{\sigma+}(\mathbf{r}, \mathbf{r}, t, t) \right]$$

Linear response:

$$\mathcal{G}_{\nu\mu}^{\sigma+}(\mathbf{r}, \mathbf{r}, t, t) = -i \left\langle T_l \left[\hat{\Psi}_{\nu}(\mathbf{r}, t_-) \hat{\Psi}_{\mu}^{\dagger}(\mathbf{r}, t_+) (-i) \int_{loop} H'(\tau) d\tau \right] \right\rangle$$

< > denotes averaging over impurity configuration

$$G_{\nu\mu}^{\sigma+}(\mathbf{r}, \mathbf{r}, \omega)$$

$$= \sum_{\eta=\pm} (-\eta) \tau_{\alpha\beta}^j \int d^2 r'' \int \frac{d\omega'}{2\pi} \Phi_j(\mathbf{r}'', \omega) \langle G_{\nu\alpha}^{-\eta}(\mathbf{r}, \mathbf{r}'', \omega + \omega') G_{\beta\mu}^{+\eta}(\mathbf{r}'', \mathbf{r}, \omega') \rangle$$

$$G^{-+}(\mathbf{r}, \mathbf{r}', \omega) = -n_F(\omega) [G^r(\mathbf{r}, \mathbf{r}', \omega) - G^a(\mathbf{r}, \mathbf{r}', \omega)]$$

$$G^{--} = G^r + G^{-+}$$

$$G^{++} = G^{-+} - G^a$$

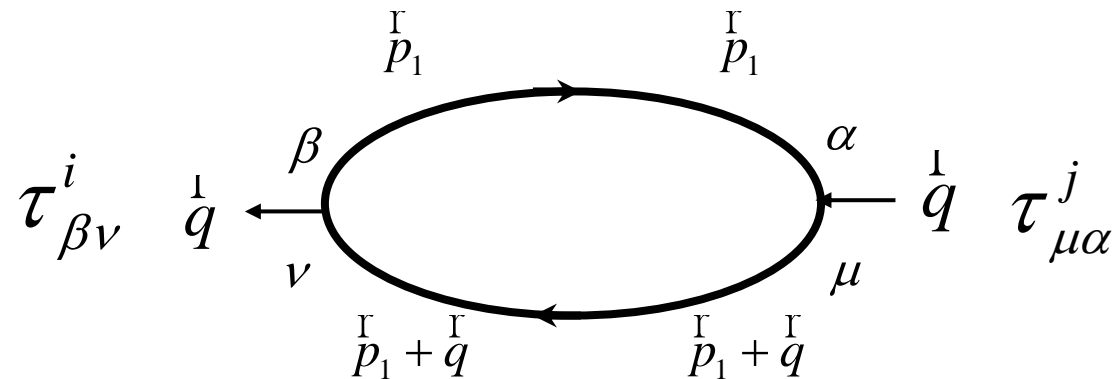
$$G^r(\mathbf{k}, \omega) = \frac{\omega - \varepsilon_k + i\Gamma + \mathbf{h}_k \cdot \boldsymbol{\sigma}}{(\omega - \varepsilon_k + i\Gamma)^2 - h_k^2}$$

$$G^a(\mathbf{k}, \omega) = \frac{\omega - \varepsilon_k - i\Gamma + \mathbf{h}_k \cdot \boldsymbol{\sigma}}{(\omega - \varepsilon_k - i\Gamma)^2 - h_k^2}$$

$$D_i(\mathbf{r}, t) = -i \text{Tr} \left[\tau^i \mathcal{G}^{\sigma+}(\mathbf{r}, \mathbf{r}, t, t) \right]$$

$$D_i(\mathbf{r}, \omega) = \int d^2 r' \sum_j \Pi_{ij}(\mathbf{r}, \mathbf{r}', \omega) \Phi_j(\mathbf{r}', \omega) + D_i^0(\mathbf{r}, \omega)$$

$$\begin{aligned} & \Pi_{ij}(\mathbf{r}, \mathbf{r}', \omega) \\ &= i\omega \int \frac{d\omega'}{2\pi} \frac{dn_F}{d\omega'} \left\langle \text{Tr} \left[G^a(\mathbf{r}', \mathbf{r}, \omega') \tau^i G^r(\mathbf{r}, \mathbf{r}', \omega + \omega') \tau^j \right] \right\rangle \end{aligned}$$



$$D_i^0(\vec{q}, \omega) = -2N_0(E_F)\Phi_i(\vec{q}, \omega)$$

$N_0(E_F)$ is the density of states per spin states at the Fermi energy

$$D_i(\vec{r}, \omega) - D_i^0(\vec{r}, \omega) = \int d^2 r' \sum_j \Pi_{ij}(\vec{r}, \vec{r}', \omega) \Phi_j(\vec{r}', \omega)$$

Fourier transform of $\int d^2 r' \Pi_{ij}(\vec{r}, \vec{r}', \omega) \Phi_j(\vec{r}', \omega)$

$$\frac{i\omega}{2\pi} \int d\omega' \frac{dn_F}{d\omega'} \tau_{\mu\alpha}^i \tau_{\beta\nu}^j \sum_{\vec{p}} \sum_{\vec{p}'} \langle G_{\alpha\beta}^r(\vec{p}, \vec{p}' + \vec{q}, \omega + \omega') G_{\nu\mu}^a(\vec{p}', \vec{p} - \vec{q}, \omega') \rangle \Phi_j(\vec{q}, \omega)$$

$$\begin{aligned}
 & \left\langle G_{\alpha\beta}^r(\vec{p}, \vec{p}', \omega + \omega') G_{\nu\mu}^a(\vec{p}' + \vec{q}, \vec{p} + \vec{q}, \omega') \right\rangle_{im.} \\
 &= G_{\alpha\beta}^r(\vec{p}, \omega + \omega') G_{\nu\mu}^a(\vec{p} - \vec{q}, \omega') \delta_{\vec{p}\vec{p}'} \\
 &+ G_{\gamma\beta}^r(\vec{p}', \omega + \omega') G_{\nu\lambda}^a(\vec{p}' - \vec{q}, \omega') \mathbf{K}_{\lambda\lambda'}^{\gamma\gamma'} G_{\alpha\gamma'}^r(\vec{p}, \omega + \omega') G_{\lambda',\mu}^a(\vec{p} - \vec{q}, \omega')
 \end{aligned}$$

$$\Psi_{\nu\lambda}^{\beta\gamma}(\omega, \omega', \vec{q}) = \begin{array}{c} \beta \xrightarrow{\vec{p}} \gamma \\ \nu \xleftarrow{\vec{p} + \vec{q}} \lambda \end{array} = \frac{c_i}{V} |V_s|^2 \sum_{\vec{p}} G_{\gamma\beta}^r(\vec{p}, \omega + \omega') G_{\nu\lambda}^a(\vec{p} - \vec{q}, \omega')$$

$$K(\omega, \omega', \vec{q}) = \frac{c_i}{V} |V_s|^2 [1 - \Psi(\omega, \omega', \vec{q})]^{-1}$$

$$\Psi^{is}(\omega, \omega', \vec{q}) = \frac{1}{2} \frac{c_i}{V} |V_s|^2 \sum_{\vec{p}} \text{Tr} \left[\tau^i G^a(\vec{p} - \vec{q}, \omega') \tau^s G^r(\vec{p}, \omega + \omega') \right]$$

To get some feeling, let's consider the case $\hbar \rightarrow 0$:

$$\Psi^{is}(\omega, \omega', \vec{q}) \Big|_{\hbar=0} = \delta^{is} \left[1 + i\omega\tau - Dq^2\tau \right]$$

$$\tau = \frac{1}{2\Gamma}$$

$$\Gamma = \pi c_i |V_s|^2 N_0(E_F)$$

$$D = v_F^2 \tau / 2$$

Dirty limit : $\hbar_p \ll \Gamma$

$$\omega \ll \Gamma, \quad v_F \cdot \vec{q} \ll \Gamma,$$

$$\Gamma \ll E_F$$

$$\Psi^{is}(\omega, \omega', \vec{q}) \Big|_{\text{linear in } \hbar \text{ and } \omega=0} = \frac{-i\varepsilon^{ism}}{\Gamma^2} \overline{(\vec{q} \cdot \vec{v}_F)} h_{p_F}^m$$

Precession of the inhomogeneous spin polarization about the effective SOI field.

$$\Psi^{is}(\omega, \omega', \vec{q}) \Big|_{\hbar=0} = \delta^{is} [1 + i\omega\tau - Dq^2\tau]$$

Angular average

$$\Psi^{ij}(\omega, \omega', \vec{q}) \Big|_{\substack{q=0, \omega=0 \\ \hbar^2 \text{ term}}} = -4\tau^2 \overline{h_{p_F}^2} (\delta^{ij} - n_k^i n_k^j)$$

D'akonov-Perel spin relaxation

$$\Psi^{l0}(\omega, \omega', \vec{q}) = \frac{\tau}{\Gamma^2} \overline{h_{p_F}^3} \frac{\partial n_{p_F}^l}{\partial p} \cdot (i\vec{q}) = \Psi^{l0}(\omega, \omega', \vec{q})$$

$$\hat{n}_k^p = \hbar_k^p / h_k^p$$

Charge-spin coupling

$$D_i(\mathbf{r}, \omega) - D_i^0(\mathbf{r}, \omega) = \int d^2 r' \sum_j \Pi_{ij}(\mathbf{r}, \mathbf{r}', \omega) \Phi_j(\mathbf{r}', \omega)$$

$$D^{ij} (D - D^0)_j = -i\omega D_i$$

$$D^{ij} = \delta^{ij} D \nabla^2 + \underbrace{4\tau \varepsilon^{ijm} \overline{h_{p_F}^m v_F^m}}_{R^{ijm} \nabla_m} - \underbrace{4\tau h_{p_F}^2 (\delta^{ij} - n_p^i n_p^j)}_{\Gamma^{ij}} + \underbrace{\frac{h_{p_F}^3}{\Gamma^2} \frac{\partial n_{p_F}^i}{\partial p} \cdot \nabla}_{M^{i0}}$$

D is the diffusion constant

Spin densities Diffusion equation for Rashba-type semiconductor strip

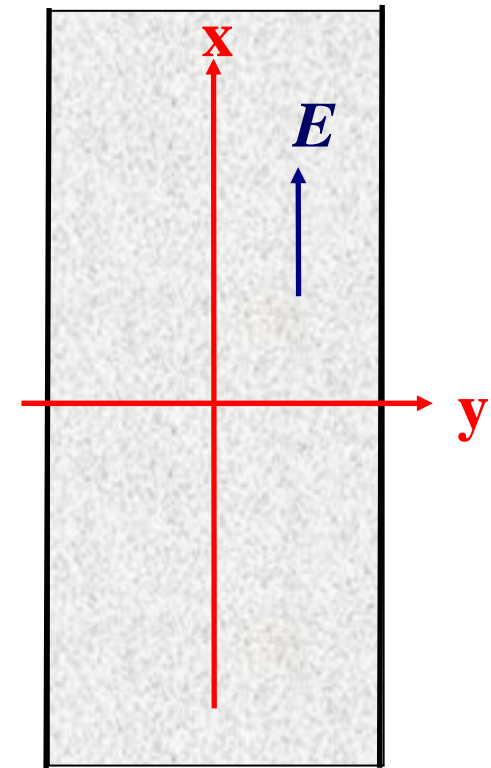
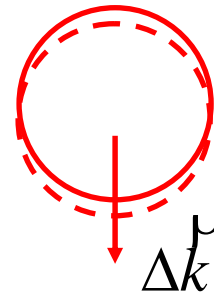
$$D \frac{\partial^2 S^z}{\partial y^2} - \Gamma^{zz} S^z = -R^{zyy} \frac{\partial S^y}{\partial y}$$

$$D \frac{\partial^2 S^y}{\partial y^2} - \Gamma^{yy} S^y = -R^{yzy} \frac{\partial S^z}{\partial y} + \frac{M_x^{y0}}{2} \frac{\partial D_0^0}{\partial x}$$

$$D \frac{\partial^2 S^x}{\partial y^2} - \Gamma^{xx} S^x = 0$$

Bulk spin density : $S^x = S^z = 0$

$$S_b^y = - \left(M_x^{y0} / 2\Gamma^{yy} \right) \frac{\partial D_0^0}{\partial x} = -N_0 e E \alpha \tau$$



V.M. Edelstein
Solid State Comm. 1990
J.I. Inoue *et al*, PRB 2003

Relating the spin flux to the spin densities

$$I_i^y(\vec{r}) = -D \frac{\partial S^i}{\partial y} - \frac{1}{2} R^{ijy} (S^j - S_b^j) + \delta_{iz} I_{SH}$$

$$I_{SH} = -\frac{1}{2} R^{zjy} S_b^j + eE \frac{N_0}{2\Gamma^2} v_F^y \overline{\left(\frac{\partial \vec{h}_k}{\partial k_x} \times \vec{h}_k \right)_z}$$

Boundary condition :

$$I_i^y(\pm d/2) = 0$$

More recent work on the boundary conditions for the spin diffusion equation:

***G. Bleibaum, Phys. Rev. B 74, 113309 (2006)**

“Boundary conditions for spin-diffusion equations with Rashba spin-orbit interaction”

**V.M. Galitski, A.A. Burkov, and S. Das Sarma,
Phys. Rev. B 74, 115331 (2006)**

“Boundary conditions for spin diffusion in disordered systems”

***Y. Tserkovnyak, B.I. Halperin, A.A. Kovalev, A. Brataas,
New Journal of Physics 9, 345 (2007)**

“Boundary spin Hall effect in a two-dimensional semiconductor system with Rashba spin-orbit coupling”

*** Work that agrees with our result for hard wall boundary.**

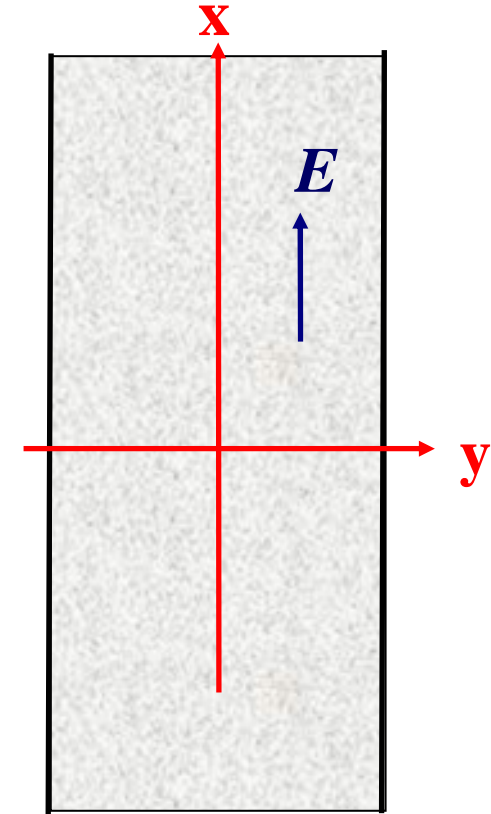
$$D \frac{\partial^2 S^z}{\partial y^2} - \Gamma^{zz} S^z = -R^{zyy} \frac{\partial S^y}{\partial y}$$

$$D \frac{\partial^2 S^y}{\partial y^2} - \Gamma^{yy} S^y = -R^{yzy} \frac{\partial S^z}{\partial y} + \frac{M_x^{y0}}{2} \frac{\partial D_0^0}{\partial x}$$

$$D \frac{\partial^2 S^x}{\partial y^2} - \Gamma^{xx} S^x = 0$$

Bulk spin density : $S^x = S^z = 0$

$$S_b^y = - \left(M_x^{y0} / 2\Gamma^{yy} \right) \frac{\partial D_0^0}{\partial x} = -N_0 e E \alpha \tau$$



NO Spin Accumulation at edges for Rashba-type strip.

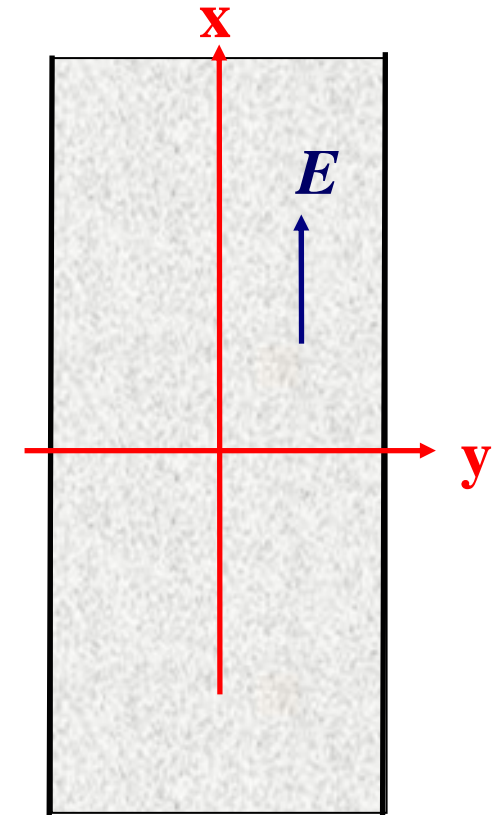
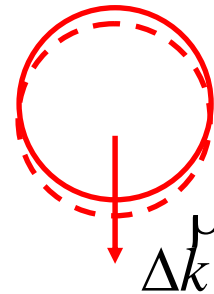
$$D \frac{\partial^2 S^z}{\partial y^2} - \Gamma^{zz} S^z = -R^{zxy} \frac{\partial S^x}{\partial y}$$

$$D \frac{\partial^2 S^x}{\partial y^2} - \Gamma^{xx} S^x = -R^{xzy} \frac{\partial S^z}{\partial y} + M_x^{x0} \frac{\partial D_0^0}{\partial x}$$

$$D \frac{\partial^2 S^y}{\partial y^2} - \Gamma^{yy} S^y = 0$$

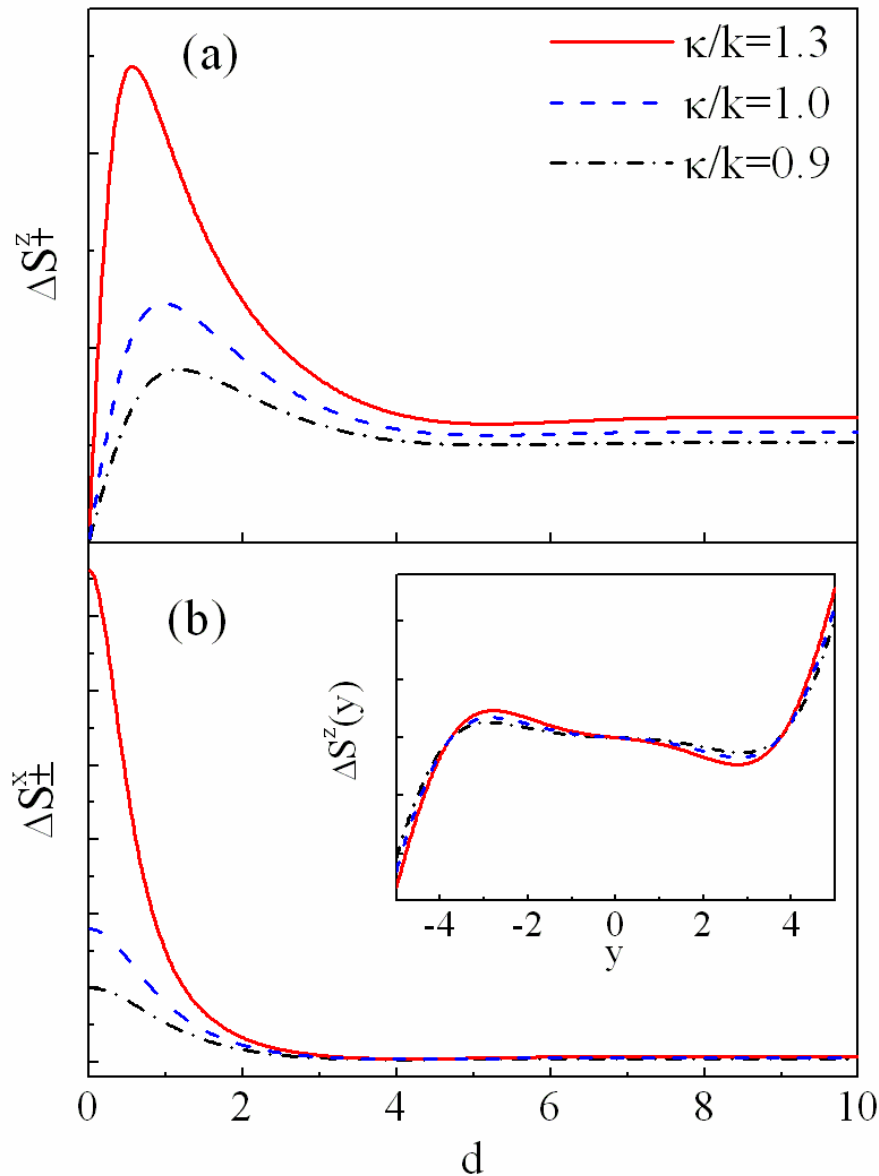
Bulk spin density : $S^y = S^z = 0$

$$S_b^x = - \left(M_x^{x0} / 2\Gamma^{xx} \right) \frac{\partial D_0^0}{\partial x}$$



$$h_k^x = \beta k_x (k_y^2 - \kappa^2);$$

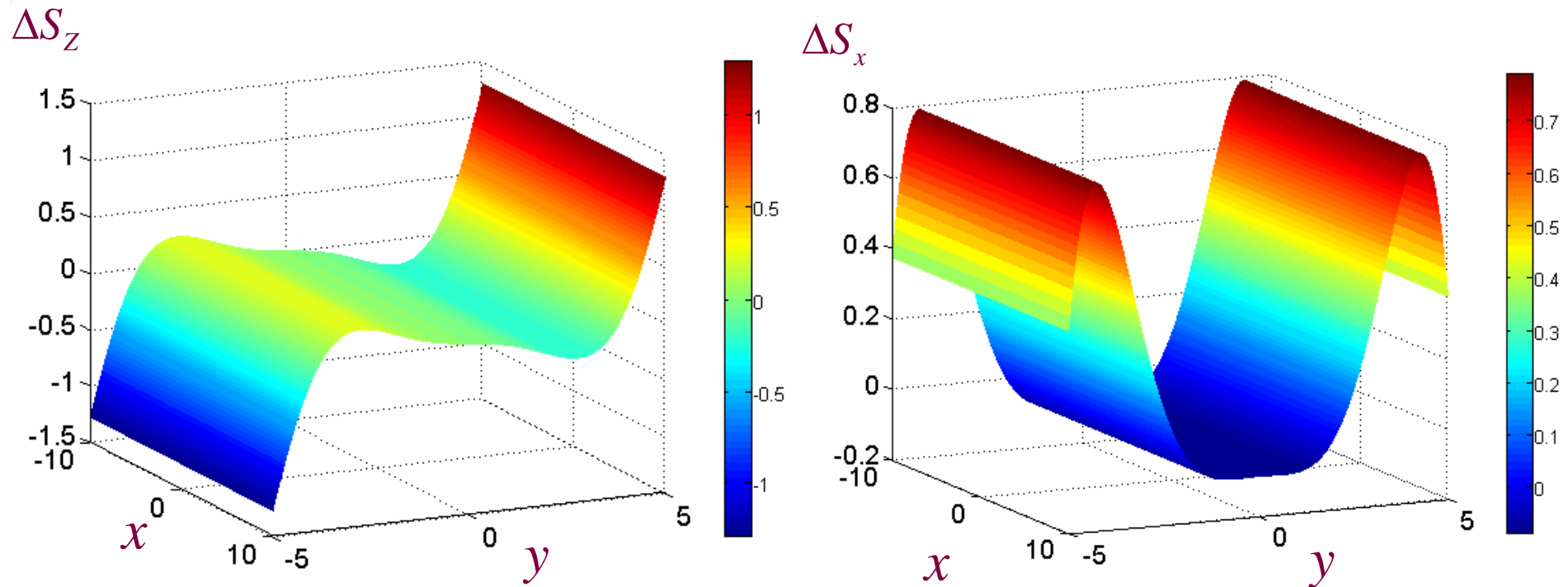
$$h_k^y = -\beta k_y (k_x^2 - \kappa^2)$$



Spin densities
for $i = x, z$ as a functions of its width
 d .

The inset shows the dependence of
 $\Delta S_z(y)$ on the transverse coordinate
 y . Lengths are measured in unit of

Phys.Rev.Lett. **95**, 146601(2005)
Mal'shukov, Wang, Chu, Chao



Spin densities of ΔS_z are of odd parity in a 2D strip with $\kappa/k=1.3$ for the strip width $d = 10$.

Spin accumulation in a Dresselhaus-type 2DEG has a comparable magnitude ($\sim 17 \mu\text{m}^{-2}$ for GaAs)

At the time the semiconductor spintronic community gradually realized that disorder due to normal impurities removes completely the Rashba SOI Spin Hall Effect.

SHE in Rashba-type spin-orbit systems vanishes in the presence of weak disorder

J.I. Inoue, *et al*, Phys. Rev. B 70, 041303 (2004)

E.I. Rashba, Phys. Rev. B 70, 201309 (2004)

O. Chalaev *et al*, Phys. Rev. B 71, 245318 (2005)

E.G. Mishchenko, *et al*, Phys. Rev. Lett. 93, 226602 (2004)

A.A. Burkov, *et al*, Phys. Rev. B 70, 155308 (2004)

O.V. Dimitrova, Phys. Rev. B 71, 245327 (2005)

R. Raimondi *et al*, Phys. Rev. B 71, 033311 (2005)

A.G. Mal'shukov *et al*, Phys. Rev. B 71, 121308(R) (2005)

B.A. Bernevig and S.C. Zhang, Phys. Rev. Lett. 95, 016801 (2005)

Cubic dependence on k is crucial.

PRL 95, 166605 (2005)

PHYSICAL REVIEW LETTERS

week ending
14 OCTOBER 2005

Theory of Spin Hall Conductivity in n -Doped GaAs

Hans-Andreas Engel, Bertrand I. Halperin, and Emmanuel I. Rashba

Department of Physics, Harvard University, Cambridge, Massachusetts 02138, USA

(Received 21 May 2005; published 13 October 2005)

We develop a theory of extrinsic spin currents in semiconductors, resulting from spin-orbit coupling at charged scatterers, which leads to skew-scattering and side-jump contributions to the spin-Hall conductivity. Applying the theory to bulk n -GaAs, without any free parameters, we find spin currents that are in reasonable agreement with experiments by Kato *et al.* [Science **306**, 1910 (2004)].

DOI: [10.1103/PhysRevLett.95.166605](https://doi.org/10.1103/PhysRevLett.95.166605)

PACS numbers: 72.25.Dc, 71.70.Ej



What should be the distribution of electrons in the momentum space if there is spin-orbit scatterers in the system (extrinsic SOI) ?

Physical Review Letters 95, 166605 (2005)

We start by refreshing our understanding on the normal Boltzmann equation.

$$-\frac{eE}{\eta} \cdot \frac{\partial f(k)}{\partial k} = - \sum_{k'} \frac{2\pi}{\eta} |W_{kk'}|^2 \delta(\varepsilon_k - \varepsilon_{k'}) \frac{1}{V^2} [f(k) - f(k')]$$

Connection to differential cross - section :

$$\frac{1}{V} \frac{\eta k}{m^*} \frac{d\sigma}{d\Omega} d\Omega_{\hat{k}'} = \int \frac{2\pi}{\eta} |W_{kk'}|^2 \delta(\varepsilon_k - \varepsilon_{k'}) \frac{1}{V^2} d\Omega_{\hat{k}'} k'^2 dk' \frac{V}{(2\pi)^3}$$

$$\frac{d\sigma}{d\Omega} = \frac{m^{*2}}{4\pi^2 \eta^4} |W_{kk'}|^2$$

RHS of the Boltzmann equation : the scattering rate

$$\begin{aligned}
 & - \sum_{\vec{k}} \frac{2\pi}{\eta} \frac{4\pi^2 \eta^4}{m^{*2}} \frac{d\sigma}{d\Omega} \delta(\varepsilon_{\vec{k}}^{\rho} - \varepsilon_{\vec{k}'}^{\rho}) \frac{1}{V^2} [f(\vec{k}^{\rho}) - f(\vec{k}'^{\rho})] \\
 & = - \frac{\eta}{m^*} \frac{1}{V} \int d\Omega_{\hat{k}'} \int d\Omega_{\hat{k}} \frac{d\sigma}{d\Omega} [f(\vec{k}^{\rho}) - f(\vec{k}'^{\rho})]
 \end{aligned}$$

For a total of N_i impurities, the total scattering rate is

$$- \frac{eE}{\eta} \cdot \frac{\partial f(\vec{k}^{\rho})}{\partial k} = -n_i \int d\Omega_{\hat{k}'} \frac{\eta k'}{m^*} \frac{d\sigma}{d\Omega} [f(\vec{k}^{\rho}) - f(\vec{k}'^{\rho})]$$

$$\begin{aligned}
 & - \frac{eE}{\eta} \cdot \frac{\partial f(\vec{k}^{\rho})}{\partial k} = - \frac{\delta f(\vec{k}^{\rho})}{\tau} \\
 \Rightarrow & \delta f(\vec{k}^{\rho}) = \frac{\tau e \eta}{m^*} E \cdot \vec{k}^{\rho} \frac{df_0}{d\varepsilon_k}
 \end{aligned}$$

$$f(\vec{k}^{\rho}) = f_0(\vec{k}^{\rho}) + \delta f(\vec{k}^{\rho})$$

For isotropic scatterers, we have $\int d\Omega_{\vec{k}'} \delta f(\vec{k}'^{\rho}) = 0$

When the impurities are spin-orbit scatterers, the distribution $f(\mathbf{k})$ will become a matrix, a 2X2 matrix.

$$\hat{f}(\mathbf{k}) = f_0(\mathbf{k}) 1_{2 \times 2} + \left(\phi(\mathbf{k}) 1_{2 \times 2} + \mathbf{f}(\mathbf{k}) \cdot \boldsymbol{\sigma} \right)$$

We may expect the scattering rate to become a scattering rate matrix.

$$-\frac{eE}{\eta} \cdot \frac{\partial \hat{f}(\mathbf{k})}{\partial k} = -n_i \int d\Omega_{\hat{\mathbf{k}}'} \frac{\eta k'}{m^*} \frac{d\sigma}{d\Omega} \left[\hat{f}(\mathbf{k}) - \hat{f}(\mathbf{k}') \right]$$

How do we come up with an appropriate definition of the scattering rate matrix ?

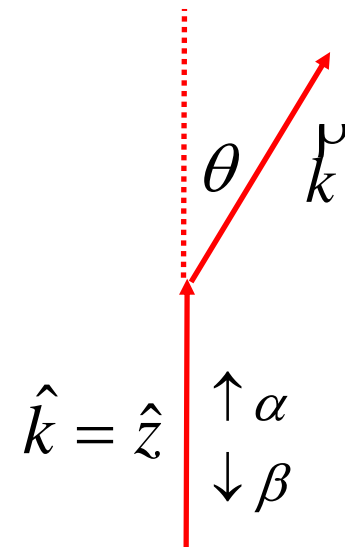
Before we go on to find the scattering rate matrix expression, it is beneficial for us to look at the physical meaning of the scattering from a spin-orbit scatterer.

$$\begin{aligned}
 & \lambda \boldsymbol{\sigma} \cdot (\mathbf{k} \times \nabla V) \\
 & \rightarrow \lambda \boldsymbol{\sigma} \cdot \left[\frac{1}{2} (\mathbf{k} + \mathbf{k}') \times (\mathbf{k} - \mathbf{k}') \right] V((\mathbf{k} + \mathbf{k}')/2) \\
 & \rightarrow \frac{\lambda}{2} \boldsymbol{\sigma} \cdot (\mathbf{k} \times \mathbf{k}' - \mathbf{k}' \times \mathbf{k}) V((\mathbf{k} + \mathbf{k}')/2) \\
 & \rightarrow \lambda \boldsymbol{\sigma} \cdot (\mathbf{k} \times \mathbf{k}') V((\mathbf{k} + \mathbf{k}')/2) \\
 & \Rightarrow \text{the effective magnetic field due to} \\
 & \quad \text{scattering event } \mathbf{k} \rightarrow \mathbf{k}' \text{ is along the} \\
 & \quad \text{direction } \mathbf{k} \times \mathbf{k}'.
 \end{aligned}$$

We first consider the scattering matrix of a spin-orbit scattering event.

Without loss of generality, we can assume that the particle is incident along z and the spin is either parallel or anti-parallel to z .

$$\begin{aligned}\psi_{\text{inc}} &= e^{ikz} \alpha \\ &\rightarrow e^{ikz} \alpha + [S_{11} \alpha + S_{21} \beta] \frac{e^{ikr}}{r}; \\ \psi_{\text{inc}} &= e^{ikz} \beta \\ &\rightarrow e^{ikz} \beta + [S_{12} \alpha + S_{22} \beta] \frac{e^{ikr}}{r}\end{aligned}$$



The scattering matrix S_{ij} are functions of θ and ϕ .

To find the ϕ dependence of S_{ij} we look at the total angular momentum along z .

$$\eta \left(\frac{1}{i} \frac{\partial}{\partial \phi} + \frac{1}{2} \sigma_z \right) \left[e^{ikz} \alpha + (S_{11} \alpha + S_{21} \beta) \frac{e^{ikr}}{r} \right] = \frac{\eta}{2} \left[e^{ikz} \alpha + (S_{11} \alpha + S_{21} \beta) \frac{e^{ikr}}{r} \right]$$

$$\left(\frac{1}{i} \frac{\partial}{\partial \phi} + \frac{1}{2} \sigma_z \right) (S_{11} \alpha + S_{21} \beta) = \frac{1}{2} (S_{11} \alpha + S_{21} \beta)$$

$$\begin{aligned} \left(\frac{1}{i} \frac{\partial}{\partial \phi} + \frac{1}{2} \right) S_{11} &= \frac{1}{2} S_{11} \\ \Rightarrow \frac{\partial S_{11}}{\partial \phi} &= 0 \end{aligned}$$

$$\begin{aligned} \left(\frac{1}{i} \frac{\partial}{\partial \phi} - \frac{1}{2} \right) S_{21} &= \frac{1}{2} S_{11} \\ \Rightarrow \frac{\partial S_{21}}{\partial \phi} &= i S_{21} \\ \Rightarrow S_{21} &\propto e^{i\phi} \end{aligned}$$

Similarly, we have

$$S_{12} \propto e^{-i\phi} \quad \text{and} \quad \frac{\partial S_{22}}{\partial \phi} = 0$$

To find the θ dependence of S_{ij} we look at the “reflection symmetry” in the yz plane.

Symmetry operator for the reflection in the yz plane :

$$P_x \sigma_x$$

P_x make changes $x \rightarrow -x$ to any function at its right hand side.

$$\sigma_x \sigma_x \sigma_x = \sigma_x ; \quad \sigma_x \sigma_y \sigma_x = -\sigma_y ; \quad \sigma_x \sigma_z \sigma_x = -\sigma_z$$

$$P_x \sigma_x (\vec{L} \cdot \vec{S}) P_x \sigma_x = \vec{L} \cdot \vec{S}$$

Applying our reflection operator to our scattering state :

$$P_x \sigma_x \left\{ e^{ikz} \alpha + [S_{11}(\theta, \phi) \alpha + S_{21}(\theta, \phi) \beta] \frac{e^{ikr}}{r} \right\}$$

$$\rightarrow e^{ikz} \beta + [S_{11}(\theta, \pi - \phi) \beta + S_{21}(\theta, \pi - \phi) \alpha] \frac{e^{ikr}}{r}$$

From reflection symmetry, we have

$$\rightarrow e^{ikz} \beta + [S_{11}(\theta, \pi - \phi) \beta + S_{21}(\theta, \pi - \phi) \alpha] \frac{e^{ikr}}{r}$$

From our previous scattering convention, we have

$$\rightarrow e^{ikz} \beta + [S_{12}(\theta, \phi) \alpha + S_{22}(\theta, \phi) \beta] \frac{e^{ikr}}{r}$$

$$S_{12}(\theta, \phi) = h(\theta) e^{-i\phi} ; \quad S_{21}(\theta, \phi) = h'(\theta) e^{i\phi}$$

$$\Rightarrow h(\theta) = -h'(\theta)$$

$$\hat{n} = \frac{\mathbf{k} \times \mathbf{k}'}{|\mathbf{k} \times \mathbf{k}'|}$$

Scattering matrix :

$$\hat{S} = \begin{pmatrix} g(\theta) & h(\theta) e^{-i\phi} \\ -h(\theta) e^{i\phi} & g(\theta) \end{pmatrix} = g(\theta) 1_{2 \times 2} + ih(\theta) \hat{n} \cdot \boldsymbol{\sigma}$$

The scattering wavefunction becomes :

$$e^{ikz} \chi_{\eta} + \hat{S} \chi_{\eta} \frac{e^{ikr}}{r}$$

Scattering rate for such a scattering wave is :

$$\psi_{sc} = \hat{S} \chi_{\eta} \frac{e^{ikr}}{r}$$

$$j_r = \frac{\eta}{2mi} \psi_{sc}^+ \frac{\partial}{\partial r} \psi_{sc} + c.c.$$

$$= \frac{\eta k}{mr^2} \chi_{\eta}^+ \hat{S}^+ \hat{S} \chi_{\eta}$$

$$\text{scattering rate} = \frac{j_r r^2 d\Omega}{V} = \frac{\eta k}{mV} \chi_{\eta}^+ \hat{S}^+ \hat{S} \chi_{\eta} d\Omega$$

Define the scattering rate matrix as follows :

$$\begin{aligned}
 -\frac{e\eta}{m^*} \mathbf{E} \cdot \mathbf{k} \frac{\partial f_0(\mathbf{k})}{\partial \varepsilon_k} 1_{2 \times 2} = & -n_i \sum_{\eta} \int d\Omega_{\hat{k}'} \frac{\eta k}{m^*} \hat{S} \chi_{\eta} \chi_{\eta}^+ \hat{S}^+ \delta f_{\eta}(\mathbf{k}) \\
 & + n_i \sum_{\eta} \int d\Omega_{\hat{k}'} \frac{\eta k}{m^*} \hat{S}(-\hat{n}) \chi_{\eta} \chi_{\eta}^+ \hat{S}^+(-\hat{n}) \delta f_{\eta}(\mathbf{k}')
 \end{aligned}$$

$$\begin{aligned}
 -\frac{e\eta}{m^*} \mathbf{E} \cdot \mathbf{k} \frac{\partial f_0(\mathbf{k})}{\partial \varepsilon_k} 1_{2 \times 2} = & -n_i \sum_{\eta} \int d\Omega_{\hat{k}'} \frac{\eta k}{m^*} \hat{S}(\hat{n}) \delta \hat{f}(\mathbf{k}) \hat{S}^+(\hat{n}) \\
 & + n_i \sum_{\eta} \int d\Omega_{\hat{k}'} \frac{\eta k}{m^*} \hat{S}(-\hat{n}) \delta \hat{f}(\mathbf{k}') \hat{S}^+(-\hat{n})
 \end{aligned}$$

$$\hat{S}(\hat{n}) \hat{f}(\vec{k}) \hat{S}^+(\vec{k})$$

$$= [g(\theta) 1_{2 \times 2} + ih(\theta) \hat{n} \cdot \vec{\sigma}] [\phi(\vec{k}) 1_{2 \times 2} + \vec{f}(\vec{k}) \cdot \vec{\sigma}] [g(\theta)^* 1_{2 \times 2} - ih(\theta)^* \hat{n} \cdot \vec{\sigma}]$$

$$\hat{S} \hat{S}^+ = |g|^2 + i(hg^* - gh^*) \hat{n} \cdot \vec{\sigma} + |h|^2$$

$$\hat{S} \vec{\sigma} \hat{S}^+ = |g|^2 \vec{\sigma} + i[hg^* (\hat{n} \cdot \vec{\sigma}) \vec{\sigma} - gh^* \vec{\sigma} (\hat{n} \cdot \vec{\sigma})] + |h|^2 (\hat{n} \cdot \vec{\sigma}) \vec{\sigma} (\hat{n} \cdot \vec{\sigma})$$

$$-\frac{e\eta}{m^*} \vec{E} \cdot \vec{k} \frac{\partial f_0(\vec{k})}{\partial \varepsilon_k} 1_{2 \times 2}$$

$$= -n_i \int d\Omega_{\hat{k}'} \frac{\eta k}{m^*} \left\{ I(\theta) [\hat{f}(\vec{k}) - \hat{f}(\vec{k}')] + I(\theta) S(\theta) \hat{n} \cdot \vec{\sigma} [\phi(\vec{k}) + \phi(\vec{k}')] \right\}$$

$$I(\theta) = |g|^2 + |h|^2$$

Sherman function

$$S(\theta) = \frac{i[h(\theta)g(\theta)^* - g(\theta)h(\theta)^*]}{I(\theta)}$$

$$\begin{aligned}
 & -\frac{e\eta}{m^*} \vec{E} \cdot \vec{k} \frac{\partial f_0(\vec{k})}{\partial \varepsilon_k} 1_{2 \times 2} \\
 & = -n_i \int d\Omega_{\hat{k}} \frac{\eta k}{m^*} \left\{ I(\theta) [\hat{f}(\vec{k}) - \hat{f}(\vec{k}')] + I(\theta) S(\theta) \hat{n} \cdot \vec{\sigma} [\phi(\vec{k}) + \phi(\vec{k}')] \right\}
 \end{aligned}$$

$$\hat{f}(\vec{k}) = f_0(\vec{k}) 1_{2 \times 2} + \left(\phi(\vec{k}) 1_{2 \times 2} + \vec{f}(\vec{k}) \cdot \vec{\sigma} \right)$$

We can see that the following ansatz must be valid:

$$\phi(\vec{k}) = \vec{k} \cdot \vec{E} C_k$$

$$C_k = \frac{e\eta\tau}{m^*} \frac{\partial f_0(\vec{k})}{\partial \varepsilon_k} ; \quad \frac{1}{\tau} = n_i \int d\Omega_{\hat{k}} \frac{\eta k}{m^*} I(\theta) [1 - \cos \theta]$$

$$0 = -n_i \int d\Omega_{\hat{k}'} \frac{\eta k}{m^*} I(\theta) \left\{ \left[\vec{f}(\vec{k}) - \vec{f}(\vec{k}') \right] \cdot \vec{\sigma} + S(\theta) \hat{n} \cdot \vec{\sigma} \left[\vec{k} + \vec{k}' \right] \cdot \vec{E} C_k \right\}$$

Another ansatz : since $\vec{f}(\vec{k})$ must change sign if $\vec{k} \rightarrow -\vec{k}$, then we let $\vec{f}(\vec{k}) = \vec{b}(\varepsilon_k) \times \vec{k}$

After some calculation, we get

$$\vec{b} = \frac{1}{2} C_k \gamma_k \vec{E} ; \quad \text{where} \quad \gamma_k = \frac{\int d\Omega_{\hat{k}'} I(\theta) S(\theta) \sin\theta}{\int d\Omega_{\hat{k}'} I(\theta) (1 - \cos\theta)}$$

$$\hat{f}(\vec{k}) = f_0(\vec{k}) 1_{2 \times 2} + C_k \vec{k} \cdot \left[\vec{E} 1_{2 \times 2} + \frac{\gamma_k}{2} (\vec{\sigma} \times \vec{E}) \right] \quad C_k = \frac{e\eta\tau}{m^*} \frac{\partial f_0(\vec{k})}{\partial \varepsilon_k}$$

Spin current:

$$\mathbf{j}_{SS}^{\mu} = n \langle \sigma_{\mu} \mathbf{v}_0 \rangle$$

$$\mathbf{v}_0 = \hbar \mathbf{k} / m^*$$

$$j_{SS,\kappa}^{\mu} = \text{Tr} \sigma_{\mu} \int \frac{d^3 k}{(2\pi)^3} \frac{\hbar k_{\kappa}}{m^*} \hat{f}(\mathbf{k}) = \frac{\gamma}{2e} \varepsilon^{\kappa\mu\nu} (\mathbf{J}_0)_{\nu},$$

where

$$\mathbf{J}_0 = 2e \int d^3 k (2\pi)^{-3} (\hbar \mathbf{k} / m^*) \mathbf{k} \cdot \mathbf{E} C_k$$

where \mathbf{J}_0 is the charge current in the absence of SO coupling.

Theory of Spin Hall Conductivity in n -Doped GaAs

Hans-Andreas Engel, Bertrand I. Halperin, and Emmanuel I. Rashba

Department of Physics, Harvard University, Cambridge, Massachusetts 02138, USA

(Received 21 May 2005; published 13 October 2005)

We develop a theory of extrinsic spin currents in semiconductors, resulting from spin-orbit coupling at charged scatterers, which leads to skew-scattering and side-jump contributions to the spin-Hall conductivity. Applying the theory to bulk n -GaAs, without any free parameters, we find spin currents that are in reasonable agreement with experiments by Kato *et al.* [Science **306**, 1910 (2004)].

DOI: [10.1103/PhysRevLett.95.166605](https://doi.org/10.1103/PhysRevLett.95.166605)

PACS numbers: 72.25.Dc, 71.70.Ej

Next, we estimate the spin-Hall currents. The measurements were performed at electrical fields $E \approx 20 \text{ mV } \mu\text{m}^{-1}$ where the conductivity increased to $\sigma_{xx} \approx 3 \times 10^3 \text{ } \Omega^{-1} \text{ m}^{-1}$ due to electron heating. We assume that γ is not very sensitive to these heating effects and we still use Eq. (8) but with the increased conductivity. For an electrical field $\mathbf{E} = \hat{x}E_x$, we find both contributions to the spin-Hall conductivity $\sigma^{\text{SH}} \equiv -j_y^z/E_x$, namely, $\sigma_{\text{SS}}^{\text{SH}} = -(\gamma/2e)\sigma_{xx} \approx 1.7 \text{ } \Omega^{-1} \text{ m}^{-1}/|e|$ and $\sigma_{\text{SJ}}^{\text{SH}} = 2n\lambda e/\hbar \approx -0.8 \text{ } \Omega^{-1} \text{ m}^{-1}/|e|$. In total, we arrive at the extrinsic spin-Hall conductivity $\sigma_{\text{theor}}^{\text{SH}} \approx 0.9 \text{ } \Omega^{-1} \text{ m}^{-1}/|e|$. The magnitude is within the error bars of the experimental value of $|\sigma_{\text{expt}}^{\text{SH}}| \approx 0.5 \text{ } \Omega^{-1} \text{ m}^{-1}/|e|$ found from spin accumulation near the free edges of the specimen [1,27].

Spin dipole around a local scatterer

- isotropic normal scatterer in a Rashba 2DEG
- extrinsic spin-orbit scatterer in a normal 2DEG

R. Landauer

Spatial Variation of Currents and Fields Due to Localized Scatterers in Metallic Conduction

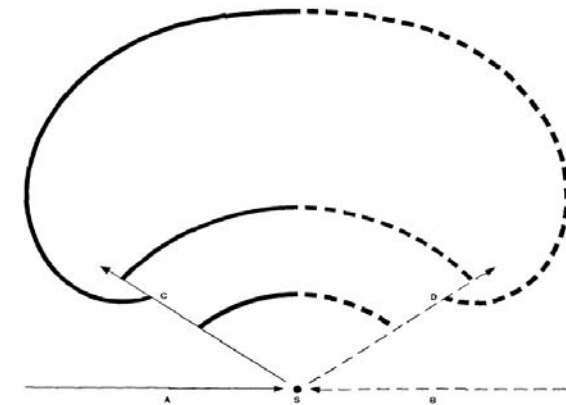
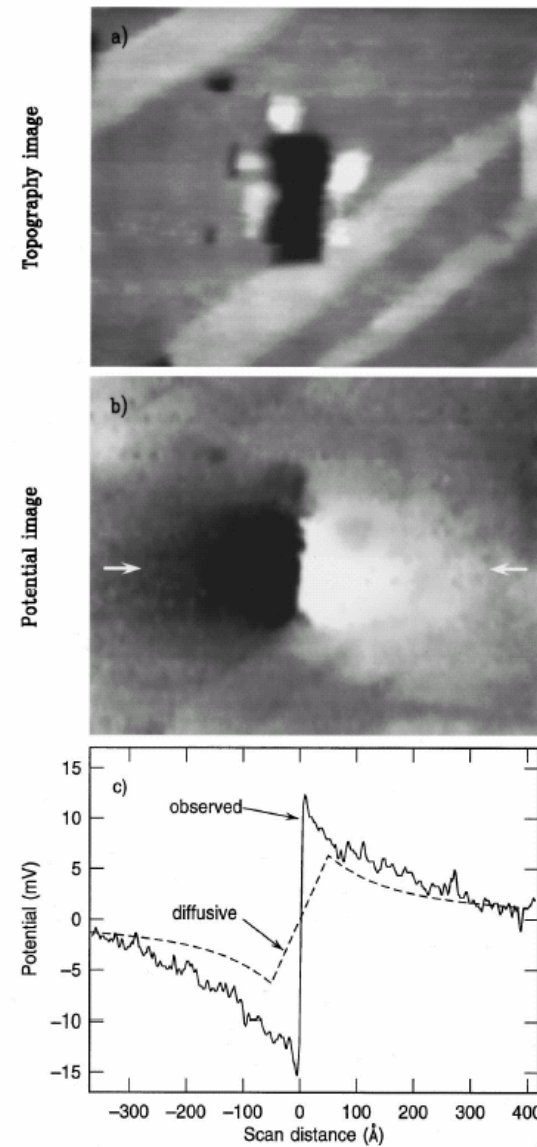
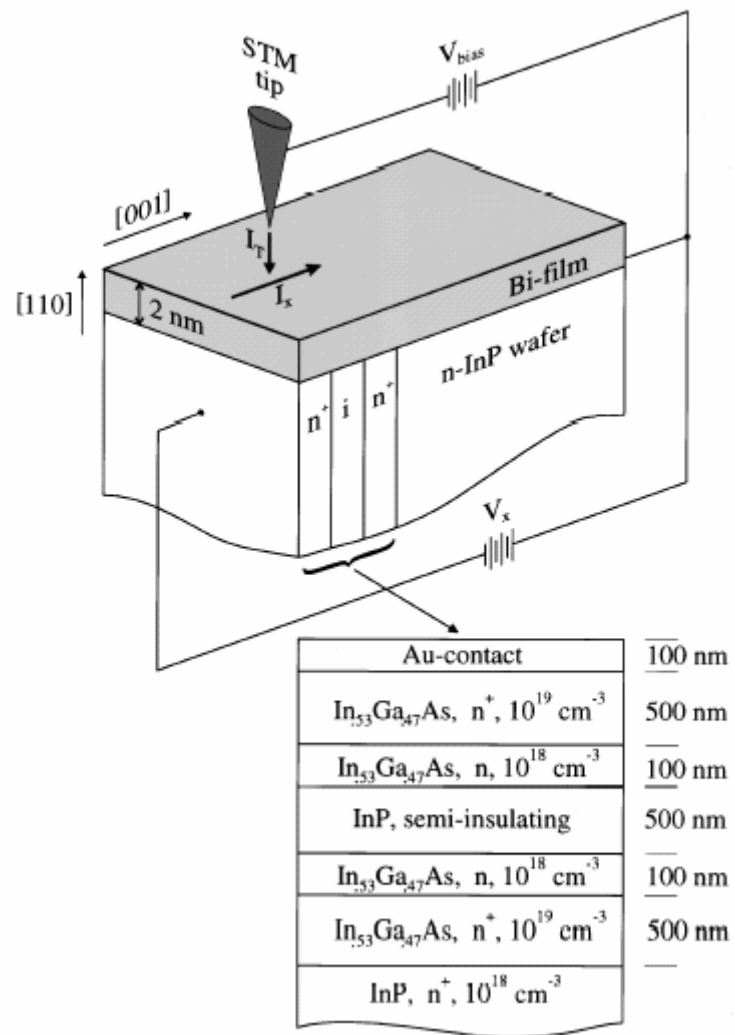


Figure 1 Schematic representation of current flow disturbed by the scatterer S . Electrons in excess numbers are incident along A , then are scattered to C , then scattered by the background. The number of electrons incident along B is less than the equilibrium number. The deficit is scattered to D , then scattered by the background. The excess and deficit diffuse together and recombine along the arcs.

Abstract: Localized scatterers can be expected to give rise to spatial variations in the electric field and in the current distribution. The transport equation allowing for spatial variations is solved by first considering the homogeneous transport equation which omits electric fields. The homogeneous solution gives the purely diffusive motion of current carriers and involves large space charges. The electric field is then found, and approximate space charge neutrality is restored, by adding a particular solution of the transport equation in which the electric field is associated only with space charge but not with a current. The presence of point scatterers leads to a dipole field about each scatterer. The spatial average of a number of these dipole fields is the same as that obtained by the usual approach which does not explicitly consider the spatial variation. Infinite plane obstacles with a reflection coefficient r are also considered. These produce a resistance proportional to $r/(1 - r)$.



PRB 54, R5283 (1996)
BG Briner, RM Feenstra
et al.

Isotropic normal scatterer in a Rashba 2DEG

Scattering amplitude
of the scatterer

$$f(\mathbf{k}, \mathbf{k}') = -\frac{m^*}{\sqrt{2\pi k_F}} \int dr^2 U(\mathbf{r}) e^{i(\mathbf{k}-\mathbf{k}')\mathbf{r}},$$

$$G_{\mathbf{k}\mathbf{k}'}^r(\omega) = \delta_{\mathbf{k}\mathbf{k}'} G_{\mathbf{k}}^{r(0)}(\omega) + G_{\mathbf{k}\mathbf{k}'}^{r(1)}(\omega) + G_{\mathbf{k}\mathbf{k}'}^{r(2)}(\omega),$$


$$G_{\mathbf{k}\mathbf{k}'}^{r(1)}(\omega) = G_{\mathbf{k}}^{r(0)}(\omega) U_{\mathbf{k}\mathbf{k}'} G_{\mathbf{k}'}^{r(0)}(\omega),$$

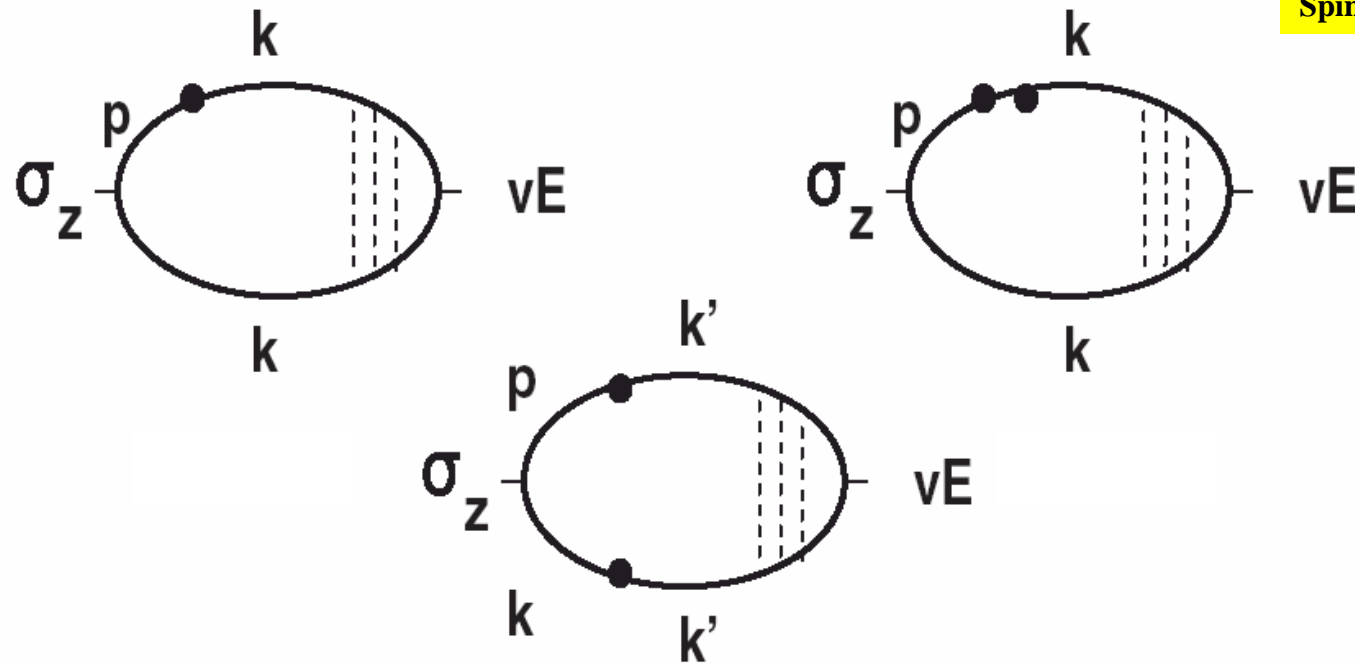
$$G_{\mathbf{k}\mathbf{k}'}^{r(2)}(\omega) = G_{\mathbf{k}}^{r(0)}(\omega) \sum_{\mathbf{k}''} U_{\mathbf{k}\mathbf{k}''} G_{\mathbf{k}''}^{r(0)}(\omega) U_{\mathbf{k}''\mathbf{k}'} G_{\mathbf{k}'}^{r(0)}(\omega).$$

Spin density in the vicinity of the scatterer

$$\sigma_z(\mathbf{r}) = \sum_{\mathbf{k}, \mathbf{k}', \mathbf{p}} e^{i(\mathbf{p}-\mathbf{k})\cdot\mathbf{r}} \int \frac{d\omega}{2\pi} \frac{dn_F(\omega)}{d\omega} \times \text{Tr}[G_{\mathbf{k}'\mathbf{k}}^a(\omega) \sigma_z G_{\mathbf{p}\mathbf{k}'}^r(\omega) \mathcal{T}(\omega, \mathbf{k}')],$$

Vertex part





Spin dipole in the ballistic regime: (PRL 97, 76601 (2006))

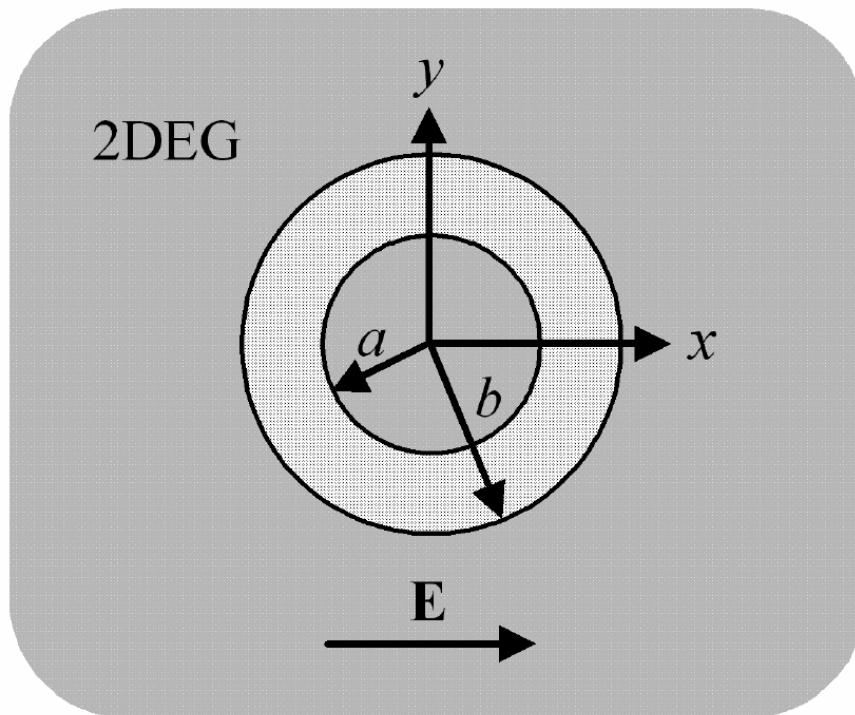
spin accumulation occurs regardless of zero spin current in the bulk

$$\sigma_z(\mathbf{r}) = -\frac{m^* v_d \sigma_t}{2\pi^2 R L_{so}} \sin\left(\frac{2R}{L_{so}}\right) \sin\theta + \frac{m^* v_d}{2\pi^2 R^2} \sin^2\left(\frac{R}{L_{so}}\right) \\ \times \sin^3\theta \left(\sigma_{tot} + \sqrt{\frac{8\pi}{k_F}} \text{Re}[f(\pi) e^{2ik_F R}] \right),$$



We invoke both the **in-plane potential gradient SOI** and the **resonant effects** for the amplification of the spin accumulation.

Chen, Chu, and Mal'shukov (Phys. Rev. B 76, 2007)



A ring-shaped potential pattern is embedded in a 2DEG. An electric field \mathbf{E} sets up a current in the 2DEG.

$$H_{\text{SO}} = \lambda \vec{\sigma} \cdot (\vec{k} \times \vec{\nabla} V)$$

$$V(\rho) = V_o [\theta(\rho - a) - \theta(\rho - b)]$$

$$S_z(\boldsymbol{\rho}) = \frac{1}{4\pi^2} \int d\mathbf{k} g(\mathbf{k}) \sum_{\sigma} \sigma \Psi_{\mathbf{k}\sigma}^{\dagger}(\boldsymbol{\rho}) \Psi_{\mathbf{k}\sigma}(\boldsymbol{\rho}),$$

Sorbello and Chu, IBM J. Res. Dev. 32, 58 (1988)

Chu and Sorbello, Phys. Rev. B 38, 7260 (1988)

$$S_z(\boldsymbol{\rho}) = n_E \operatorname{Re} \sum_{\sigma} \sigma \sum_{l=0}^{\infty} R_l^{\sigma}(\rho) R_{l+1}^{\sigma*}(\rho) \sin\phi_{\rho}$$

Dipole-like

Radial wavefunction

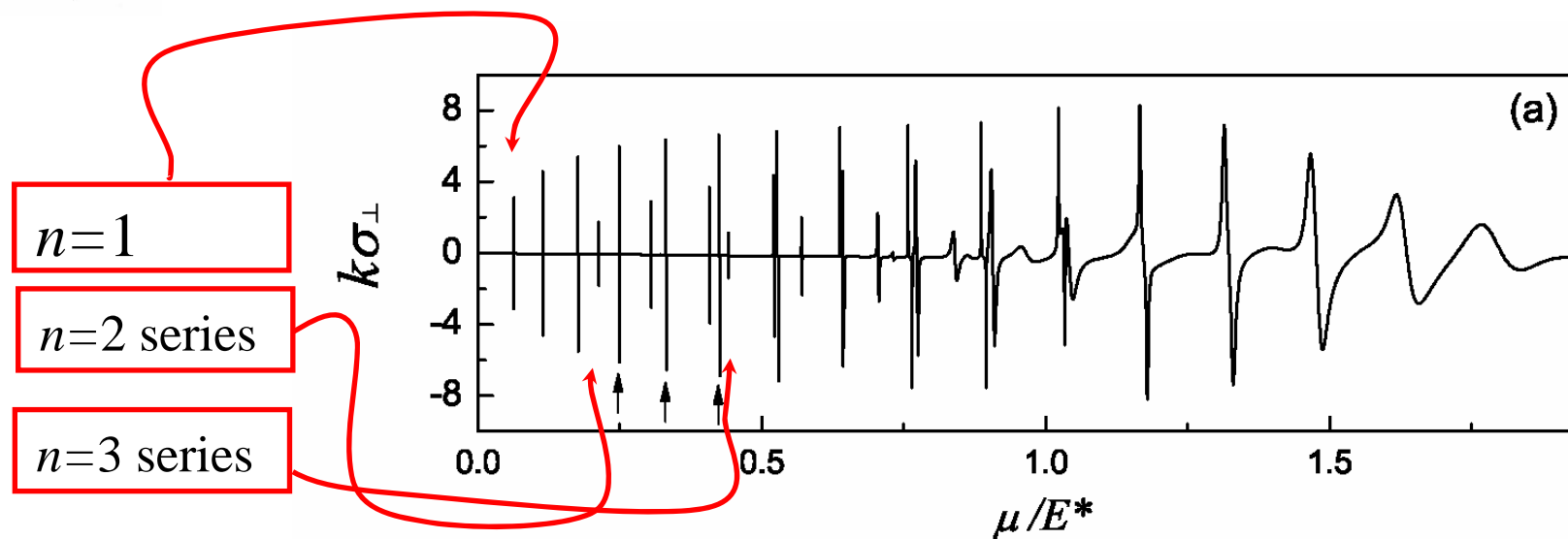
**Asymptotic
form:**

$$S_z = \frac{\sin\phi_\rho}{k^*\rho} \left[p_s + \frac{\wp_s}{k^*\rho} \right]$$

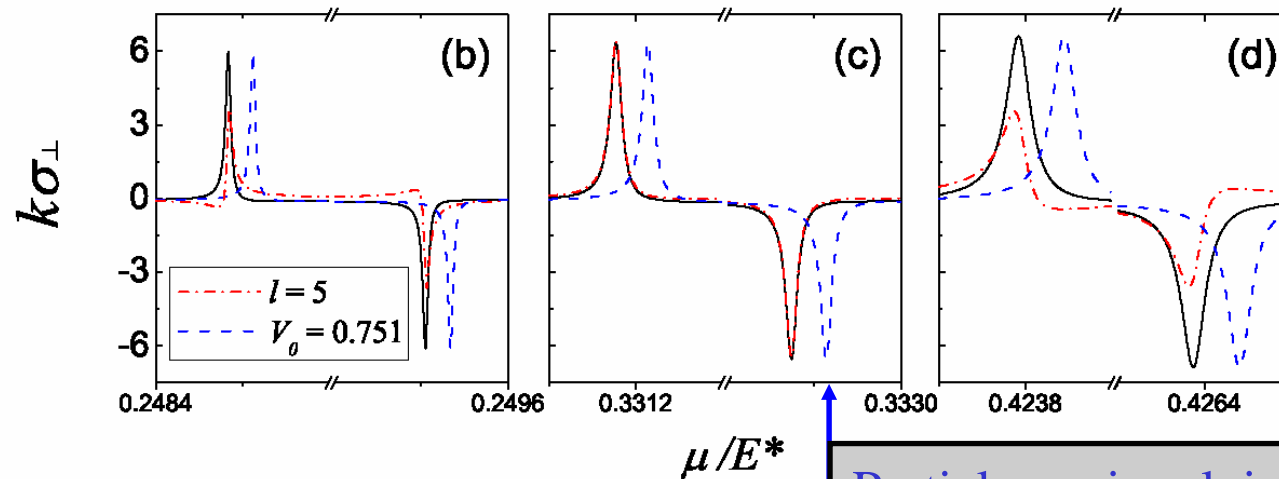
$$p_s = -\frac{n_E^* k \sigma_\perp}{4\pi}$$

$$n_E^* = \frac{m^* e E_0 l_0^*}{\pi \hbar^2}$$

$$\sigma_\perp = \frac{2}{k} \sum_\sigma \sigma \sum_{l=0}^{\infty} \sin [2 (\delta_l^\sigma - \delta_{l+1}^\sigma)]$$



$V_0 = 0.75$



$E^* = 77.1 \text{ meV}$

Partial sum involving
 $\delta_l=5$

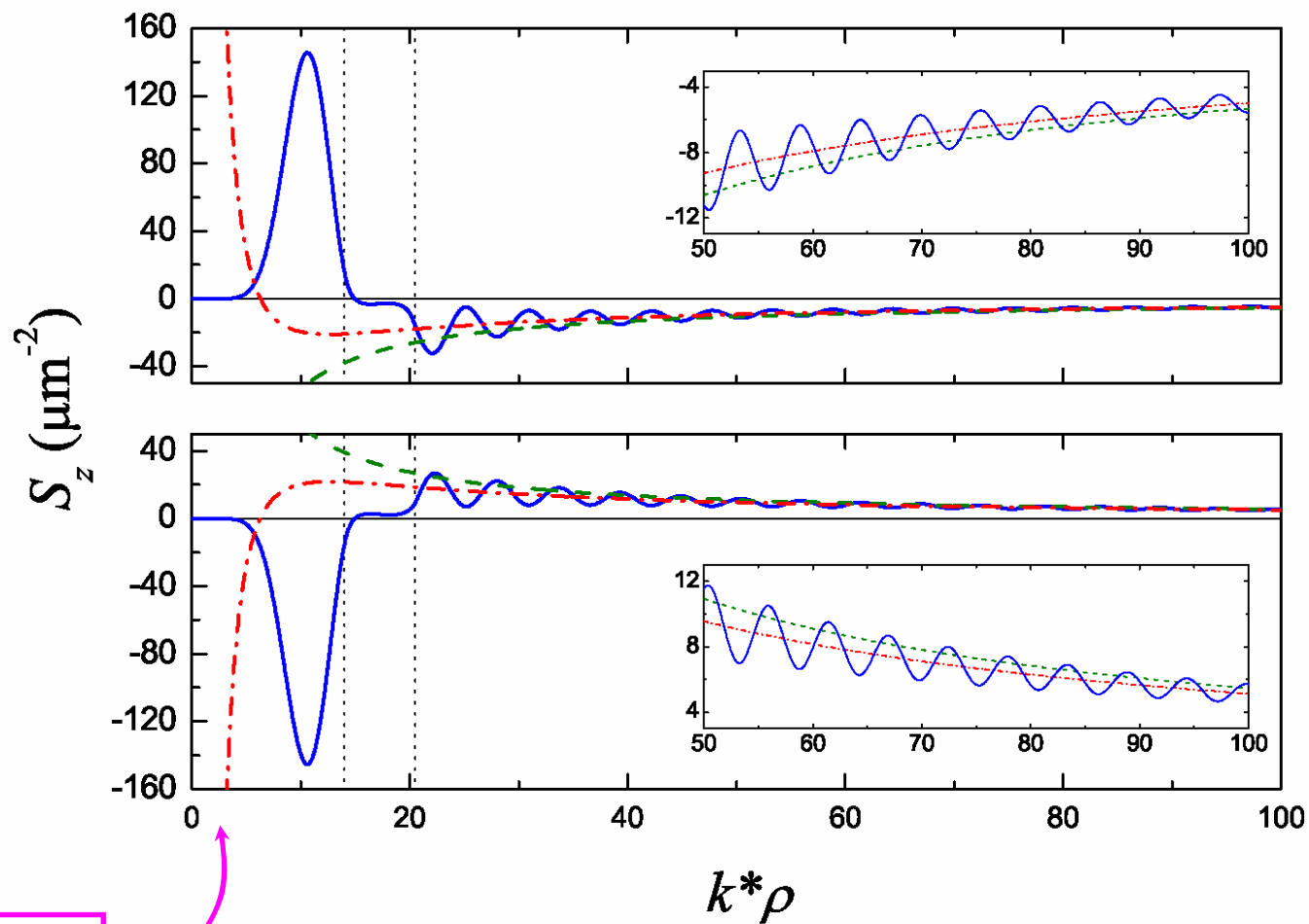
$$n=1,$$

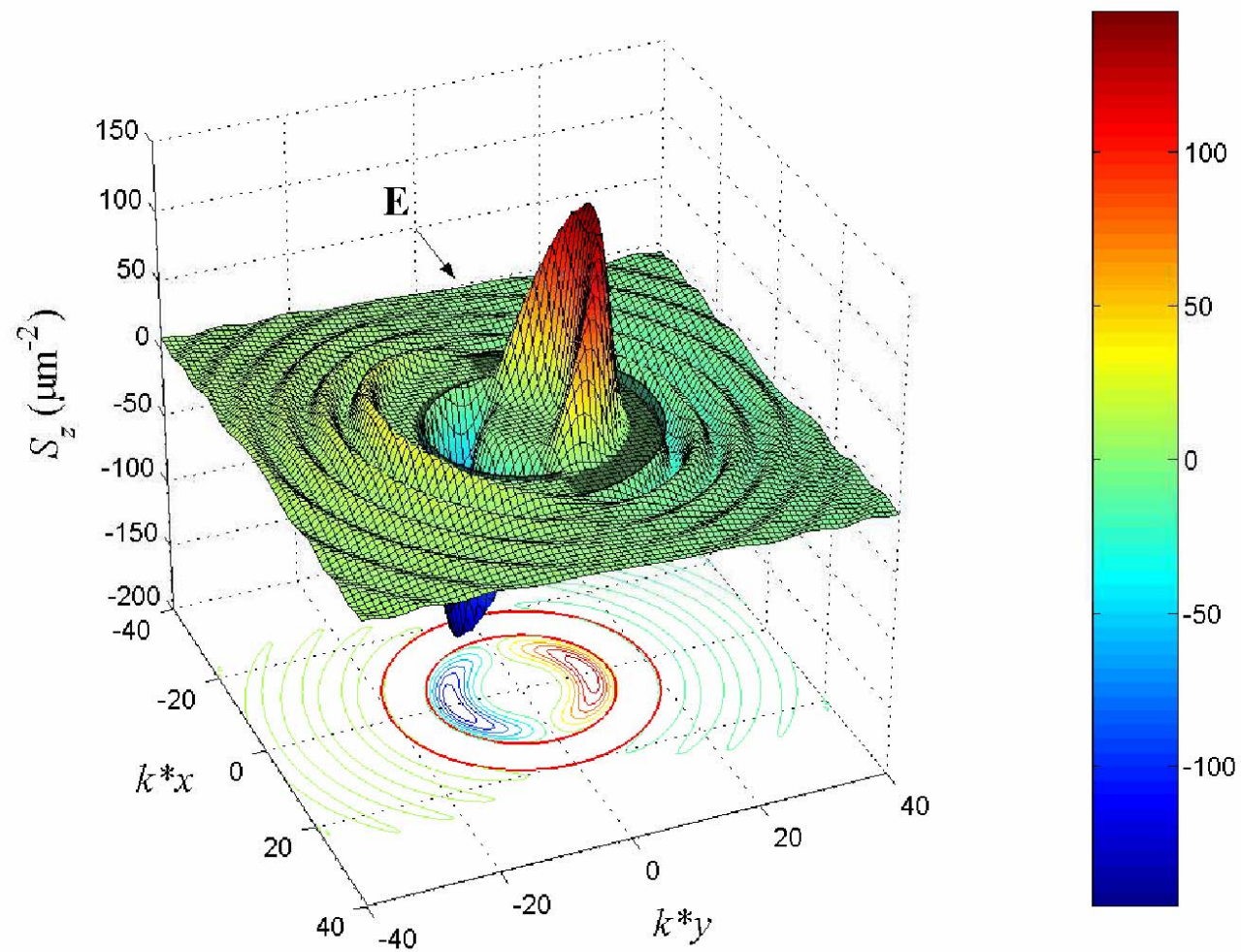
$$l=$$

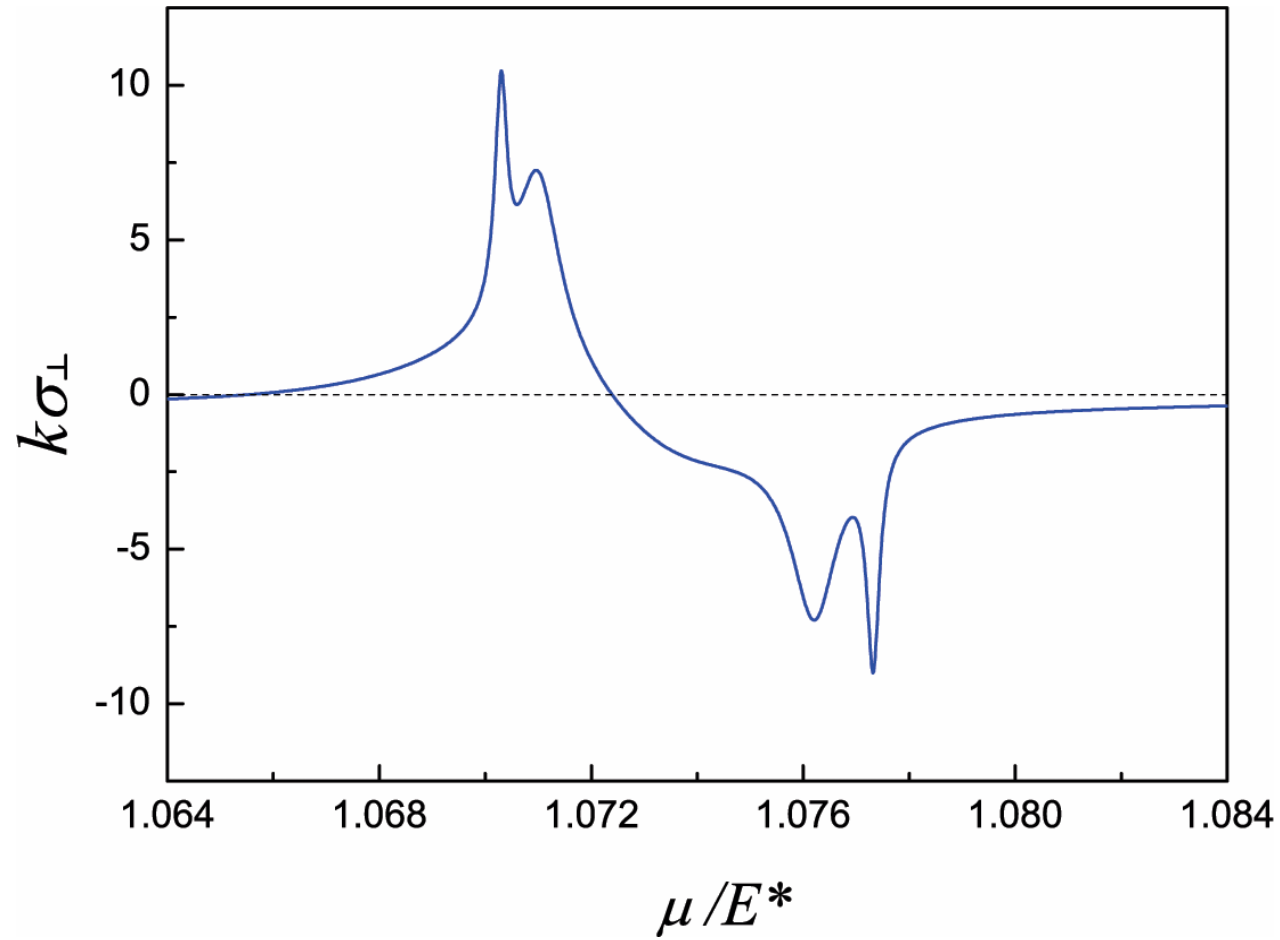
$$5$$

Length
scale =
46.3 Å

Asymptotic



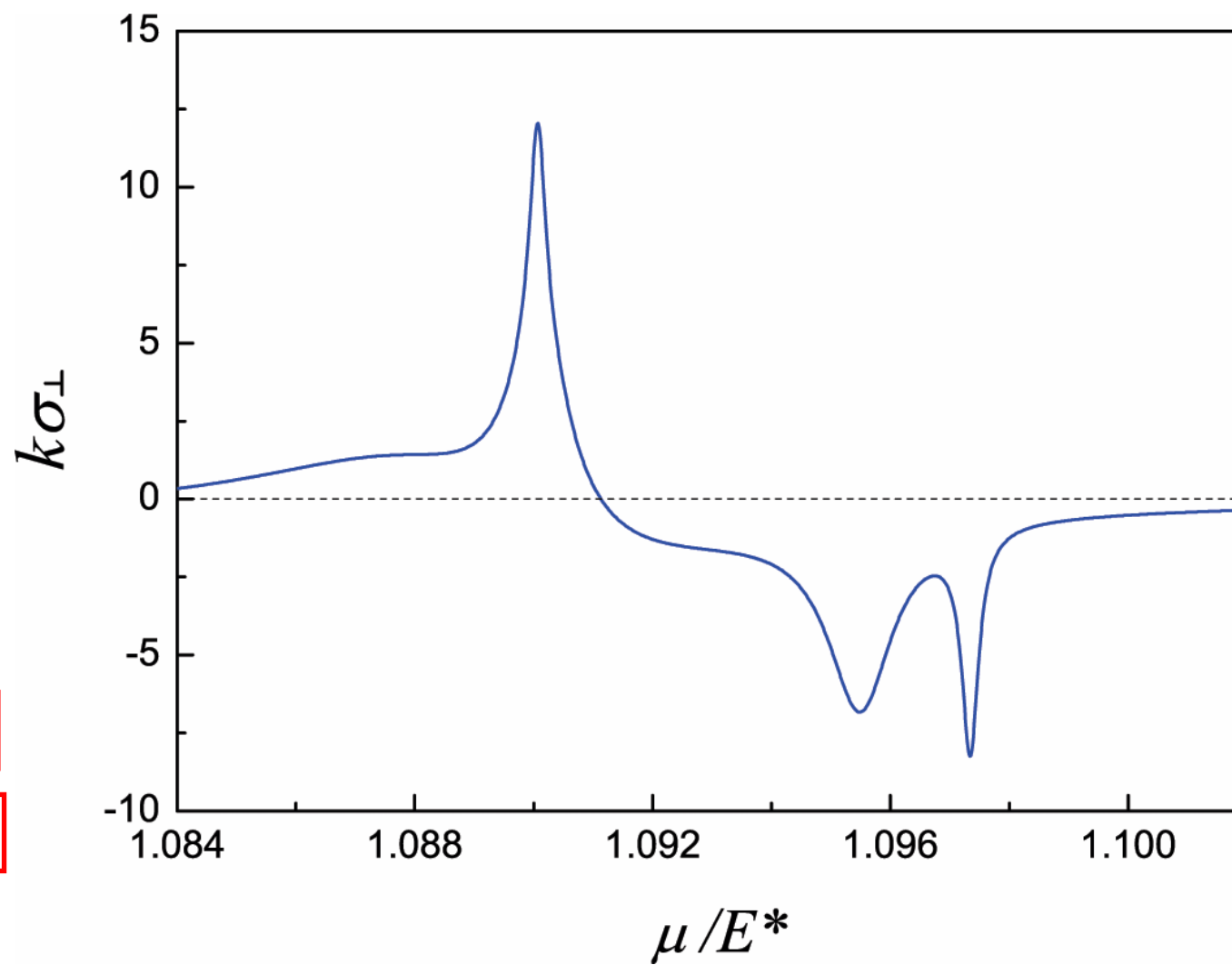




$$V_0 =$$

$$a = 20$$

$$b = 26.5$$



$$V_0 =$$

$$a = 19.8$$

$$b = 26.3$$

Possible realization of the microstructure:

1. Gate-patterning on the 2DEG
2. Carrier distribution profiles in Si-doped layers formed by focused ion beam implanatation and successive overlayer growth

Ref. J. Vac. Sci. Technol. B 18, 3158 (2000)

Summary

1. **Nonequilibrium spin accumulation (spin cloud or spin dipole) is found in the absence of bulk “spin current”.**
2. **For the case of Rashba SOI, nonequilibrium spin cloud is formed around a normal impurity.**
3. **For the case of a normal 2DEG, nonequilibrium spin cloud is formed around a local SOI structure.**
4. **The interplay between the in-plane potential gradient SOI and quantum resonances can lead to significant effects.**

Other recent work that invoked the importance of in-plane potential gradient:

Phys. Rev. Lett. 98, 186807 (2007)

Giant Spin Splitting through Surface Alloying

Christian R. Ast,^{1,2,*} Jürgen Henk,³ Arthur Ernst,³ Luca Moreschini,² Mihaela C. Falub,² Daniela Pacilé,^{2,†}
Patrick Bruno,³ Klaus Kern,^{1,2} and Marco Grioni²

¹Max-Planck-Institut für Festkörperforschung, D-70569 Stuttgart, Germany

²Ecole Polytechnique Fédérale de Lausanne (EPFL), Institut de Physique des Nanostructures, CH-1015 Lausanne, Switzerland

³Max-Planck-Institut für Mikrostrukturphysik, D-06120 Halle (Saale), Germany

(Received 26 October 2006; published 3 May 2007)

The long-range ordered surface alloy **Bi/Ag(111)** is found to exhibit a giant spin splitting of its surface electronic structure due to spin-orbit coupling, as is determined by angle-resolved photoelectron spectroscopy. First-principles electronic structure calculations fully confirm the experimental findings. The effect is brought about by a strong in-plane gradient of the crystal potential in the surface layer, in interplay with the structural asymmetry due to the surface-potential barrier. As a result, the spin polarization of the surface states is considerably rotated out of the surface plane.

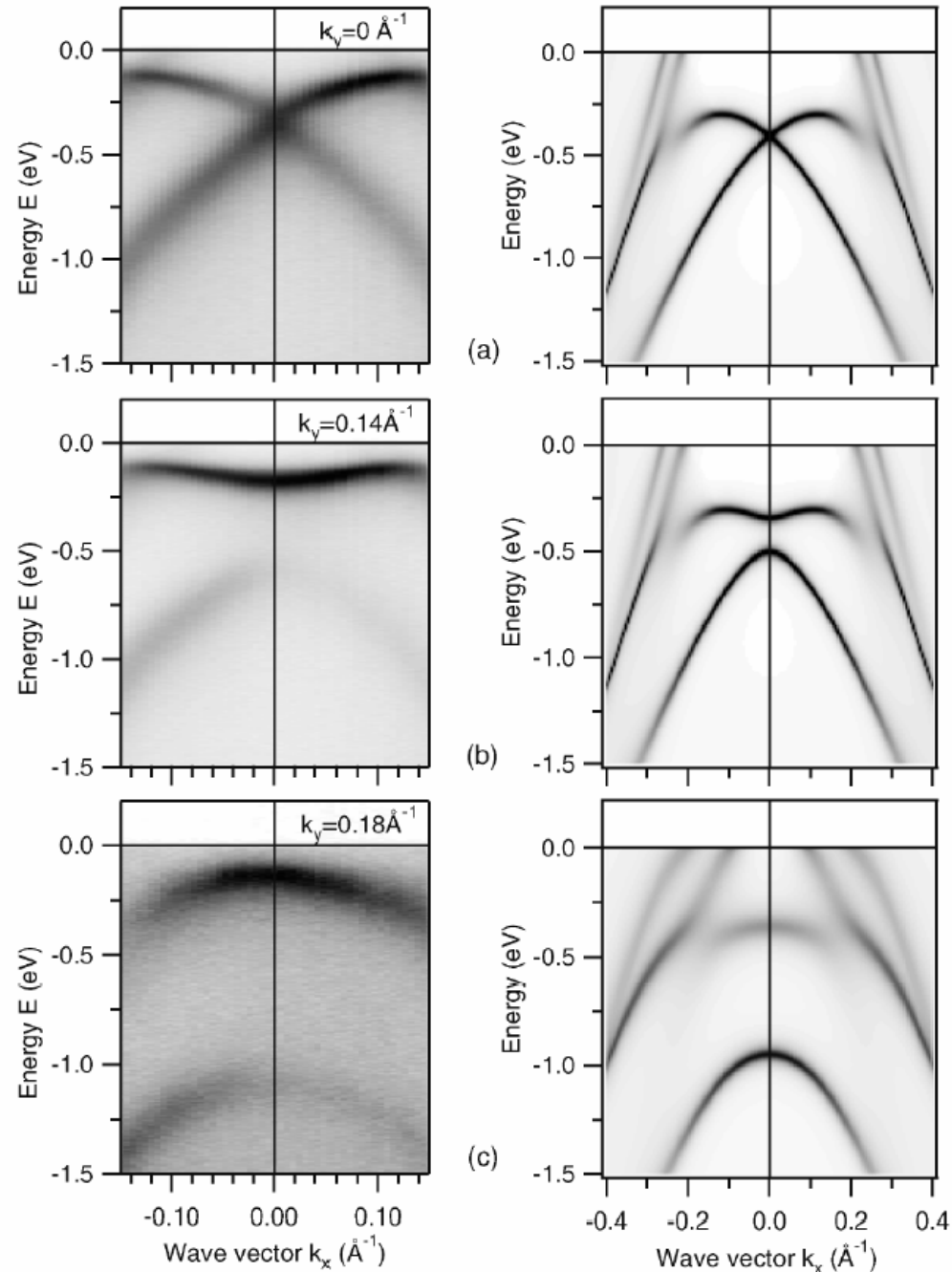
TABLE I. Selected materials and parameters characterizing the spin splitting: Rashba energy of split states E_R , wave number offset k_0 , and Rashba parameter α_R .

| Material | E_R (meV) | k_0 (\AA^{-1}) | α_R (eV \AA) | Reference |
|-------------------------------|----------------|--------------------------------|----------------------------------|-----------|
| InGaAs/InAlAs heterostructure | <1 | 0.028 | 0.07 | [4] |
| Ag(111) surface state | <0.2 | 0.004 | 0.03 | [5,6] |
| Au(111) surface state | 2.1 | 0.012 | 0.33 | [6,7] |
| Bi(111) surface state | ~ 14 | ~ 0.05 | ~ 0.56 | [8] |
| Bi/Ag(111) surface alloy | 200 | 0.13 | 3.05 | This work |

Band structure measurements by ARPES (left-hand panels) and calculations (right-hand panels) in the vicinity of the Γ point.

Note the different horizontal scales.

Giant spin splitting in surface metallic alloy



PHYSICAL REVIEW B 77, 081407(R) (2008)

Spin-orbit split two-dimensional electron gas with tunable Rashba and Fermi energyChristian R. Ast,^{1,2,*} Daniela Pacilé,^{2,†} Luca Moreschini,² Mihaela C. Falub,² Marco Papagno,² Klaus Kern,^{1,2} and
Marco Grioni²¹*Max-Planck-Institut für Festkörperforschung, D-70569 Stuttgart, Germany*²*Ecole Polytechnique Fédérale de Lausanne (EPFL), Institut de Physique des Nanostructures, CH-1015 Lausanne, Switzerland*Jürgen Henk, Arthur Ernst, Sergey Ostanin, and Patrick Bruno
Max-Planck-Institut für Mikrostrukturphysik, D-06120 Halle (Saale), Germany

(Received 15 January 2008; published 15 February 2008)

We demonstrate that it is possible to tune the Rashba energy, introduced by a strong spin-orbit splitting, and the Fermi energy in a two-dimensional electron gas by a controlled change of stoichiometry in an artificial surface alloy. In the $\text{Bi}_x\text{Pb}_{1-x}/\text{Ag}(111)$ surface alloy, the spin-orbit interaction maintains a dramatic influence on the band dispersion for arbitrary Bi concentration x , as is shown by angle-resolved photoelectron spectroscopy. The Rashba energy E_R and the Fermi energy E_F can be tuned to achieve values larger than one for the ratio E_R/E_F , which opens up the possibility for observing phenomena, such as corrections to the Fermi liquid or a superconducting state. Relativistic first-principles calculations explain the experimental findings.

DOI: [10.1103/PhysRevB.77.081407](https://doi.org/10.1103/PhysRevB.77.081407)

PACS number(s): 73.20.At, 79.60.-i, 71.70.Ej

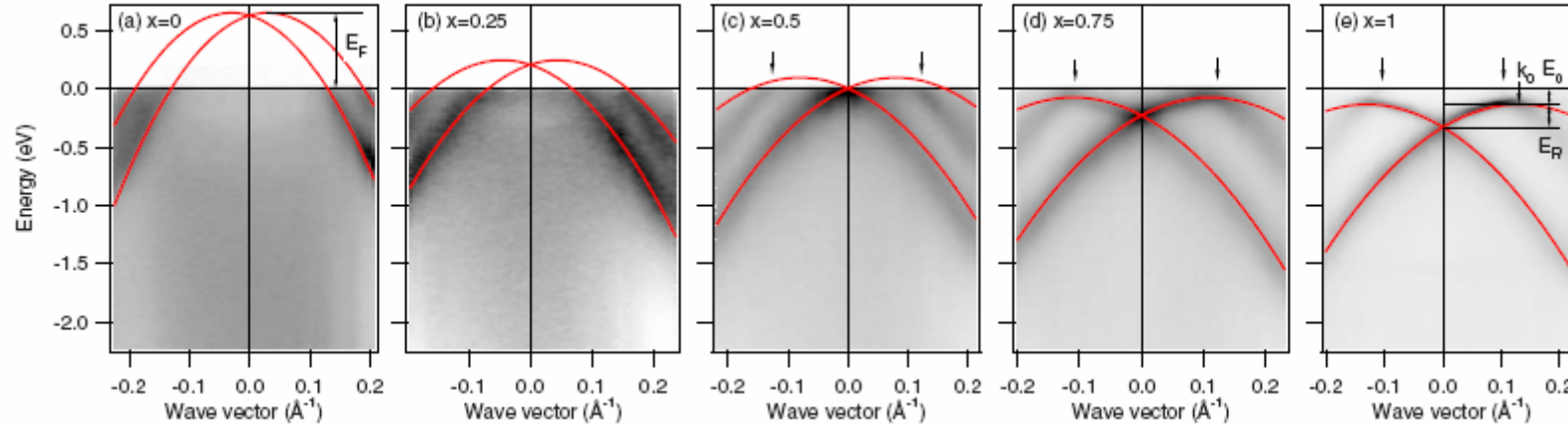
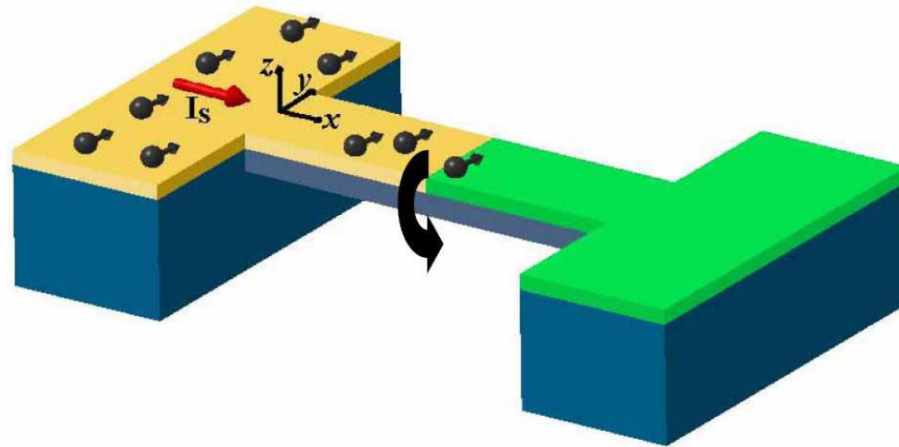


FIG. 1. (Color online) Experimental band structures of $\text{Bi}_x\text{Pb}_{1-x}/\text{Ag}(111)$ surface alloys for x as indicated. The photoemission intensity is depicted as linear gray scale, with dark corresponding to high intensity, versus energy E and wave vector k along $\bar{\text{K}}\bar{\Gamma}\bar{\text{K}}$. Data are taken at 21.2 eV (HeI). Red (dark gray) lines represent parabolic fits to the surface-state bands. The Fermi energy of the holes is indicated in (a). The spin-orbit splitting k_0 , the Rashba energy E_R as well as the energy offset E_0 are defined in (e).

Spin Current Detection

- **A nano-mechanical proposal**
- **An Inverse spin-Hall proposal and experiment**

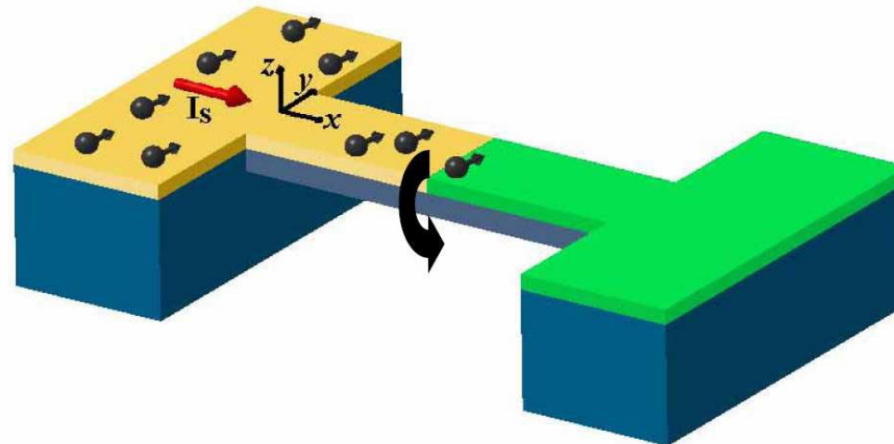
Nanobridge consists of:
Semiconductor (yellow region); Metal (green region);
Insulator (blue region)



Semiconductor provides the strain-induced SOI;
Metal provides a rapid spin relaxation;
Insulator is to provide an asymmetric environment for the semiconductor so as to allow for a net torsional stress.

- Relate torsional energy to spin current
- Derive equation of motion for the torsion angle
- Relate the spin current to the spin density
- Estimate torsion angle and its thermal fluctuation

Target: To study the torsion angle the nanobridge is to twist upon the diffusion of electron spin into the nanobridge from the semiconductor side.



Dimension of the Nanobridge:

b : the width L_t : total length of the nanobridge
 $c/2$: thickness of the semiconductor
 L : length of the semiconductor in the nanobridge
 $c/2$: thickness of the insulator

Strain-induced SOI in semiconductor

$$H_{\text{SOI}} = \alpha \left[\sigma_x (u_{zx} k_z - u_{xy} k_y) + \sigma_y (u_{xy} k_x - u_{yz} k_z) + \sigma_z (u_{yz} k_y - u_{zx} k_x) \right] \\ + \beta \left[\sigma_x k_x (u_{yy} - u_{zz}) + \sigma_y k_y (u_{zz} - u_{xx}) + \sigma_z k_z (u_{xx} - u_{yy}) \right]$$

u_{ij} are elements of the strain tensor

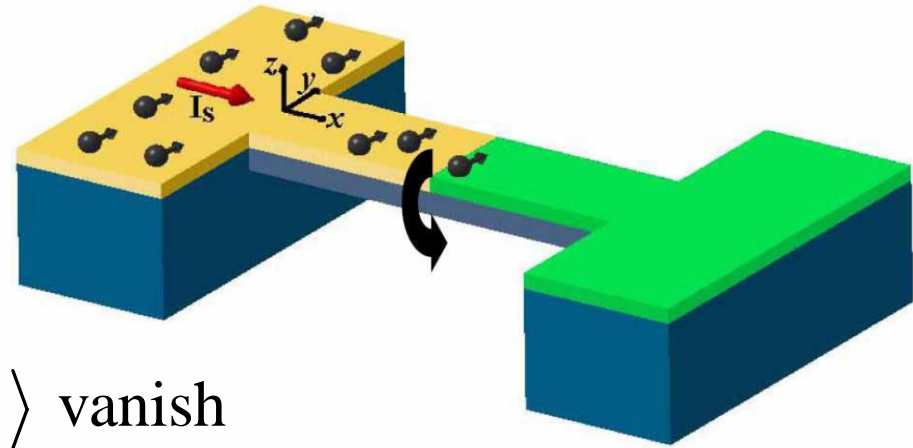
α is the coupling constant for torsional motions

β is the coupling constant for flexural motions

$\beta \ll \alpha$ for narrow gap semiconductors

$$H_{\text{SOI}} = \alpha \left[\sigma_x (u_{zx} k_z - u_{xy} k_y) + \sigma_y (u_{xy} k_x - u_{yz} k_z) + \sigma_z (u_{yz} k_y - u_{zx} k_x) \right]$$

$u_{yz} = 0$ for torsional motion
along x axis



terms involving $\langle k_y \rangle$ and $\langle k_z \rangle$ vanish

$$H_{\text{SOI}} = \alpha \left[\sigma_y u_{xy} - \sigma_z u_{zx} \right] k_x$$

$$H_{\text{SOI}} = \alpha \left[\sigma_y u_{xy} - \sigma_z u_{zx} \right] k_x$$

$$u_{yx} = \tau(x) \frac{\partial \chi}{\partial z}; \quad u_{zx} = -\tau(x) \frac{\partial \chi}{\partial y}$$

$$\tau(x) = \frac{\partial \theta}{\partial x}$$

$$\nabla^2 \chi(y, z) = -1 \quad \text{with the boundary condition } \chi = 0$$

An influx of diffusive spin current can be represented by a Boltzmann distribution function $F_k^i(r)$ from which we can calculate the spin distribution function $P_k^i(r)$. We assume $P_k^i(r)$ to be uniform within the cross section of the semiconductor.

Torsional energy:

$$\begin{aligned}
 E_{\text{SO}} &= \int \sum_{\vec{k}} \text{Tr} \left[F_{\vec{k}}^{\uparrow}(\vec{r}) H_{\text{SOI}} \right] dx dy dz \\
 &= 2\alpha \int_0^L dx \frac{\partial \theta}{\partial x} \sum_{\vec{k}} k_x \left[P_{\vec{k}}^y \frac{\partial \chi}{\partial z} + P_{\vec{k}}^z \frac{\partial \chi}{\partial y} \right] dy dz
 \end{aligned}$$

From the above expression it is clear that the insulator plays a very important role in providing a net torsional stress.

$$J^y(x) = S \sum_{\vec{k}} v_x P_{\vec{k}}^y(x)$$

$$E_{\text{SO}} = -\gamma \int_0^L dx J^y(x) \frac{\partial \theta}{\partial x}$$

$$\rho I \frac{d^2 \theta}{dt^2} - K \frac{d^2 \theta}{dx^2} - \gamma \frac{d}{dx} [J^y(x) \eta(L-x)] = 0$$

$$\theta_L = \frac{L(L_t - L)}{L_t} \frac{\mathfrak{T}}{K}$$

The SOI torque on the nanobridge $\mathfrak{T} = \gamma \frac{1}{L} \int_0^L dx J^y(x)$

$$\bar{J}^y \equiv \frac{1}{L} \int_0^L dx J^y(x) = \frac{D_S P^y(0) S}{L}$$

$$\overline{\delta\theta_L^2} = \frac{k_B T L_t}{\pi^2 K} \sum_{n \geq 1} \frac{1}{n^2} \sin^2 \left(\frac{\pi n L}{L_t} \right)$$

$$\theta_L = \frac{L(L_t - L)}{L_t} \frac{\mathfrak{I}}{K}$$

$$b = 400 \text{ nm}$$

$$c = 200 \text{ nm}$$

$$\alpha/\hbar = 4 \times 10^5 \text{ m/s (GaAs)}$$

$$\gamma = 2.4 \times 10^{-32} \text{ J sec}$$

$$\text{For } e\bar{J}^y = 10^{-8} \text{ Amp.}$$

$$\mathfrak{J} = 1.5 \times 10^{-21} \text{ Nm}$$

**within the sensitivity of
P. Mohanty's group,
Phys. Rev. B 70, 195301
(2004)**

**A.G. Mal'shukov, C.S. Tang,
C.S. Chu, K.A. Chao,
Phys. Rev. Lett. 95, 107203
(2005)**

$$\text{For } L_t = 5 \text{ } \mu\text{m}$$

$$L = 2 \text{ } \mu\text{m}$$

$$Q \approx 10^4$$

$$\delta\theta \approx 0.5 \times 10^{-4} \text{ }^\circ$$

Summary

- 1. Strain-induced SOI provides a nanomechanical scheme for the detection of spin current**
- 2. The effect can be inverted for the generation of spin current from torsional motion**

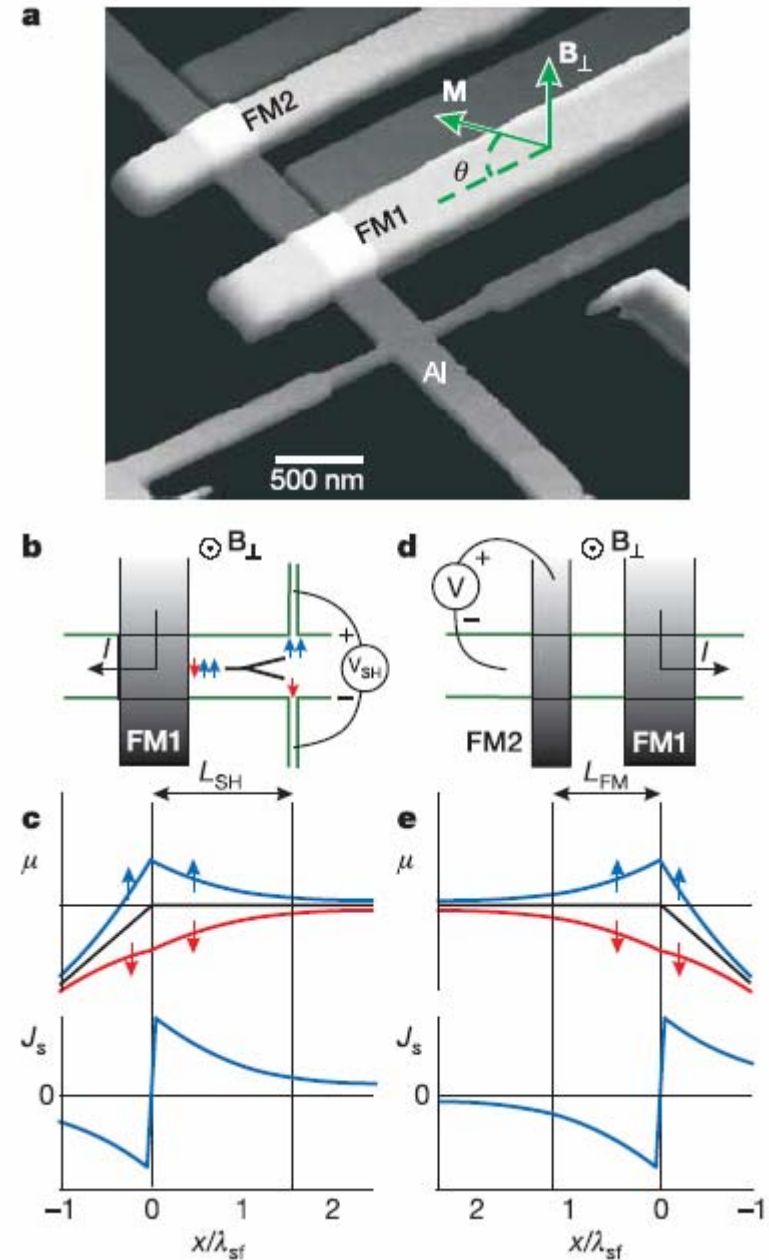
LETTERS

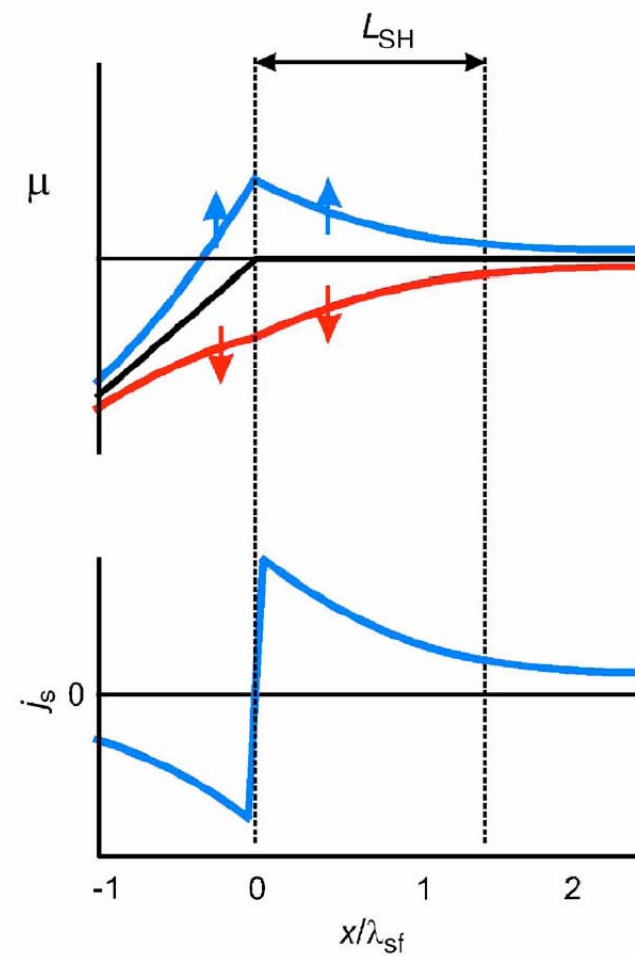
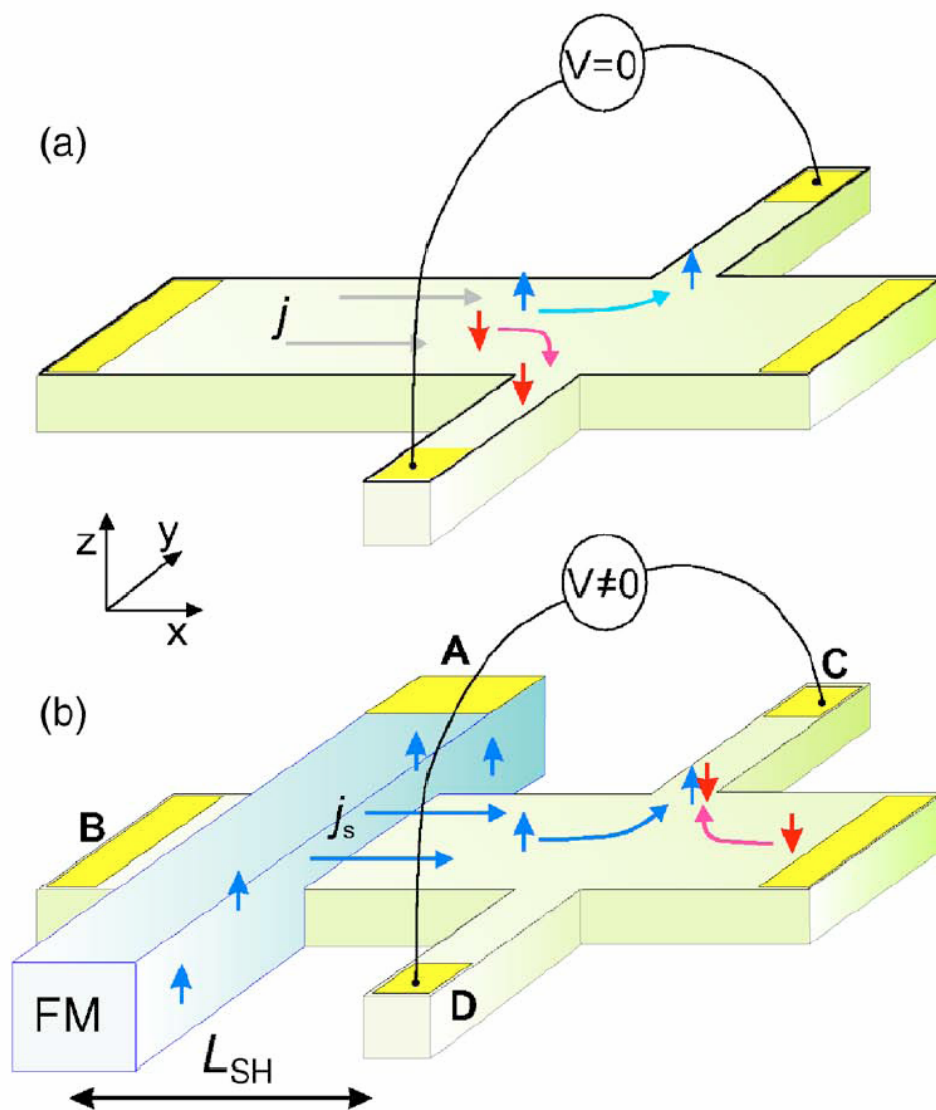
Direct electronic measurement of the spin Hall effect

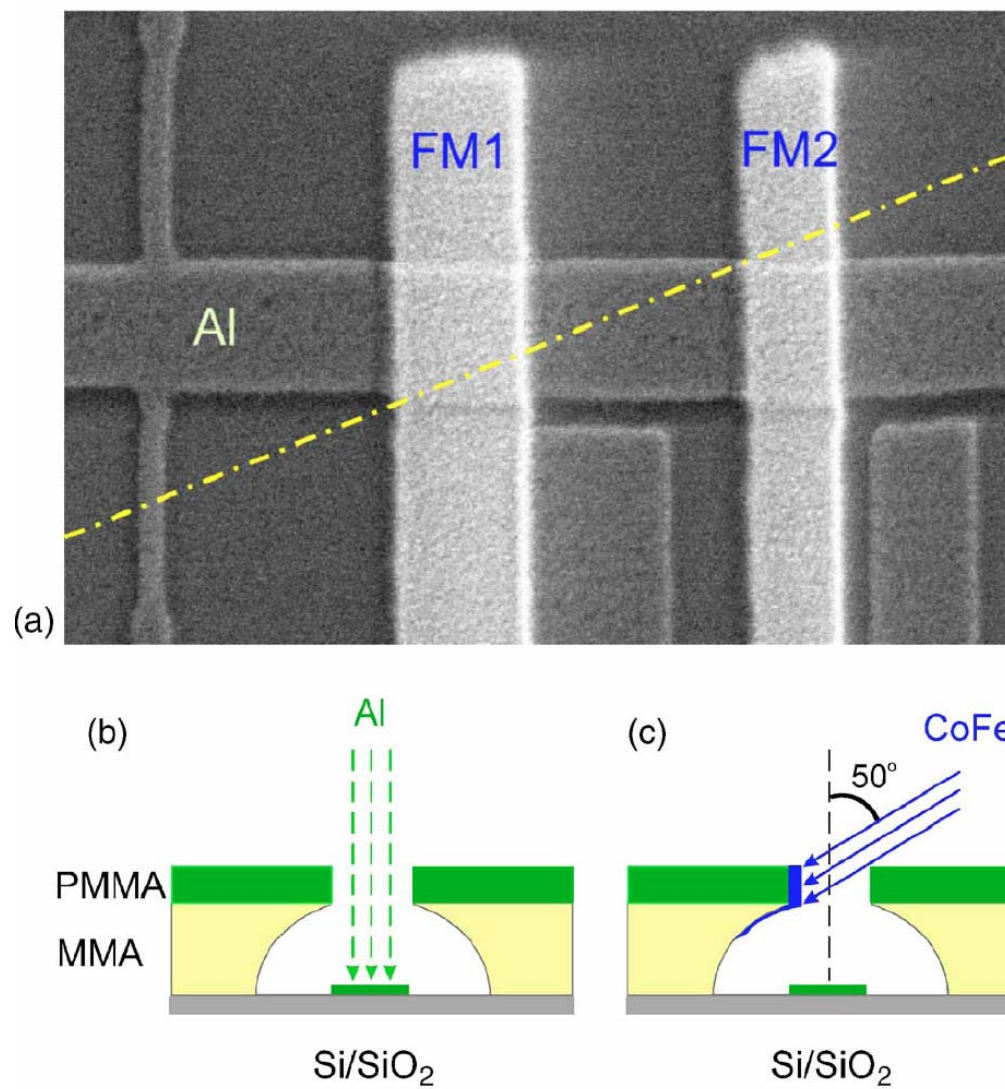
S. O. Valenzuela¹† & M. Tinkham¹

The generation, manipulation and detection of spin-polarized electrons in nanostructures define the main challenges of spin-based electronics¹. Among the different approaches for spin generation and manipulation, spin-orbit coupling—which couples the spin of an electron to its momentum—is attracting considerable interest. In a spin-orbit-coupled system, a non-zero spin current is predicted in a direction perpendicular to the applied electric field, giving rise to a spin Hall effect^{2–4}. Consistent with this effect, electrically induced spin polarization was recently detected by optical techniques at the edges of a semiconductor channel⁵ and in two-dimensional electron gases in semiconductor heterostructures^{6,7}. Here we report electrical measurements of the spin Hall effect in a diffusive metallic conductor, using a ferromagnetic electrode in combination with a tunnel barrier to inject a spin-polarized current. In our devices, we observe an induced voltage that results exclusively from the conversion of the injected spin current into charge imbalance through the spin Hall effect. Such a voltage is proportional to the component of the injected spins that is perpendicular to the plane defined by the spin current direction and the voltage probes. These experiments reveal opportunities for efficient spin detection without the need for magnetic materials, which could lead to useful spintronics devices that integrate information processing and data storage.

Figure 1 | Geometry of the devices and measurement schemes. **a**, Atomic force microscope image of a device. A thin aluminium (Al) Hall cross is oxidized and contacted with two ferromagnetic electrodes with different widths (FM1 and FM2). A magnetic field perpendicular to the substrate, B_{\perp} , sets the orientation of the magnetization M of FM1 (and FM2), which is characterized by an angle θ . **b**, Spin Hall measurement. A current I is injected out of FM1 into the Al film and away from the Hall cross. A spin Hall voltage, V_{SH} , is measured between the two Hall probes at a distance L_{SH} from the injection point. V_{SH} is caused by the separation of up and down spins due to spin-orbit interaction in combination with a pure spin current. **c**, Top: spatial dependence of the spin-up and spin-down electrochemical potentials, $\mu_{\uparrow, \downarrow}$. The black line represents the electrochemical potential of the electrons in the absence of spin injection. λ_{sf} is the spin diffusion length. Bottom: associated spin current, J_s . The polarized spins are injected near $x = 0$ and diffuse in both Al branches in opposite directions. The sign change in J_s reflects the flow direction. **d**, Spin-transistor measurement for device characterization. I is injected out of FM1 into the Al film and away from FM2, which is located at a distance L_{FM} from FM1. A voltage V is measured between FM2 and the left side of the Al film. **e**, As in **c** but for the conditions shown in **d**. Note that both V_{SH} in **b** and V in **d** vary with θ .







$$\nabla^2 \delta\mu(\mathbf{r}) = \frac{\delta\mu(\mathbf{r})}{\lambda_{sf}^2}, \quad \delta\mu(\mathbf{r}) = \frac{\mu^\uparrow(\mathbf{r}) - \mu^\downarrow(\mathbf{r})}{2}$$

$$\mathbf{j}_c(\mathbf{r}) = \sigma_c \mathbf{E}(\mathbf{r}) + \frac{\sigma_{SH}}{\sigma_c} (\hat{\mathbf{z}} \times \mathbf{j}_s),$$

$$\mathbf{j}_s(\mathbf{r}) = -\sigma_c \nabla \delta\mu(\mathbf{r})$$

$$j_s(x) = \frac{1}{2} P \frac{I}{A_N} e^{-x/\lambda_{sf}},$$

New Journal of Physics

The open-access journal for physics

Extracting current-induced spins: spin boundary conditions at narrow Hall contacts

i Adagideli^{1,3}, M Scheid¹, M Wimmer¹, G E W Bauer²
and K Richter¹

¹ Institut für Theoretische Physik, Universität Regensburg, D-93040, Germany

² Kavli Institute of Nanoscience, TU Delft, Lorentzweg 1,
2628 CJ Delft, The Netherlands

E-mail: inanc.adagideli@physik.uni-regensburg.de

New Journal of Physics 9 (2007) 382

Received 30 July 2007

Published 24 October 2007

Online at <http://www.njp.org/>

doi:10.1088/1367-2630/9/10/382

Abstract. We consider the possibility to extract spins that are generated by an electric current in a two-dimensional electron gas with Rashba–Dresselhaus spin–orbit interaction (R2DEG) in the Hall geometry. To this end, we discuss boundary conditions for the spin accumulations between a spin–orbit (SO) coupled region and a contact without SO coupling, i.e. a normal two-dimensional electron gas (2DEG). We demonstrate that in contrast to contacts that extend along the whole sample, a spin accumulation can diffuse into the normal region through finite contacts and be detected by e.g. ferromagnets. For an impedance-matched narrow contact the spin accumulation in the 2DEG is equal to the current induced spin accumulation in the bulk of R2DEG up to a geometry-dependent numerical factor.

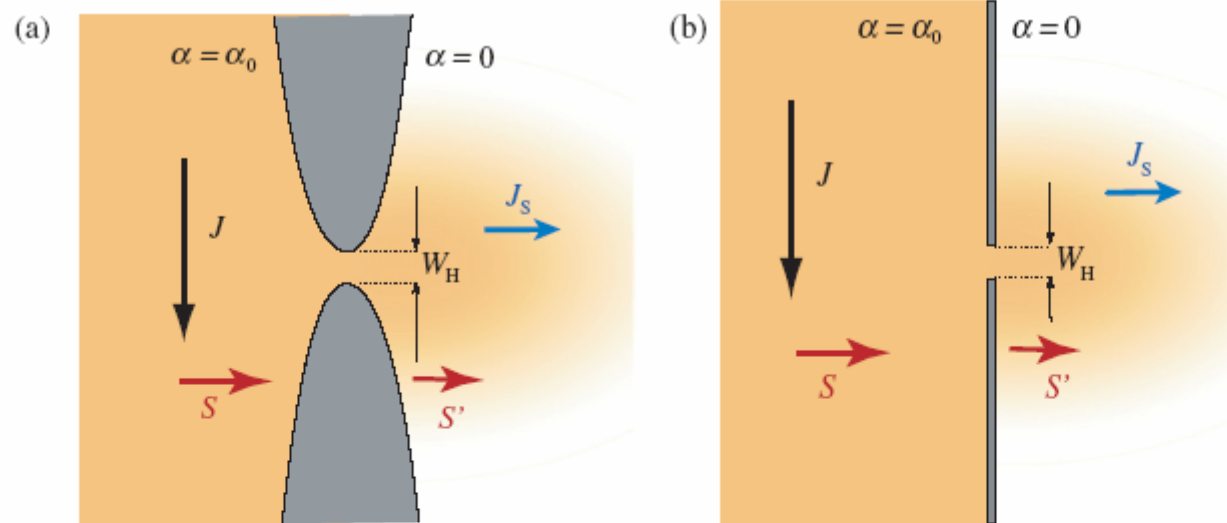
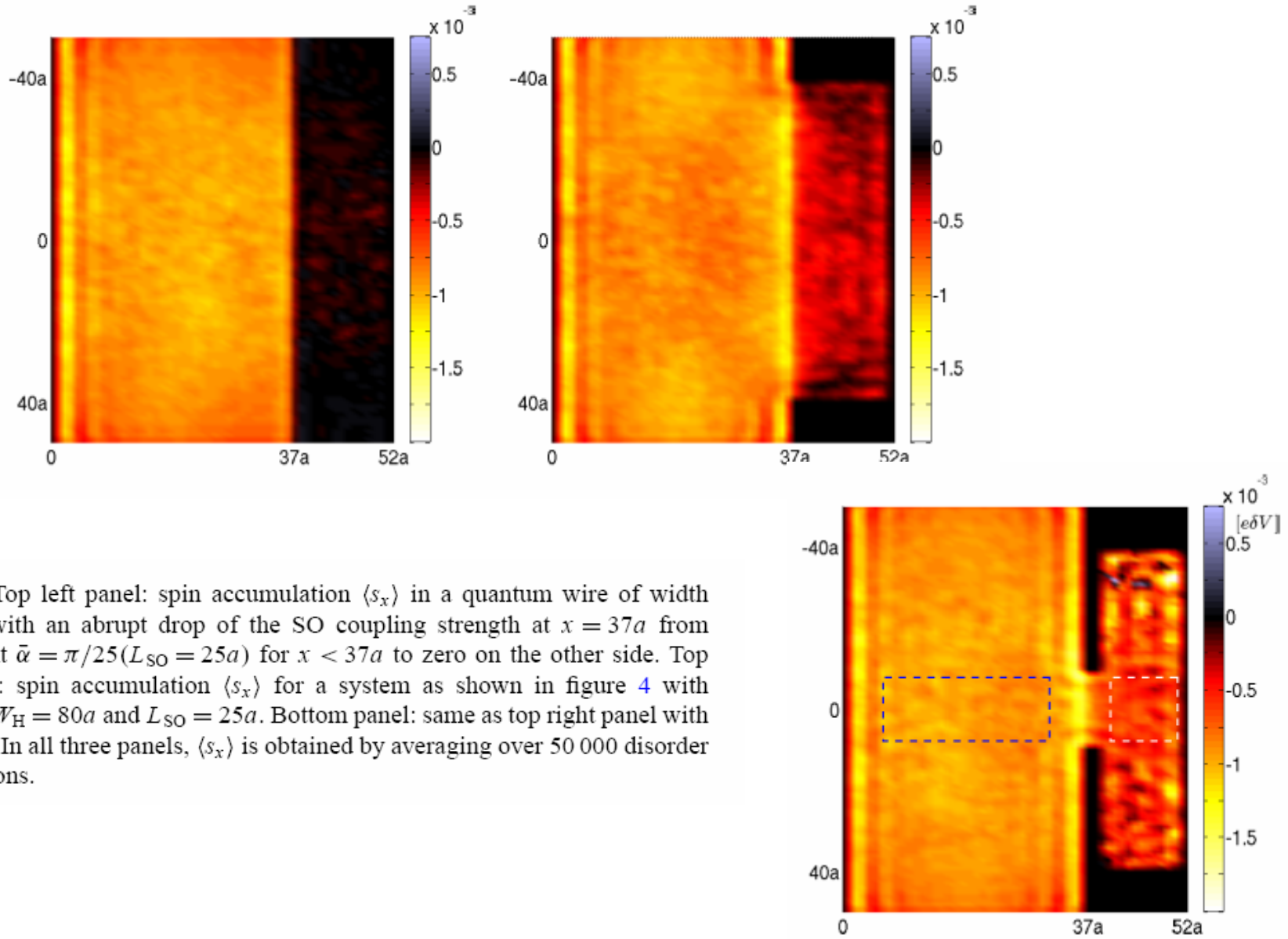


Figure 3. Geometry of the contact: (a) 2DEG with a constriction in the middle. On the left side there is an applied homogeneous current density which is modified near the opening. On the right side, the current density far away from the contact as well as the net charge current flowing from the left region to the right region is zero. However, there is a finite spin current and a finite spin accumulation in the right region. The respective mobilities of the left and right regions are assumed to be the same but the Rashba coefficients are different. (b) An idealized version of (a) used in the calculations of this section. The origin is chosen at the center of the opening with width W_H .



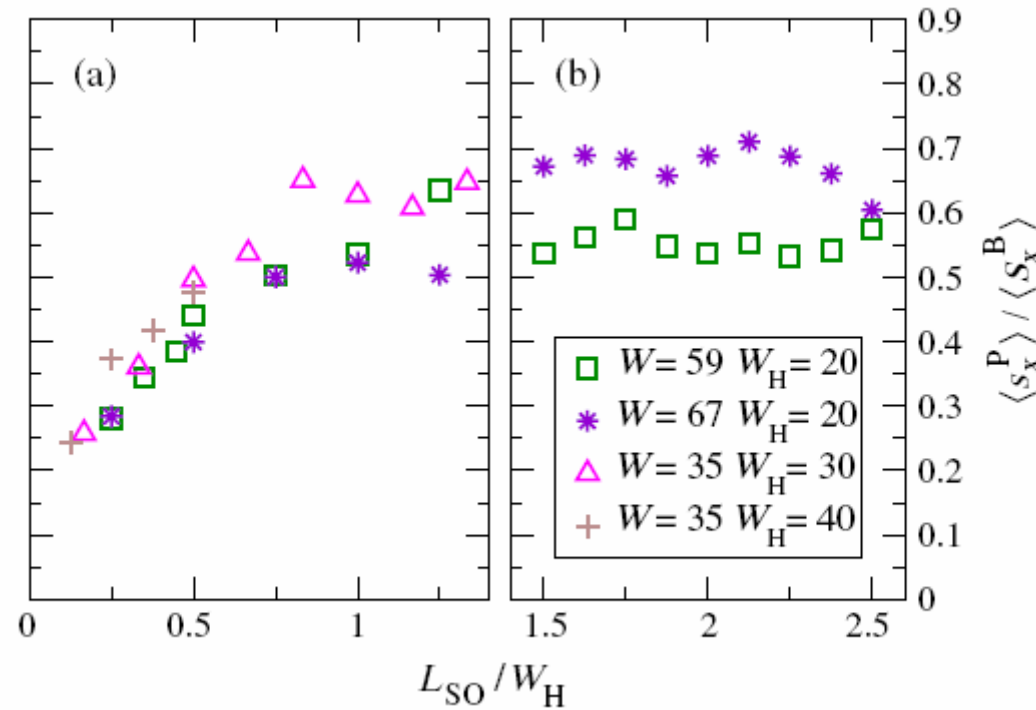
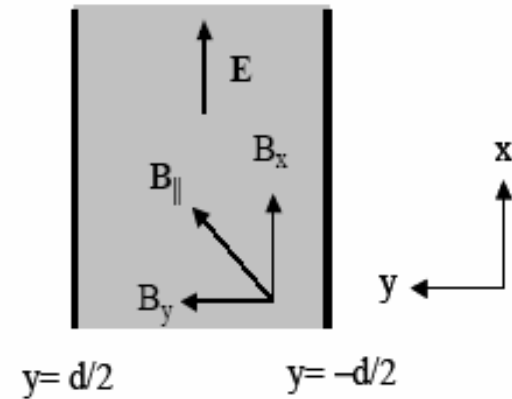
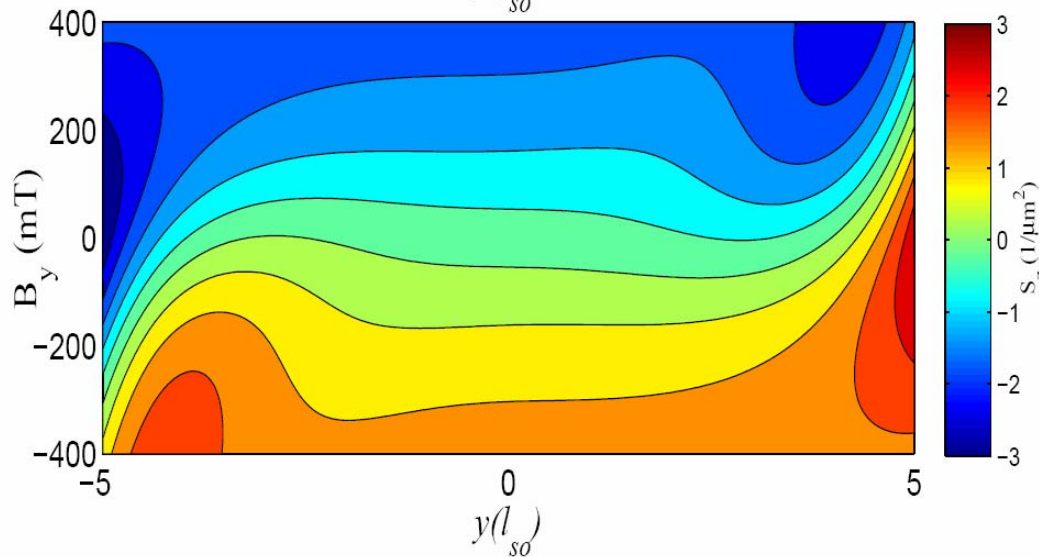
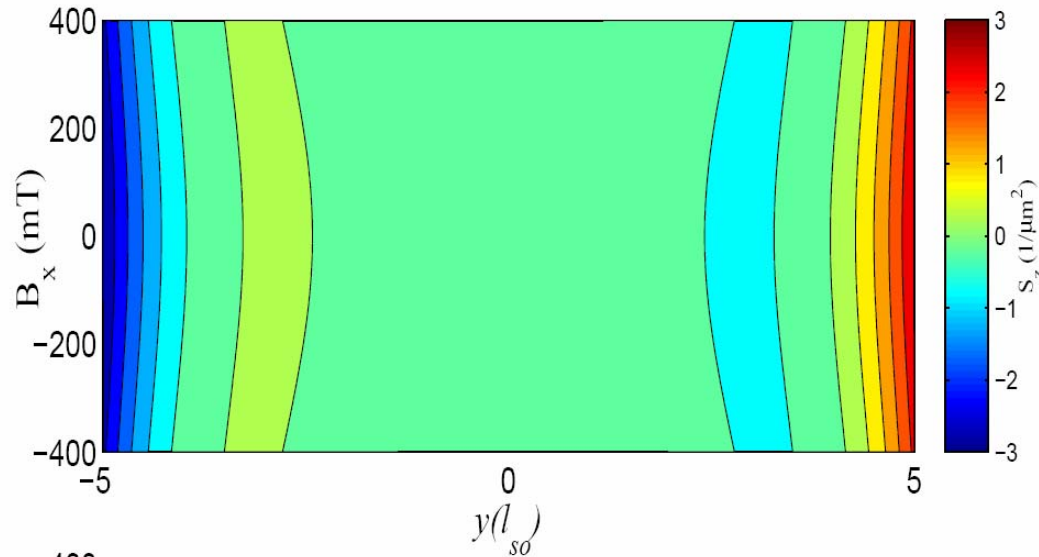


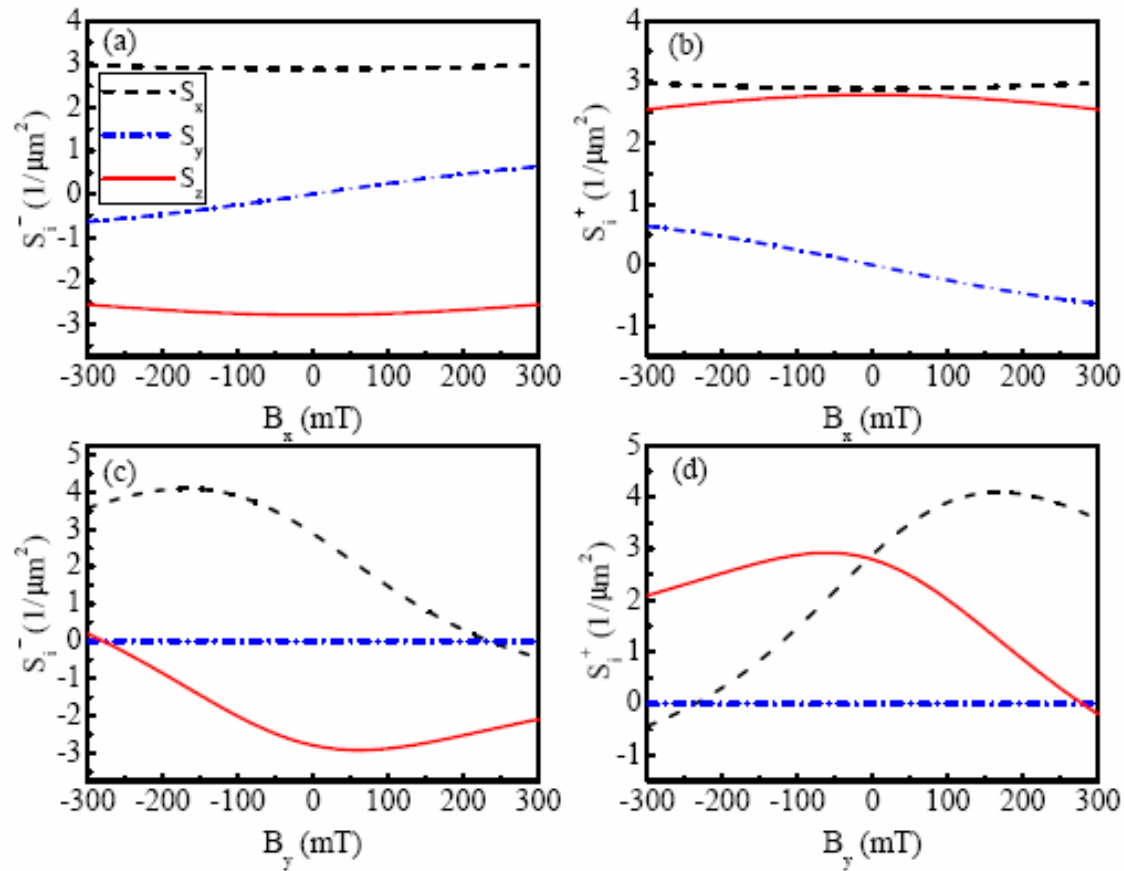
Figure 7. Left panel: average spin accumulation inside the normal region $\langle s_x^P \rangle$ relative to the accumulation in the bulk of the SO region $\langle s_x^B \rangle$ for various geometries averaged over 20 000 disorder configurations as a function of L_{SO}/W_H . Right panel: $\langle s_x^P \rangle / \langle s_x^B \rangle$ for two different geometries averaged over 60 000 disorder configurations.

Weak in-plane magnetic field as a probe for the SOI mechanism in a sample

Symmetries of spin accumulation in weak in-plane magnetic fields



L.Y. Wang, C.S. Chu, A.G. Mal'shukov, 2008





Thank you for your attention

Quantum Spin Hall Effect and Topological Phase Transition in HgTe Quantum Wells

B. Andrei Bernevig,^{1,2} Taylor L. Hughes,¹ Shou-Cheng Zhang^{1*}

We show that the quantum spin Hall (QSH) effect, a state of matter with topological properties distinct from those of conventional insulators, can be realized in mercury telluride–cadmium telluride semiconductor quantum wells. When the thickness of the quantum well is varied, the electronic state changes from a normal to an “inverted” type at a critical thickness d_c . We show that this transition is a topological quantum phase transition between a conventional insulating phase and a phase exhibiting the QSH effect with a single pair of helical edge states. We also discuss methods for experimental detection of the QSH effect.

The spin Hall effect (1–5) has recently attracted great attention in condensed matter physics, not only for its fundamental scientific importance but also because of its potential application in semiconductor spin-

tronics. In particular, the intrinsic spin Hall effect promises the possibility of designing the intrinsic electronic properties of materials so that the effect can be maximized. On the basis of this line of reasoning, it was shown (6) that the intrinsic spin

Hall effect can in principle exist in band insulators, where the spin current can flow without dissipation. Motivated by this suggestion, researchers have proposed the quantum spin Hall (QSH) effect for graphene (7) as well as for semiconductors (8, 9), where the spin current is carried entirely by the helical edge states in two-dimensional samples.

Time-reversal symmetry plays an important role in the dynamics of the helical edge states (10–12). When there is an even number of pairs of helical states at each edge, impurity scattering or many-body interactions can open a gap at the edge and render the system topologically trivial. However, when there is an odd number of pairs of helical states at each edge, these effects cannot open a gap unless time-reversal symmetry is

¹Department of Physics, Stanford University, Stanford, CA 94305, USA. ²Kavli Institute for Theoretical Physics, University of California, Santa Barbara, CA 93106, USA.

*To whom correspondence should be addressed. E-mail: sczhang@stanford.edu

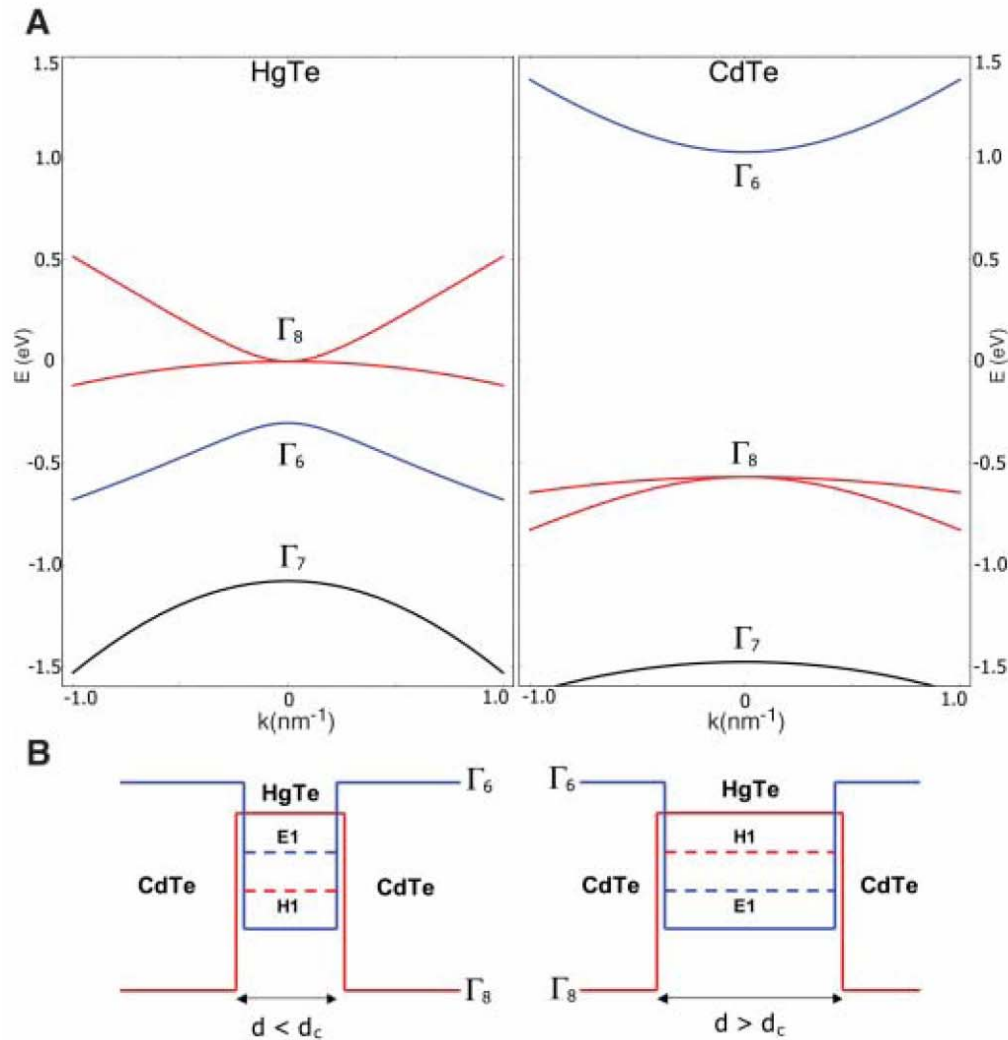
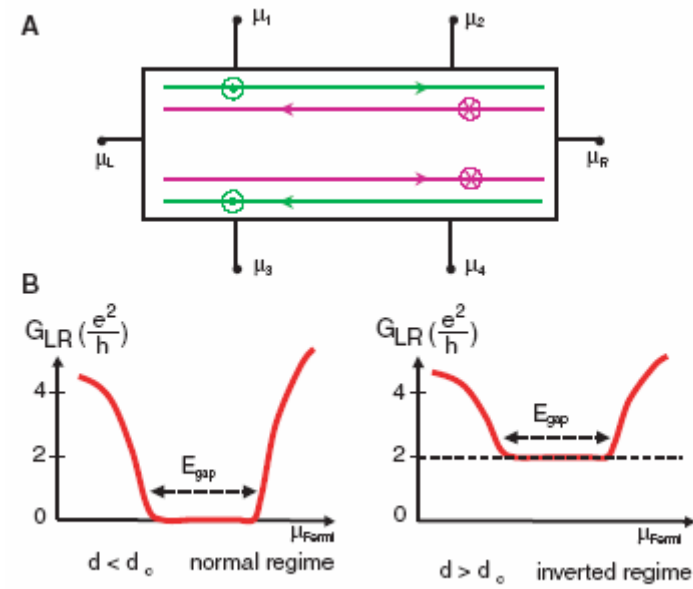
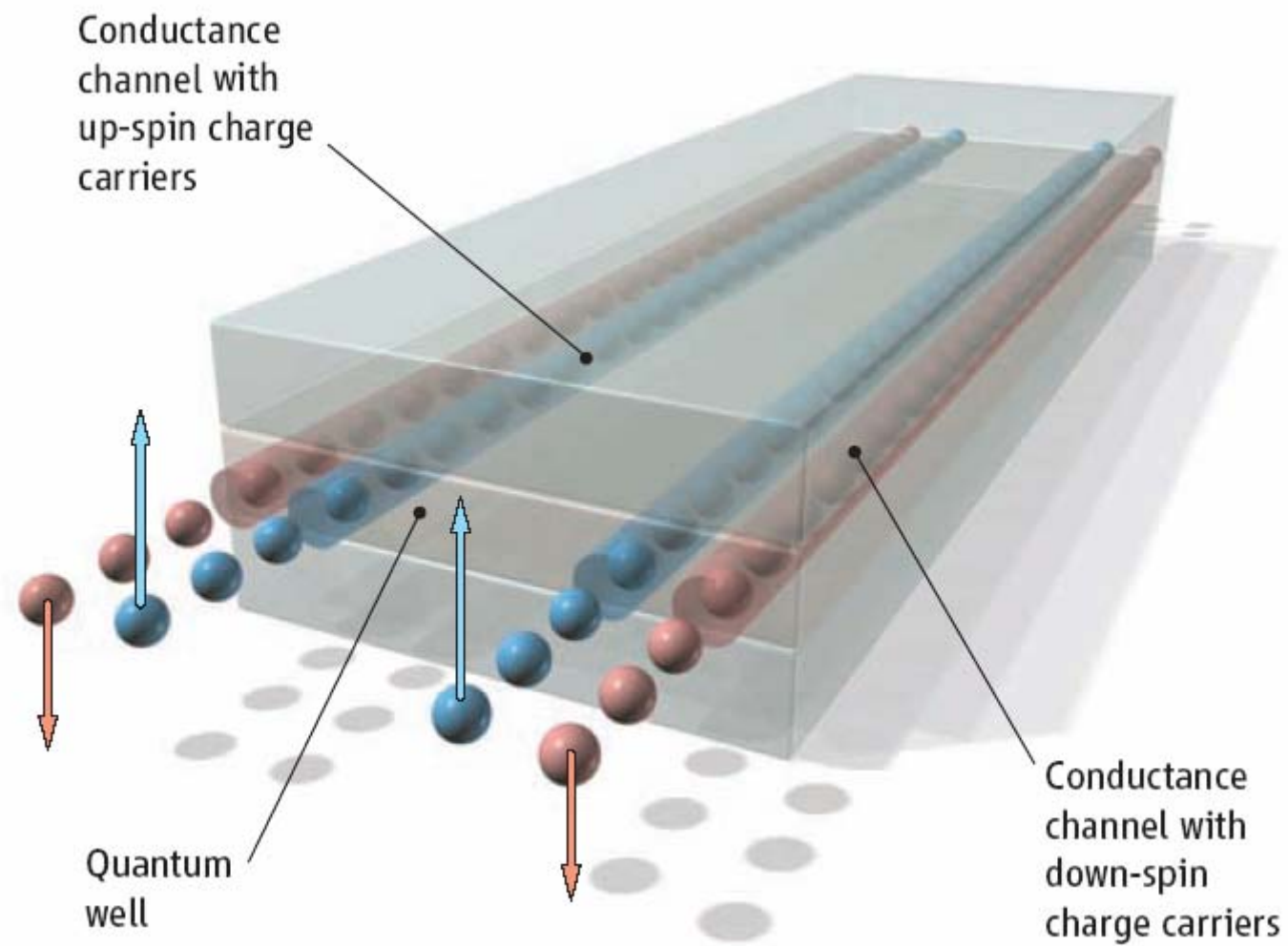


Fig. 1. (A) Bulk energy bands of HgTe and CdTe near the Γ point. (B) The CdTe-HgTe-CdTe quantum well in the normal regime $E1 > H1$ with $d < d_c$ and in the inverted regime $H1 > E1$ with $d > d_c$. In this and other figures, $\Gamma_8/H1$ symmetry is indicated in red and $\Gamma_6/E1$ symmetry is indicated in blue.





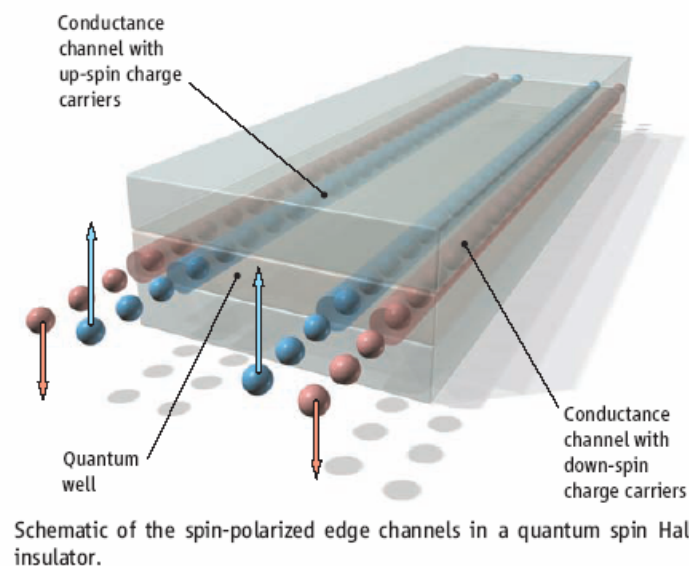
Quantum Spin Hall Insulator State in HgTe Quantum Wells

Markus König,¹ Steffen Wiedmann,¹ Christoph Brüne,¹ Andreas Roth,¹ Hartmut Buhmann,¹ Laurens W. Molenkamp,^{1*} Xiao-Liang Qi,² Shou-Cheng Zhang²

AUTHORS' SUMMARY

The discovery more than 25 years ago of the quantum Hall effect (*I*), in which the “Hall,” or “transverse electrical” conductance of a material is quantized, came as a total surprise to the physics community. This effect occurs in layered metals at high magnetic fields and results from the formation of conducting one-dimensional channels that develop at the edges of the sample. Each of these edge channels, in which the current moves only in one direction, exhibits a quantized conductance that is characteristic of one-dimensional transport. The number of edge channels in the sample is directly related to the value of the quantum Hall conductance. Moreover, the charge carriers in these channels are very resistant to scattering.

Not only can the quantum Hall effect be observed in macroscopic samples for this reason, but within the channels, charge carriers can be transported without energy dissipation. Therefore, quantum Hall edge channels may be useful for applications in integrated circuit technology, where power dissipation is becoming more and more of a problem as devices become smaller. Of course, there are some formidable obstacles to overcome—the quantum Hall effect only occurs at low temperatures and high magnetic fields.



theoretically that the electronic structure of inverted HgTe quantum wells exhibits the properties that should enable an observation of the quantum spin Hall insulator state. Our experimental observations confirm this.

These experiments only became possible after the development of quantum wells of sufficiently high carrier mobility, combined with the lithographic techniques needed to pattern the sample. The patterning is especially difficult because of the very high volatility of Hg. Moreover, we have developed a special low-deposition temperature Si-O-N gate insulator (7), which allows us to control the Fermi level (the energy level up to which all

electronics states are filled) in the quantum well from the conduction band, through the insulating gap, and into the valence band. Using both electron beam and optical lithography, we have fabricated simple rectangular structures in various sizes from quantum wells of varying width and measured the conductance as a function of gate voltage.

We observe that samples made from narrow quantum wells with a “normal” electronic structure basically show zero conductance when the

